1-1-1981

Analytical electron microscope study of precipitate-free zones in Al-Ag.

Sailesh M. Merchant

ANALYTICAL ELECTRON MICROSCOPE STUDY OF PRECIPITATE-FREE ZONES IN Al-Ag

by

Sailesh M. Merchant

A Thesis

Presented to the Graduate Committee

of Lehigh University

in Candidacy for the Degree of

Master of Science

in

Metallurgy and Materials Engineering

Lehigh University

1981

CERTIFICATE OF APPROVAL

This thesis is accepted and approved in partial fulfillment of the requirements for the degree of Master of Science.

September 16, 1981
(date)

Professor in Charge

Chairman of Department

ACKNOWLEDGEMENTS

I would like to express my sincere appreciation and gratitude

- to my advisor, Dr. M. R. Notis for his continuous guidance, kind support and understanding throughout the course of this investigation;
- to Dr. D. B. Williams who was much more than a co-advisor and guide--he was the driving force;
- to Dr. Y. T. Chou for the useful discussions on vacancies and dislocations;
- to Steve Baumann and Joseph Michael for the valuable advice in phase transformations and electron microscopy;
- to Dave Calvert for his efforts to make me a microscopist;
- to James Kerner and C. Narayan for help with the microprobe;
- to Andrea Weiss (D^2) for the state-of-the-art in printing and photography;
- to Louise and Betty for deciphering the hieroglyphs and the excellent typing work;
- to the fellow Graduate Students of Zoo' - Cal, Chen, Nicky, Raymond and Steve and others in the department for their constant encouragement;
- to the various organizations and the department in providing financial support;

and

- to the members of my family, to whom this thesis is dedicated.

TABLE OF CONTENTS

LIST OF TABLES

LIST OF FIGURES

ABSTRACT

The mechanism of formation of precipitate-free zones (PFZ) around grain boundaries in an aged Al-4.5 at% (~ 16 wt%) Ag alloy has been studied. The aim of this investigation was to distinguish between the solute depletion and vacancy depletion mechanisms suggested to explain PFZ formation. Earlier studies in the system, carried out using the electron-probe microanalyzer (EPMA), indicated the competitive occurrence of both mechanisms. The relatively poor resolution of the EPMA limited microanalysis to $\gtrsim 1$ μm. In the present study, the high spatial resolution capability of Analytical Electron Microscopy (AEM)has been used to measure solute concentration profiles with a spatial resolution of $\lesssim 50$ nm in thin foils of the alloy aged for various times at 433 K, 523 K and 598 K. Results indicate that the absence of heterogeneous nucleation sites combined with the presence of solute depletion near grain boundaries, are jointly responsible for the formation of two distinct types of PFZ, a white PFZ (WPFZ) immediately adjacent to the grain boundary, and a grey PFZ (GPFZ) containing Guinier-Preston zones bounding the WPFZ. Deformation and subsequent ageing of previously aged samples show the heterogeneous nucleation of γ' within the original GPFZ, confirming the presence therein of excess solute. A comparison of results has been made with recent models suggested for PFZ formation in Al-Zn-Mg and Cu-Ni-Nb alloys. The equilibrium (solid) solubility of Ag in Al and the

metastable miscibility gap have been determined at each of the ageing temperatures using AEM and these values show good agreement with previous work. Measurements of the WPFZ width have been used to calculate a diffusion coefficient and activation energy which are both in good agreement with previous literature studies and appear consistent with kinetic control of the process by the bulk diffusion of Ag in Al.

I. INTRODUCTION

In recent years there have been a significant number of investigations concerned with the formation of precipitate-free zones (PFZ) adjacent to grain boundaries in aged Al-based alloy systems. Much of the interest arose because it was believed that the PFZ could be due to solute depletion by grain boundary precipitates and could act as anodic paths for stress corrosion. Later work demonstrated that a vacancy concentration gradient and hence a vacancy depletion, could be developed near grain boundaries. The absence of vacancies, which are necessary for the nucleation of precipitates, could cause these PFZ . Either mechanism would preclude precipitation in the regions adjoining grain boundaries.

Clark used the electron-probe microanalyzer (EPMA) to study solute concentration profiles across grain boundary PFZ in aged Al-Ag alloys. Two distinct zones free of the metastable γ' precipitate were observed: a narrow ($\sim$ 500 nm wide) white PFZ (WPFZ) immediately adjacent to the grain boundary, which he attributed to the effects of solute depletion and a surrounding grey PFZ (GPFZ) with a constant solute content similar to that of the bulk composition, and therefore caused by effects of vacancy depletion. However, the relatively poor spatial resolution of the EPMA ($\gtrsim$ 1 μm) limited microanalysis to profiles across the GPFZ and Clark was unable to experimentally measure the solute distribution in the WPFZ.

The aim of this investigation was to use analytical electron microscopy (AEM), a technique with enhanced spatial resolution ($\lesssim$ 50 nm), to study composition variation in both the WPFZ and the GPFZ, and to distinguish between the two mechanisms suggested to explain PFZ formation in aged Al-Ag alloys. The Al-Ag system was chosen because it is well-documented, and because the results would be directly comparable to the earlier work of Clark using the EPMA.

II. BACKGROUND

A. Previous Work on PFZ --Chronology 1930-1980.

In a review article on precipitation from solid solutions in age-hardenable alloys, Geisler (1951) described the causes and mechanism of formation of "denuded zones" along grain boundaries observed as a result of "local impoverishment of the adjoining solid solution" by diffusion in aged Al-Zn, Al-Ag and Inconel (Fe-Ni-Cr) alloys. Interestingly, Geisler cited the work of Mehl and Barrett (1931) in the Al-Ag system, the first classical paper on Widmanstatten precipitates. These authors were probably the first workers to observe PFZ in this system but have made no mention of this feature to have been seen in their metallographic observations. Geisler summarized earlier studies by Dix (1940) wherein he had examined stress corrosion cracking and intergranular failure in several Al-based alloys and tried to explain them as a consequence of the "improverished solid solution adjacent to the grain boundary" being anodic to the grain, causing preferential attack along such regions.

Hopkinson and Carroll (1959) used electron probe microanalysis to test the validity of the "solute impoverishment" hypothesis in sensitized austenitic stainless steel and measured the Cr content with linear scans across grain boundaries. They could not find any significant Cr depletion in regions around grain-boundary carbides although corrosion studies indicated contrary results. They concluded that the Cr depletion profile was either too shallow or was confined to a distance less than the "effective diameter" of the

electron beam used for analysis.

The inherent limitations, in terms of the spatial resolution of EPMA, were also highlighted by Fleetwood (1961/62) who used the technique to measure Cr depletion around a grain boundary due to precipitation of grain boundary carbides. While he was able to observe a large concentration gradient, his analysis was limited to a closest distance of approach to the grain boundary without interference from Cr-carbides of 1.5 μm, the limit imposed by electron dispersion in the specimen. He concluded that much greater denudation of Cr would occur closer to the grain boundary at distances < 1.5 μm.

Alm and Kiessling (1962/63), using the same technique obtained linear traverses for Cr content across grain boundary carbides in austenitic stainless steels and showed that heat treatment conditions play an important role in determining the extent of solute depletion (and therefore the width of the depleted zone). However, in some cases, depending upon the width of the zone, the EPMA was not a sufficiently sensitive instrument to register the depletion.

At about the same time as the above investigations, Rosenbaum and Turnbull (1958/59) while studying nucleation phenomena in Al-Si alloys, found that point defects "quenched-in" from the supersaturated solid solution, condensed to form defect clusters and/or dislocation loops and helices which would serve as nucleating sites during ageing. This would explain the higher-than-predicted precipitation rates and precipitate densities in such

alloys. They found a "particle-free," depleted zone near grain boundaries with "particles" immediately adjacent to the zone larger than those within the matrix. As no grain boundary precipitation was observed prior to ageing, the authors suggested that the depleted region could not be caused by solute segregation and found that cold work prior to ageing would eliminate the depleted zone. Decreased quenching rates increased the width of the zone. It was concluded that these zones could be attributed to the migration of vacancies to grain boundaries (and also dislocations) during the quench and prior to high-temperature ageing. As slower quenches would offer large diffusion distances for the vacancies, the depleted zones were caused by an absence of potential nuclei rather than a lowering of solute concentration during the quench by segregation at the grain boundaries.

A similar hypothesis was put forth by Thomas and Nutting (1959/60) for aged Al-Zn-Mg alloys who also suggested that if the grain boundary precipitates were large enough, they would be able to draw solute atoms from adjoining regions, as would the precipitates at the edge of the zone and therefore solute depletion would, to some extent, be present and both mechanisms may operate to form the PFZ.

Embury and Nicholson (1963) tried to explain the importance of a high solute atom/vacancy ratio for copious precipitation to occur within the grains. They showed that in an Al-Zn-Mg alloy quenched directly to an ageing temperature above the Guinier-Preston zone solvus, the PFZ is caused entirely by solute depletion by the grain

boundary precipitate rather than by vacancy depletion. The solute atom/vacancy ratio is very low in this case and consequently large precipitates are observed in comparison to specimens quenched to room temperature and then aged for the same time as the direct-quenched sample. However, similar observations to support the vacancy depletion mechanism were made by Taylor (1963/64) who studied the effects of the ageing and solution-treatment temperatures on the width of the PFZ.

In their review on precipitation hardening, Kelly and Nicholson (1963) supported the vacancy depletion mechanism to cause PFZ in Al-based systems. However, in an Al-15.6 wt% (4.4 at%) Ag alloy, water quenched from 525°C (798 K) and aged 5 days at 160°C (433 K), they observed a 30 nm wide PFZ which they attributed to solute depletion effects. It was explained that the grain boundary precipitates cause a solute impoverishment of the adjoining areas and hence the narrow zone. They presumed a vacancy-free region, of about 0.5 to 1.0 μm width, probably corresponding to the grey precipitate free zone (GPFZ) as suggested later by Clark (1964).

Clark (1964) studied the formation of PFZ in an Al-15 wt% (4.2 at%) Ag alloy aged at 160°C (433 K) and 325°C (598 K). He indicated the relative competition between the vacancy depletion and solute depletion mechanisms to cause PFZs. He recognized two distinct PFZ at 160°C; the larger (~ 4 μm) precipitate free (of γ') GPFZ was solute-rich as indicated by an electron probe microanalysis trace across the zone, indicating that it was caused by vacancy de-

pletion and, a narrow ($\sim$ 500 nm) white PFZ (WPFZ) immediately adjacent to the grain boundary, caused by solute depletion. Once again, as in previous studies, Clark was unable to analyze the solute distribution within the impoverished region because of spatial resolution limits when using a 0.5 μm diameter probe on the electron probe microanalyzer. However he attributed the PFZ formed after ageing at 325^{o}C (598 K) to be caused by solute depletion effects.

A very systematic study on PFZ in aged Al-Zn-Mg alloys was carried out by Embury and Nicholson (1965) and Lorimer and Nicholson (1966). According to their model, on quenching from the solution treatment temperature, a vacancy concentration gradient develops adjacent to the grain boundaries. A size distribution of Guinier-Preston zones would then develop near the grain boundaries depending upon the ageing treatment. They classified PFZ formation depending upon the quenching conditions, temperature, ageing time and temperature above or below the Guinier-Preston zone solvus line. A critical Guinier-Preston zone size is then thought to determine whether these should or should not transform to precipitates. The edge of the PFZ would then occur at a distance from the grain boundary where Guinier-Preston zones smaller in size than the critical diameter have dissolved. In a subsequent paper Unwin, Lorimer and Nicholson (1979) suggested that because of the presence of grain boundary precipitates, effects of a superimposed solute concentration profile should be taken into account to completely characterize the nature of PFZs. Many of these findings were also observed in the work of Subramanya (1968).

Smith and Grant (1969) showed that the width of PFZ is a function of the ageing treatment in Al-Zn-Mg alloy specimens, solution treated and quenched to room temperature and aged, depending upon whether the ageing was above or below the Guinier-Preston zone solvus temperature. In the latter case, the PFZ width increased with time at the same ageing temperature. They suggested that PFZ formed in alloys with such a heat treatment would be caused due to both the vacancy depletion and solute depletion mechanisms, and also due to some other mechanism causing competitive growth and dissolution of the Guinier-Preston zones at the edge of the PFZ.

Sperry (1970) argued that the effects of solute depletion must always be considered whenever a systematic comparison and study of the mechanisms of formation of PFZ is made. Citing volume differences between the equilibrium grain boundary precipitates and the matrix, a migration of solute atoms would always occur in the immediate vicinity of a grain boundary in order that the grain boundary precipitate may thicken. Consequently, the Guinier-Preston zone solvus temperature would vary within a given solute depleted zone as a function of the solute supersaturation and he suggested that effects of grain boundary misorientation should also be accounted for in determining the width of the PFZ.

Jacobs and Pashley (1969) proposed a "Kinetic" model for the nucleation of precipitates and suggested that in a specimen directly quenched after solution treatment, to the ageing temperature (the ageing temperature being less than T_c--the critical temperature at

which nucleation can occur when no excess vacancies are present at the ageing temperature), nucleation would occur right up to the grain boundary, except for a very small solute depletion zone.

Starke (1970) summarized most of the work published describing the effects and causes of denuded zones in the Al-based alloy systems. He has made comparisons between the "thermodynamic" model of Nicholson and co-workers (1965, 1969) and "kinetic" model of Pashley et al. (1969).

In the years to follow a significant number of investigations were made by workers in aged Al-based systems, mostly Al-Zn-Mg, studying the formation of PFZ and their detrimental effects on properties such as loss of hardness and stress corrosion cracking. Analytical methods were used and techniques such as the electron probe microanalysis, electron energy loss spectrometry and scanning transmission electron microscopy were employed. Lorimer et al. (1971) were probably the first to utilize the analytical electron microscope (AEM) to study solute distribution around a grain boundary in an Al-Zn-Mg alloy. They measured the Zn concentration in samples that were water-quenched and furnace cooled from 465^{o}C (738 K). In the water quenched samples no significant variation was detected in the Zn concentration around the grain boundary. Significant Zn depletion was observed in the furnace-cooled sample, indicating effects of solute diffusion around the grain boundary. Doig and Edington (1973,1974,1975) and Doig et al., (1973) used various heat-treatment conditions to obtain specifically solute depletion or vacancy depletion induced PFZ in Al-X (X = Cu, Mg, Zn-Mg) alloys. Electron

energy loss spectrometry was used to obtain solute concentration profiles across grain boundaries in alloys step-quenched to remove effects of excess vacancies and to induce the formation of solute depleted PFZ. They used the Grube method to determine the low temperature diffusion coefficients of Cu and Mg in Al; values of Q and D_o were also calculated. Later, AEM profiles were obtained by the same workers (1975) and solute depletion was attributed to cause PFZ formation.

Pande et al. (1977) followed Hopkinson and Carroll (1959) to check for Cr depletion in sensitized 304 stainless steels. Recognizing the limitations of the EPMA, they used a 10 nm diameter AEM probe to determine Cr concentration across a grain boundary between precipitates. Taking beam broadening effects into account, the quantitative x-ray data was collected at step distances of 50 nm, and marked Cr depletion was observed.

The most recent study concerning microanalysis of PFZ was conducted by Raghavan (1980) on Al-Zn-Mg and Cu-Ni-Nb alloys. For samples which were solution treated, air cooled to room temperature and aged for various times, he obtained concentration profiles for Zn and Mg in Al-Zn-Mg and Nb in the water quenched Cu-Ni-Nb alloys. In this work, a Philips EM400T with an EDAX energy-dispersive x-ray analyzer and a 40 nm probe was used to obtain concentration profiles across PFZ adjoining grain boundaries. He has suggested two different models for the alloy systems concerned; both models are based upon solute distribution with reference to the matrix solute concentration within the grains and at the grain boundary.

For either alloy, he did not find any significant solute depletion in the as-quenched samples. For the Al-Zn-Mg system, significant solute depletion was observed upon ageing and the amount of depletion increased with ageing time. However even after ageing for 4 hours the solute concentration in the PFZ was higher than the matrix solute concentration. Deformation experiments followed by ageing indicated hetrogeneous nucleation of precipitates within the original PFZ, which demonstrated that the PFZ were supersaturated with respect to solute even after the 4 hours ageing treatment. A model for PFZ formation in Al-Zn-Mg alloys was suggested such that its width upon ageing would be determined by the intersection of the vacancy concentration profile developed near the grain boundaries and the horizontal describing the critical vacancy concentration required for nucleation [after Embury and Nicholson (1965)], see Figure 1(a). As Guinier-Preston zones would serve as nuclei for the next transition (η') or equilibrium (η) precipitates, the absence of Guinier-Preston zones would not allow the η precipitates to form within the PFZ. Direct formation of η from the α-matrix within this zone is precluded due to free energy conditions. Meanwhile precipitation of η' or η within the main regions of the grains causes this region of the matrix to approach the equilibrium concentration; thus, the PFZ remains supersaturated with respect to the grain interiors. This causes concentration gradients to be set up both with respect to the grain boundary and also the edge of the PFZ causing precipitates there to coarsen. Grain boundary precipitates grow and thicken simultaneously. The process

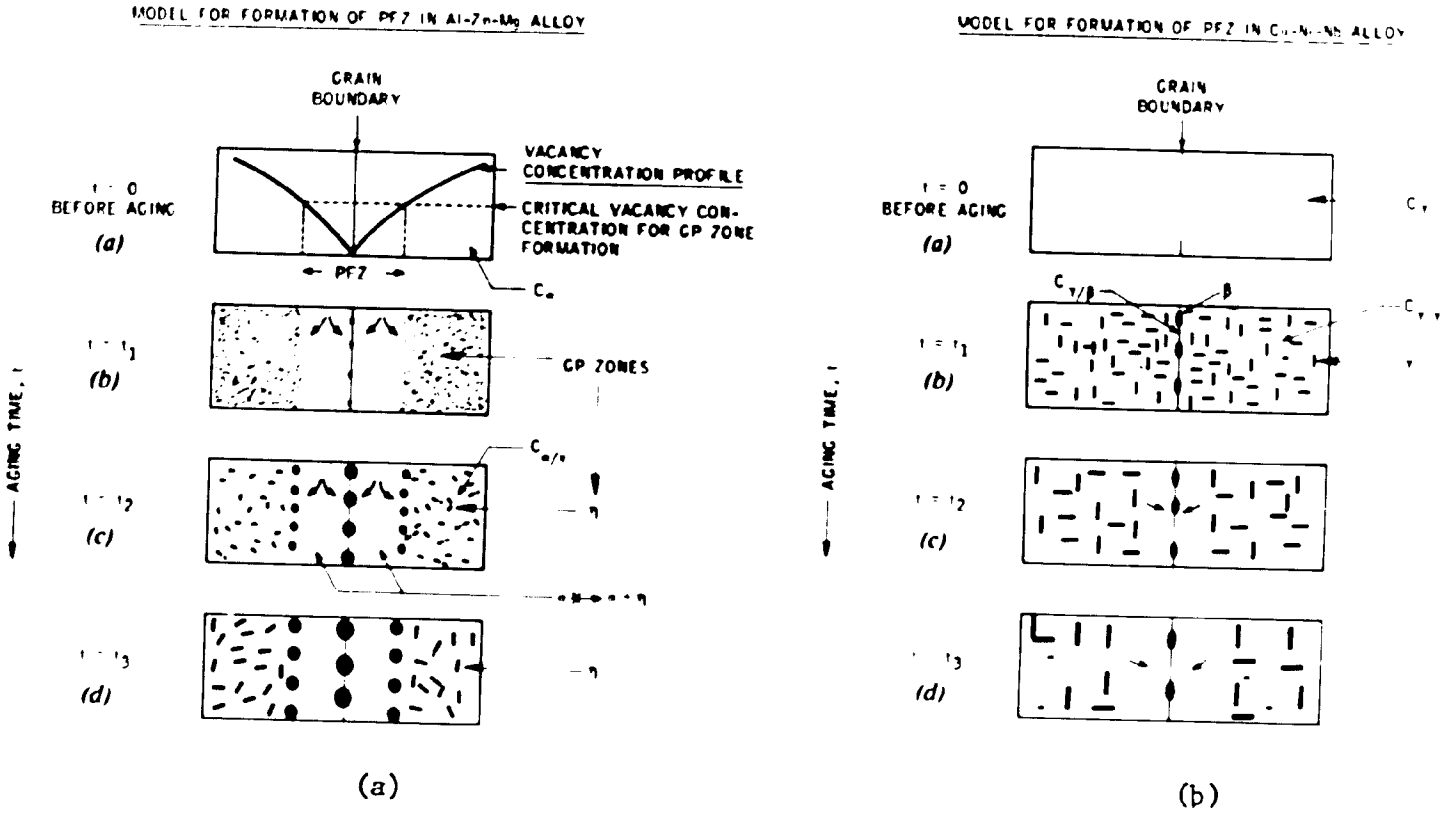

(a) (b)

Fig. 1: Schematic illustrations of the formation of PFZ in (a) Al-Zn-Mg and (b) Cu-Ni-Nb alloys. [From Raghavan (1980)]

continues until the solute concentration of the matrix is uniform across the PFZ. Thus the initiation of the PFZ due to a vacancy concentration profile and the lack of nucleation sites would primarily be responsible for the formation of PFZ in this system.

In Cu-Ni-Nb, PFZ were initially proposed to be caused by solute depletion [Raghavan, (1977)] and this model was later expanded [Raghavan, (1980)] in more recent work. In the as-quenched condition no appreciable Nb depletion was observed; however significant Nb depletion was seen in the PFZ after ageing. The PFZ was found to be depleted of the metastable γ'' phase, but supersaturated with respect to the equilibrium β-phase. The solute depletion in regions adjoining the grain boundary was caused by the nucleation of the β phase at the grain boundaries, causing the solute level in this region to fall between the composition of the matrix in equilibrium with the β and the γ'' phase. Nucleation of γ'', however, occurs within the rest of grain, beyond the edge of the solute depleted zone. The zone is thus caused by a process of diffusion of Nb atoms, and consequently increases in width with ageing time at the temperature studied. As diffusion of Nb occurs only towards the grain boundary, preferential coarsening of the precipitates at the edge of the zone does not occur. Figure 1(b) schematically demonstrates this model [from Raghavan, (1980)].

In order to provide a better understanding of the mechanism of formation of PFZ in Al-Ag alloys, and to ascertain solute depletion and supersaturation effects, it is necessary to obtain concentration profiles across the width of PFZ adjoining grain boundaries. From

the earlier studies of Hopkinson and Carroll (1959), Fleetwood (1962) and Alm and Kiessling (1962) followed by Clark (1964), it is apparent that the width of the solute depleted zone is less than 1 μm. Since this is approximately the size of the 'excited volume' or the region where x-rays are produced and detected in the EPMA, the spatial resolution of the conventional EPMA is not sufficient to reveal the solute concentration distribution in depleted zones. The approach of Clark (1964) might be followed, but concentration profiles should be measured on heat-treated thin-foils using analytical electron microscopy (AEM), a technique with enhanced spatial resolution as compared to the microprobe. A comparison of results obtained, may then be made with models suggested by Raghavan (1980) for PFZ formation in Al-Zn-Mg and Cu-Ni-Nb alloys.

The Al-Ag system was chosen because of the extensive documentation concerning phase transformations available in this system. It was believed that a prior detailed study of the available literature on the phase diagram and physical metallurgy of this alloy system would help in interpreting the results obtained from this work. The next sections therefore describe some of these studies.

B. Phase Diagram Data in the Al-Ag System

(i) The equilibrium solvus line

The extensive solid solubility of Ag in Al was first recognized by Hansen (1928), who had studied the system in great detail. It was found to increase from about 0.75 wt% (~ 0.19 at%) Ag at 200°C (473 K) to about 48 wt% (18.75 at%) Ag at the eutectic, ~ 560°C (833 K). However, the purity of the alloy was not adequate and subsequent work using purer materials by Crepaz (1930), Wakeman and Raynor (1948/49), Raynor and Wakeman (1949) and Rotherham and Larke (1952/53) showed discrepancies in the solid solubility of Ag in Al at low temperatures [below 400°C (673 K)]. Williams and Easton (1974) used the data of Raynor and Wakeman (1949) and Rotherham and Larke (1952/53) to obtain a theoretical expression to determine the solid solubility of Ag in Al at temperatures less than 300°C (573 K):

$$\log_{10} x = 1.85 - \frac{1140}{T}$$

$$\text{i.e.} \quad x = \exp\left[4.261 - \frac{2625.42}{T}\right] \qquad (1)$$

where x is the concentration of Ag in at% and T is the corresponding absolute temperature. The latest comprehensive study on the Ag-Al system was made by Elliott and Shunk (1980), for the ASM Bulletin on Phase Diagrams. The diagram lacks solid solubility data at temperatures below 200°C (473 K) at the Al-rich end and, moreover, is labelled as being provisional. Table I shows the solid solubility limit of Ag in Al as obtained by previous workers.

TABLE I

Terminal Solid Solubility Limits of Ag in Al
(the Equilibrium Solvus Line) as Determined by
Previous Workers at the Temperatures
Used in This Investigation
All Compositions in At% (Wt%) Ag. Balance Al

Temperature	Hansen (1928)	Crepaz (1930)	Rotherham & Larke (1952/53)	Williams & Easton (1974)	Elliott & Shunk (1980)
160°C (433 K)	--	--	0.19 (0.75)	0.17[1] (0.66)	--
250°C (523 K)	0.64 (2.5)	0.96 (3.75)	0.51 (2.0)	0.47[1] (1.85)	0.51 (2.0)
325°C (598 K)	1.46 (5.6)	1.79 (6.8)	1.03 (4.0)	0.95[2] (3.7)	1.16 (4.5)

[1] Theoretical value

[2] Experimental value

Doig and Edington (1973) used AEM to determine the variation of solute concentration across grain boundaries and between grain boundary precipitates in aged Al-Mg and Al-Cu alloys with well-formed PFZ. Following Aaron and Aaronson's "collector-plate" mechanism (1968), i.e., assuming diffusion along the grain boundary to be significantly faster than within the bulk of the grain, the composition of the solute at the grain boundary would effectively be constant and approximately equal to the equilibrium solute concentration expected in the matrix. Therefore, an AEM profile taken across the grain boundary, in suitably aged alloys, would be able to measure this concentration of the solute at the grain boundary plane and hence could be used to measure the equilibrium composition for the matrix. A similar rationale has been developed by Romig (1979) and Romig and Goldstein (1980) who used AEM microanalysis to determine the Fe-Ni and Fe-Ni-P phase diagrams at low temperatures. They have, however, taken concentration profiles perpendicular to phase interfaces and the concentration values at the interphase interface were assumed to represent "local equilibrium" compositions. Any deviations from true equilibrium at the interphase interface would be too small to be detected by AEM. Hence, by using several ageing temperatures, the technique can be extended to develop equilibrium and metastable solvus curves for any alloy system using a single alloy composition.

It was decided, therefore, to use AEM x-ray microanalysis to determine the solid solubility limit of Ag in Al at low temperatures ($160^{o}C$, $250^{o}C$ and $325^{o}C$, in particular) while analyzing solute distribution within the PFZ in aged Al-Ag specimens. The solute con-

centration measured at the grain boundary would be useful to extend the available data below 325°C (598 K) and would allow for a comparison to be made with the solid solubility values predicted at these temperatures from the expression suggested by Williams and Easton (1974).

(ii) The metastable Guinier-Preston zone solvus line.*

The metastable Guinier-Preston zone solvus has been determined for Al-rich, Al-Ag alloys by Borelius and Larsson (1956), Baur and Gerold (1962), Gerold (1963) and Hirano (1967) using various techniques such as small-angle x-ray scattering, resistometry and calorimetry and specific heat measurements. Table II lists the metastable solvus compositions for the three temperatures under investigation. None of the workers have actually reported these values directly; they have been obtained from plots containing data for a wide range of temperatures. Although Hirano's study is the most recent work on the determination of the Guinier-Preston zone metastable solvus line, because of the large differences between the compositions that he reports compared with those obtained by other workers, his study will not be considered further and is only mentioned here.

In Clark's (1964) investigation on PFZ in aged Al-Ag alloys, he indicated that the narrow WPFZ immediately adjacent to the grain boundary was caused by effects of solute depletion. The absence of Guinier-Preston zones in this narrow (~ 500 nm for an Al-15 wt% Ag alloy aged at 160°C for 120 hrs.) white region indicated that the solute concentration there had been lowered below the composition of the Guinier-Preston zone solvus at the ageing temperature; the extent

TABLE II

Metastable Guinier-Preston Zone Solvus Composition [Ag in At% (Wt%)] for the Temperatures Studied as Obtained by Previous Investigations

Temperature	Baur & Gerold (1962)[a]	Gerold (1963)[b]	Hirano (1967)[c]
160°C (433 K)	0.6 (2.36)	0.64 (2.51)	0.15 (0.6)
250°C (523 K)	1.2 (4.63)	1.44 (5.52)	0.6 (2.36)
325°C (598 K)	---	---	2.5 (9.3)

[a] Small-angle x-ray scattering

[b] Resistivity

[c] Resistivity and specific heat variations

of solute depletion could be estimated by the limit of Guinier-Preston zone formation and the composition of the immiscibility gap at that ageing temperature. He pointed out that the limit of Guinier-Preston zone formation indicated only one point on the solute depletion gradient. He was unable to analyze the Ag distribution within the WPFZ, as the PFZ was of the same order of size as the diameter of the analyzing probe.

Consequently, it was decided to obtain values of the Ag concentrations which would define the Guinier-Preston zone metastable solvus line at the three ageing temperatures used in this investigation. This concentration would be available from the concentration profile taken across the grain boundary WPFZ, defined by the edge of the WPFZ, namely the limits of Guinier-Preston zone formation.

*[Although the first stages of decomposition of a supersaturated solid solution of Al-Ag alloys are identified as ε, η or η' by Borelius and Larsson (1956) or Hirano (1967), these will be collectively known in the text as Guinier-Preston zones, following Lorimer (1978).]

C. Phase Transformations in the Al-Ag System

Precipitation reactions in aged Al-Ag alloys have been studied in great detail and are well documented. Early work by Mehl and Barrett (1931), Barrett et al. (1941) and Guinier (1952) was useful in predicting the phase transformations in the system. The first TEM studies were performed by Koda and Takeyama (1952,1953) who used oxide replicas and later by Nicholson and Nutting (1961), using self-supporting thin metal foils of an Al-16 wt% (4.5 at%) Ag alloy. The

appropriate region of the Al-Ag equilibrium diagram is shown in Figure 2; under equilibrium conditions a supersaturated solid solution of Ag in Al would yield a two-phase structure of Al (the matrix) and an intermetallic compound Ag_2Al, called the γ-phase.

A freshly quenched, solution-treated ($520^{o}C$/793 K) sample of the alloy, upon examination showed two prominent types of defects--dislocation loops formed by the collapse of discs of aggregated vacancies, containing regions of stacking faults within them, and helical dislocations. These defects play an important role for they serve as nucleating sites for the metastable γ' precipitates and hence in determining the width of the GPFZ. Upon ageing at $160^{o}C$ (433 K) for various times Nicholson and Nutting (1961) observed a sequence of precipitation in the alloy.

The first stage of decomposition of the supersaturated solid solution is the copious homogeneous nucleation of Ag-rich nominally spherical Guinier-Preston zones in an Al matrix. These possess the same fcc structure as the matrix and do not exhibit any strain fields around them because of the close proximity of the lattice parameters of Ag 0.4086 nm and Al 0.4049 nm. Kelly and Nicholson (1963) indicated that the Guinier-Preston zones nucleate on Ag-rich clusters formed during the quench and/or the "pre-precipitation" period. Hren and Thomas (1963) have shown that clusters are also observed in specimens having compositions within the equilibrium single phase field. The kinetics of Guinier-Preston zone formation have been investigated by Baur and Gerold (1962), Murty and Vasu (1969,1971) and Federighi and Passari (1959) and these workers have performed some

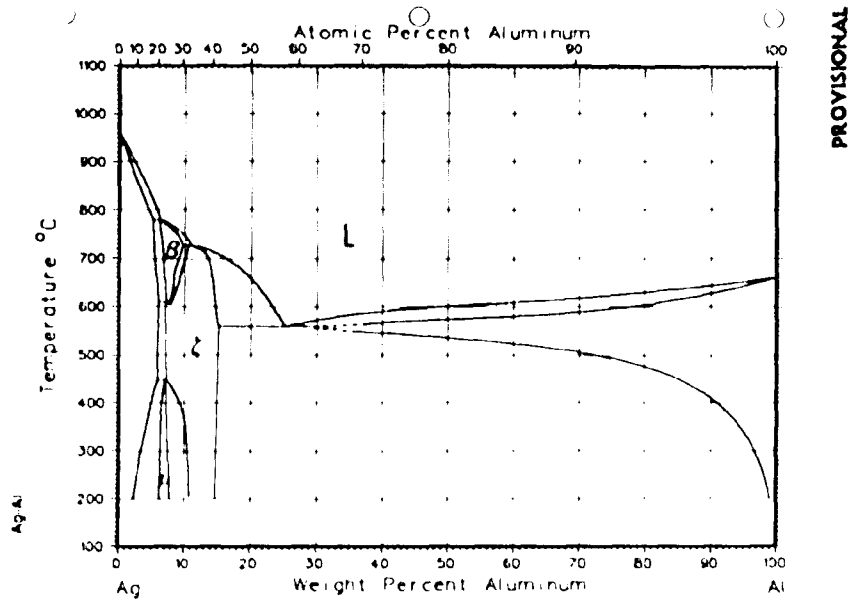

Fig. 2: The Al-Ag equilibrium diagram
[From Elliott and Shunk (1980)]

studies demonstrating the influence of vacancies upon the nucleation role of the zones. Gragg and Cohen (1971) have shown that a shape change occurs on ageing above 170°C (443 K) such that octahedral zones change to spherical ones with an attendant loss in Ag content, and they have developed a computer-simulated model to describe the configuration of atoms within each zone.

The second stage in the precipitation sequence is the nucleation of metastable γ' precipitates, having a h.c.p.-based structure with alternate close-packed layers corresponding to the approximate compositions of Ag_2Al and Ag. The lattice parameters of the γ' phase are c = 0.4607 nm and a = 0.2858 nm and c/a = 1.612 (Barrett et al.1941) and it exhibits a characteristic orientation relationship with the matrix, $(0001)_{\gamma'} \parallel (111)_{\alpha}$ and $[11\bar{2}0]_{\gamma} \parallel [\bar{1}10]_{\alpha}$. Nicholson and Nutting (1961) found that the γ' nucleates heterogeneously, mostly on helical dislocations. They suggested that because of a "finite binding energy" between a Ag-atom and a vacancy, the solute atom-vacancy pairs would migrate to a screw dislocation where vacancies would be annihilated to form a helical dislocation and consequently the local Ag concentration would be raised. Therefore, helical dislocations would serve as favourable sites for the precipitation of an Ag-rich phase. This increased Ag concentration would lower the stacking fault energy of the dislocation which would then climb onto {111} planes by forming jogs and split into two partial dislocations by a reverse Kuhlmann-Wilsdorf (1958) reaction:

$$\frac{a}{2}[\bar{1}10] \rightarrow \frac{a}{3}[\bar{1}11] + \frac{a}{6}[\bar{1}1\bar{2}].$$

Such a mechanism had been proposed by Suzuki (1952), whereby, when a glissile dislocation in an fcc lattice splits into a pair of partial dislocations, the partials are separated by a stacking fault containing a thin layer of hcp structure [see Read, (1953)]. Because of this difference in structure, the equilibrium concentration of solute in the faulted layer may differ from that of the surrounding matrix. This would lead to segregation of solute in the region, causing a local change in the stacking fault energy and hence alter the fault width. Segregation of the solute at the fault would then lead to nucleation of a precipitate, if the fault and this phase have the same crystal structure. This mechanism of formation of γ' precipitates gives rise to contrast affects similar to those seen due to stacking faults and is called "displacement-fringe" contrast. This is characteristics of γ' plate precipitates and is easily observed during the early stages of ageing. For a detailed explanation see Hirsch, et al. (1965).

Hren and Thomas (1963) using "in-situ" hot-stage microscopy found that all dislocations were effective as nucleation sites for the γ' precipitates. Subsequent work on γ' precipitation has been done by Nemoto and Koda (1964/65), Watanabe et al. (1963), Passoja and Ansell (1971) and Dobromyslov (1972). A good electron microscope study has been performed by Fujime et al. (1964) who have explained the effects of double diffraction in selected area diffraction patterns from an Al-20 wt% (5.88 at%) Ag alloy containing γ' and γ precipitates. It should be noted, however, that Hren and Thomas (1963) could not find evidence for nucleation of γ' at Guinier-Preston zones

as had been suggested by Guinier (1952). That γ' nucleates only on heterogeneities has been confirmed by studies performed during the early stages of ageing at 160°C [Nicholson and Nutting, (1961)] where it is shown that the density of γ' precipitates is the same as the density of vacancy loops and dislocations in the quenched supersaturated solid solution.

The equilibrium γ-phase nucleates at grain boundaries of the Al matrix, and growth occurs by means of a discontinuous or cellular reaction, see Nicholson and Nutting (1961) or Aaronson and Clark (1967) where the grain boundary migrates with the growing γ precipitates and the attendant dissolution of γ' takes place in front of the advancing boundary and precipitation of γ occurs within the transformed region. The γ phase can also form "in-situ" from the γ' by the acquisition of misfit dislocations [Laird and Aaronson, (1967) and (1969)]. The γ has a composition Ag_2Al and is hexagonal with a = 0.2879 nm, c = 0.4573 nm, c/a = 1.588, see Barrett, et al.(1941). It has the same orientation relationship with the matrix as does γ'.

Laird and Aaronson (1967, 1969) studied the structure of the γ plates and found that the interface consisted of partial dislocations, predominantly of the edge orientation, and suggested that their growth would occur by the "ledge mechanism" (Aaronson, 1962). Abbott and Haworth (1973) used the electron probe microanalyzer to study the solute distribution around isolated γ plates during dissolution. They found that the solute concentration of the precipitate/matrix interface was lower than the equilibrium value, indicating an interface-controlled dissolution reaction.

D. Diffusion Data of Ag in Al

Diffusion is fundamental to most metallurgical phenomena, but, for low-temperature reactions such as precipitation, reliable diffusion data is not generally available, and it becomes necessary to rely on values of diffusion coefficients of the solute in the matrix, extrapolated from high temperatures. Moreover there is considerable scatter in the literature for the activation energies required to calculate low-temperature diffusion coefficients.

Doig and Edington (1973) examined the reasons for the lack of such data. They suggested that the absence of low-temperature data arises for two main reasons:

- in cases of limited solid solubility, the changes in composition may be too small to measure accurately with available techniques.
- diffusion distances are small in terms of the spatial resolution made available by conventional methods of microanalysis.

A similar situation exists for the Al-Ag system, where there is a lack of low-temperature diffusion data, and a range of values is reported for the activation energy as a function of Ag concentration, depending upon the technique utilized for its determination.

High temperature diffusion studies of Ag in Al have been made by Beerwald (1939), Mehl, et al. (1941), von Koster and Sperner (1953), Heumann and Dittrich (1957), Kahkonen and Syrjanen (1970) using diffusion couples. Anand and Agarwala (1967) used residual

activity measurements while studying the diffusion of Ag^{110}. Ag-isotopes were also used by Heumann and Bohmer (1968), whereas Hren and Thomas (1963) and Abbott and Haworth (1973) obtained diffusion constants from dissolution kinetics of γ' and γ precipitates respectively. Diffusion data in thin-films of Al-Ag have been obtained by Weaver and Brown (1968). A summary of the studies that have been performed, the technique used, and the activation energy obtained is given in Table III. The activation energy is plotted as a function of percent Ag in Figure 3.

Doig and Edington (1973) suggested that values of the diffusion coefficient and the activation energy for solute depletion could be obtained from AEM profiles taken across grain boundaries. As described previously, following the "collector-plate" mechanism suggested by Aaron and Aaronson (1968), at temperatures below 0.8 T_m (T_m = melting point of alloy) in the absence of matrix precipitation, the rate controlling step in the growth of a grain boundary precipitate from a supersaturated solid solution is the volume diffusion of the solute to the grain boundary. The process is shown schematically on the following page together with the associated solute concentration profile in the adjoining matrix. As solute diffusion occurs rapidly along the grain boundary, the grain boundary composition can be taken as being constant, and approximately equal to that predicted by the equilibrium diagram (the terminal solid solubility in the matrix). Using the Grube analysis, the composition of the matrix, C_x, at any point in the profile is given as

TABLE III

Activation Energy Studies in the Al-Ag System

Investigators	Activation Energy, Q (kcals/mole)	Experimental Technique
Beerwald (1939)	32.6	Diffusion Couples
Mehl et al. (1941)	38.5	Diffusion Couples
von Koster & Sperner (1953)	29.0 for Al-20 wt% Ag Theoretical expression: Q = 32600 - 560 at% Ag, 30.06 for Al-16 wt% Ag	Warm Hardening
Borelius & Larsson (1956)	Not reported for 4.5 at% Ag	Resistivity
Heumann & Dittrich (1957)	35.0	Interdiffusion
Baur & Gerold (1962)	22.5	Resistivity
Hren & Thomas (1963)	37.5 ± 4.0	Dissolution of γ' precipitates
Anand & Agarwala (1967)	29.0 $D_o = 0.21$	Ag^{110} residual activity in Al
Weaver & Brown (1958)	26.4 $D_o = 9$	Evaporated thin-films of Ag-Al, formation of Ag_2Al
Heumann & Bohmer (1968)	28.9 $D_o = 0.39$	Diffusion of Ag^{110} in Al

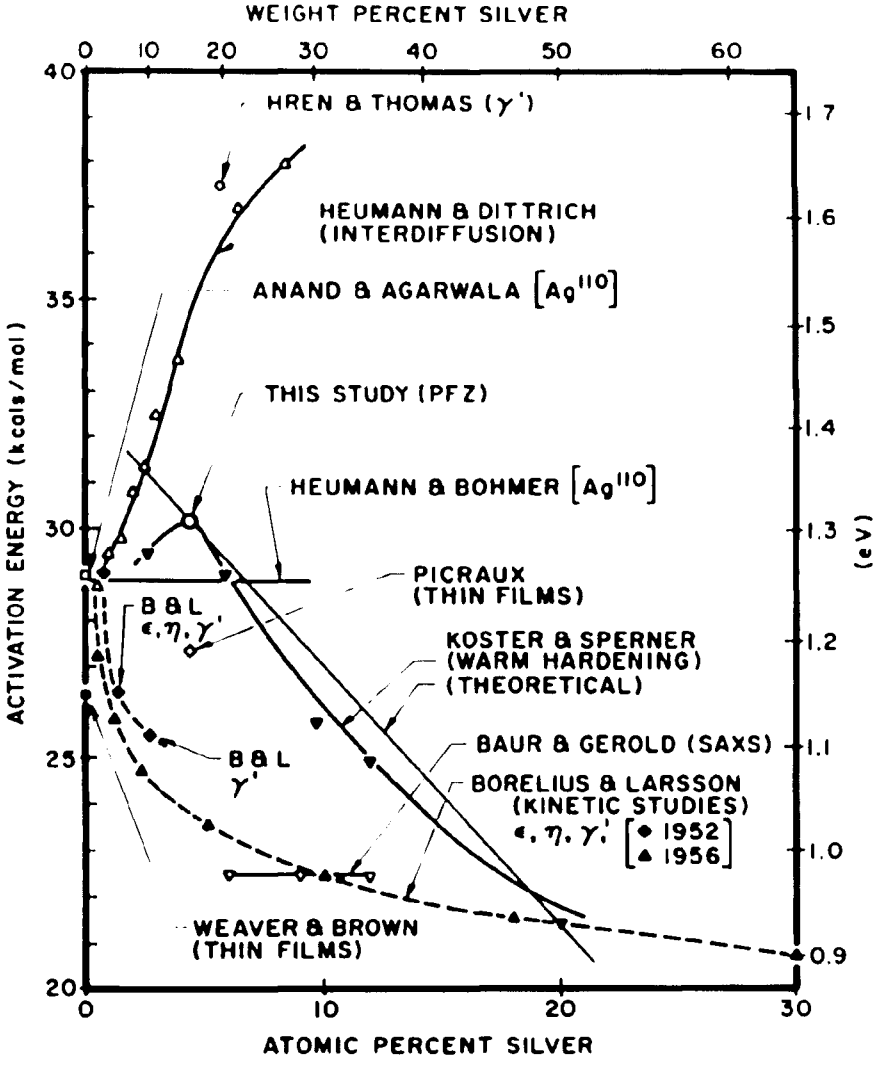

Fig. 3: Dependence of the activation energy on concentration. [After Hirano (1967)]

$$C_x = C_o + (C_1 - C_o) \text{ erf } \left[\frac{x}{2\sqrt{D_v t}}\right] \qquad (2)$$

where t = ageing time.

C_o = equilibrium solute concentration at the ageing temperature

C_1 = the bulk solute concentration.

D_v = volume diffusion coefficient of the solute.

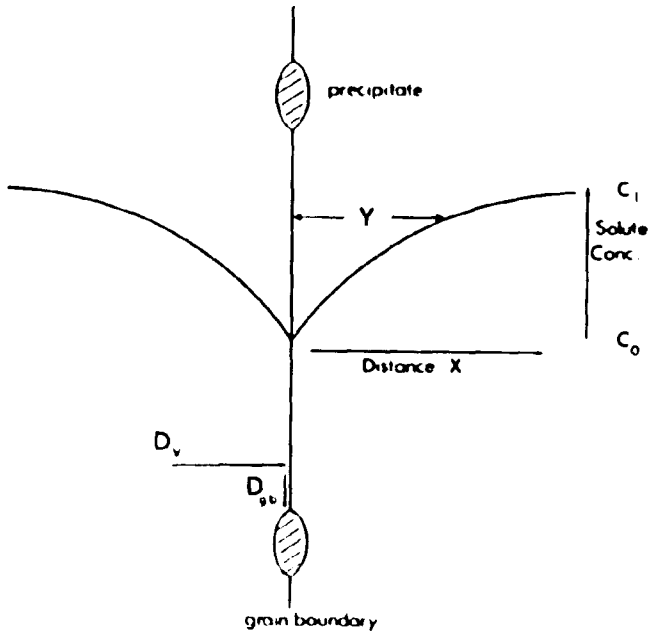

Schematic diagram of the processes occurring during growth of grain boundary allotriomorphs [from Doig and Edington, (1973)].

The width, Y, of the solute depletion region can be defined as,

$$Y = 2\sqrt{D_v t} \text{ when } \left[\frac{C_x - C_o}{C_1 - C_o}\right] = \text{erf } 1 \simeq 0.84 \qquad (3)$$

Thus the width of the solute depleted region, Y, is the distance

away from the grain boundary, at which the composition profile, C_x vs. X, yields a concentration ratio of 0.84. If specimens are evaluated at known times and at different temperatures, both the diffusion coefficient and activation energy may be calculated. The Doig and Edington (1973) study was made on both aged Al-Cu and Al-Mg samples containing well-defined PFZ but without matrix precipitates. The difficulties involved in their approach are:

(a) the concentration profile must first be measured and the values of the solute concentrations in equation (2) must be accurately known (from the phase diagram equilibrium solvus data and AEM measurements) in order to determine Y. Therefore a large number of concentration profiles are required in order to obtain a Y vs. $\sqrt{t}$ relationship at a given ageing temperature so that D_{Ag} and Q may be determined. Moreover, C_o may not be accurately known.

(b) Experimentally, conventionally aged alloys could contain matrix precipitates, and therefore it is possible that the value for Y at which $\frac{C_x - C_o}{C_1 - C_o} \simeq 0.84$ (equation (3)) could occur in the region where Guinier-Preston zones are observed. Therefore the value measured for C_x might be erroneous due to the presence of precipitates.

As the ageing temperatures used in the present investigation were below the Guinier-Preston zone solvus limits for the Al-16 wt% Ag alloy there was copious matrix precipitation present. An estimate of the diffusion coefficient of Ag in Al, D_{Ag} can therefore be obtained by equating the half-width (Y) of the solute depleted WPFZ to the characteristic diffusion distance, where

$$Y = 2\sqrt{D_{Ag} \cdot t} \qquad (4)$$

As there is no available diffusion data at low temperatures, it is first necessary to obtain extrapolated values of D_{Ag} at the ageing temperatures of this investigation, 160°C, 250°C and 325°C, so that a comparison with experimental results can be made. A plot of $\ell n\ D$ vs. $1/T$, where T is the absolute ageing temperature would be useful to obtain a value for the activation energy for diffusion of Ag in Al.

Using the approach suggested by Hren and Thomas (1963) for extrapolation, i.e., since

$$\ell n\ D = \ell n\ D_o - \frac{Q}{RT}, \qquad (5)$$

then at two different temperatures, T_1 and T_2,

$$\ell n\ D_{T_1} - \ell n\ D_{T_2} = \frac{Q}{R}\left(\frac{1}{T_2} - \frac{1}{T_1}\right). \qquad (6)$$

Table IV shows the values of D_{Ag} obtained by extrapolation, using the above equation from the two sets of higher temperature diffusion data given by Hren and Thomas (1963) and Heumann and Dittrich (1957). These studies were chosen because they were performed on specimens nearest in composition to the alloy (Al-16 wt% Ag) used in this investigation while they represent two different experimental techniques.

TABLE IV

Values of D_{Ag} Obtained from Extrapolation of High-Temperature Results Using Eqn. 6

Workers	Activation Energy, Q (kcals/mole)	Value of D_{Ag} at T		Extrapolated Values of D_{Ag}	
		T	$D_{Ag}(cm^2/s)$	T	$D_{Ag}(cm^2/s)$
Hren & Thomas (1963)[1]	37.5 ± 4	450°C	4×10^{-11}	325°C	1.7×10^{-13}
				250°C	1.8×10^{-15}
				160°C	1.0×10^{-18}
Heumann & Dittrich (1957)[2]	35.0 (interpolated)	500°C	0.7×10^{-9}	325°C	8.98×10^{-13}
				250°C	1.32×10^{-14}
				160°C	1.2×10^{-17}

[1]Hren & Thomas: data obtained from D_{Ag} measurements on dissolution of γ' precipitates in Al-20 wt% Ag alloy.

[2]Heumann & Dittrich: data obtained from diffusion-couple experiments for Al-15.85 Ag alloy.

III. EXPERIMENTAL PROCEDURES

A. Synopsis

Since a major aspect of this study was to follow the treatments carried out by Clark (1964) in his work on PFZ in Al-Ag alloys, similar alloy compositions and heat-treatments were chosen, and the work repeated. As Clark makes no statements about the solution treatment temperature, quenching procedure (direct quenched to ageing temperature or otherwise), or quenching medium, time spent at room temperature before ageing; these parameters were chosen and, as far as possible, kept identical.

Formation of PFZ would also be studied at an intermediate temperature of 250°C (523 K), which would supplement this investigation with an additional series of profiles across the PFZ at an intermediate temperature. Moreover, an intermediate temperature value would also help in determining the solid solubility and metastable Guinier-Preston zone solvus limits and therefore extend the phase diagram below 325°C (598 K). The solute depletion profile (if any) would be used to obtain a value of D_{Ag} at 250°C (523 K) and hence the activation energy of solute diffusion, Q, could also be measured.

B. Alloy Preparation and Homogenization

The alloys used in this investigation were obtained from three different sources. The first was an Al-16 wt% Ag alloy obtained in the form of cold rolled strips of 0.2-0.3 mm thickness (courtesy of Prof. D. B. Williams, Lehigh University). The second alloy composition was prepared at Lehigh from zone-refined

(99.9995% purity) Al and spectroscopically pure Ag (99.995 + purity). The Al was received in the form of 13 mm x 13 mm slugs and the Ag was in powder form. Each constituent was weighed carefully and the charge was placed in a 2 ml high purity alumina crucible (Coors Porcelain, Golden, Colorado). The alloy was melted in a high frequency induction furnace (Lepel H. F. Generator) at 60 Hz in a reducing atmosphere of Ar + H_2 (20:1 by volume) within a container of fused silica (National Scientific Company, Quakertown, Pa.) as shown in Fig. 4. A boron nitride block was used to serve as a support for the alumina crucible. The silica container was purged with the reducing gas atmosphere for several minutes. A moderate heating rate was employed to avoid thermal shock and cracking of the crucible and the alloy was kept molten for several minutes to allow complete mixing. The melt was slowly cooled to avoid porosity and allowed to reach room temperature before removing the crucible from the reducing atmosphere in the container.

After casting, surface oxides were removed and the samples were encapsulated together with an "oxygen-getter" Ta foil in evacuated SiO_2 tubes. The homogenization treatment was carried out for a period of 100 hours at 550°C (823 K) in a furnace previously stabilized at that temperature (accurate to $\pm$ 1°C). After the homogenization heat treatment, the samples were quenched in water by crushing the glass tube. Any surface oxide was removed and the alloy cold rolled to about 0.5-1 mm thickness, with intermediate anneals. A third alloy lot was prepared from the same

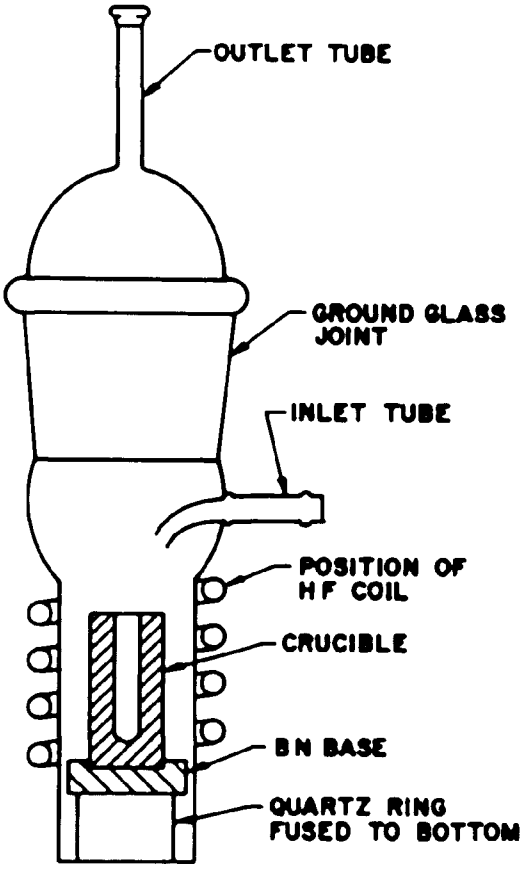

Fig. 4: Alloy melting apparatus.
[From Romig (1979)]

high purity Al and Ag described above, but was sent to Alfa Ventron Inc., Danvers, MA. and was vacuum induction melted and then cast in chill molds. Since this material was obtained towards the end of the present work, it was used only for some of the deformation studies.

After a homogenization treatment of 4 to 5 hours, the composition of the alloys was determined using the EPMA as Al + 15.73 $\pm$ 0.13 wt% (4.46 $\pm$ 0.03 at%) for the alloy obtained from Prof. Williams, Al + 16 wt% (4.54 at%) Ag for the Alfa Ventron casting and Al + 9.395 wt% (2.53 at%) Ag for the ingot cast at Lehigh. The Al-9.395 wt% Ag alloy was used for "k-factor" determination. For simplicity, the alloys will be referred to as Al-16 wt% Ag and Al-9.5 wt% Ag alloys.

Discs, three millimeters in diameter were punched out of the cold rolled strips to be used for all heat-treatments and deformation experiments and for subsequent TEM/AEM investigations.

C. Heat Treatments

All heat-treatments were carried out directly on Al-16 wt% Ag alloy discs 3 mm in diameter punched out from the cold-rolled material. These discs were encapsulated in evacuated fused silica tubes and solution-treated for 1 hr. at 550^{o}C (823 K). The specimens were quenched into water at room temperature by crushing the silica tubes with a pair of tongs. A room temperature ageing treatment of 4-5 mins. was unavoidable because the specimens had to be dried and wrapped securely in Al-foil for isothermal ageing.

Isothermal ageing was carried out for various times at 160^{o}C

(433 K), 250°C (523 K), and 325°C (598 K) after wrapping the specimens securely in Al-foil. After the ageing treatment the samples were quenched into water and then stored continuously in liquid N_2 for further specimen preparation. The isothermal heat treatments were carried out in a platinum wire-wound furnace. Temperatures were monitored using a calibrated chromel-alumel thermocouple placed next to the evaculated tubes or foils. It was observed that it would take approximately 1-2 mins. for the samples to attain the required temperature. Details of any other heat treatments carried out will be described, when necessary, in their appropriate contexts. All temperatures were held within $\pm$ 0.5°C and reported temperatures are accurate to $\pm$ 1°C. Figure 5 shows a schematic of the heat treatments carried out for the Al-16 wt% Ag alloy used in this investigation.

D. Deformation Experiments

Some of the samples that were solution treated and aged for 50 hrs. at 160°C were then deformed about 10% or 40% at room temperature and subsequently reaged at 160°C for 2 and 3 hours respectively to determine if heterogeneous nucleation of precipitates could be induced in the PFZ. A similar treatment was carried out by Raghavan (1980) for Al-Zn-Mg samples and precipitation within the original PFZ, due to the second thermo-mechanical treatment was reported.

E. Thin-foil Preparation for TEM/AEM

Self-supporting 3 mm diameter discs were used in all TEM/AEM studies performed on the alloy. After the appropriate heat treat-

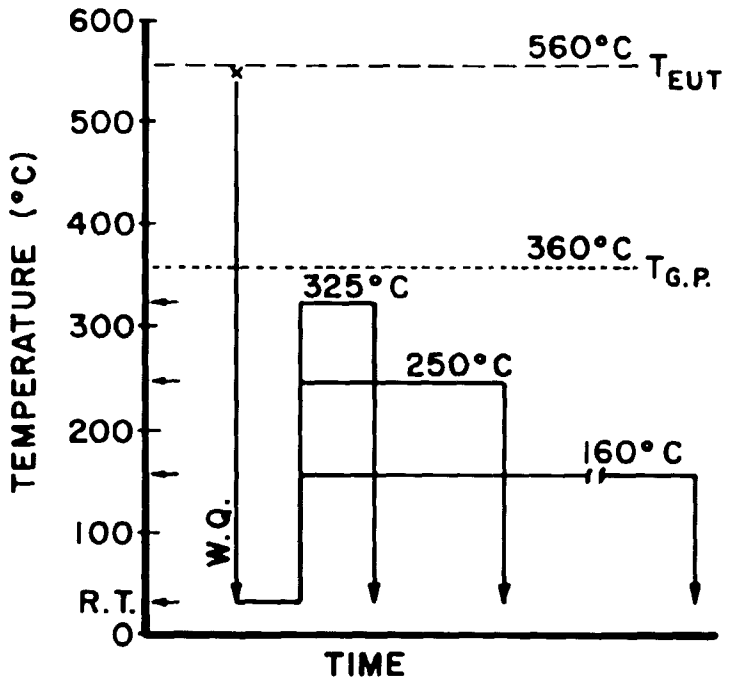

Fig. 5: Schematic diagram of heat treatment procedures for specimens used in this investigation. Solution treatment for 1 hr. + water quench (W.Q.) to room temperature (R.T.) + room temperature age for 4 to 5 minutes + isothermal ageing at 160°C, 250°C, and 325°C for various times. T_{EUT}: eutectic temperature; $T_{G.P.}$: Guinier-Preston zone solvus temperature.

ments, the samples were preserved in liquid N_2 before any further specimen preparation. Any oxide residue on the samples was removed by grinding it off manually on 600 grit SiC paper and the foil was reduced to a thickness of about 0.08 to 0.1 mm (2 to 4 mils).

The samples were thinned for TEM/AEM examination using a Fischionne twin-jet electropolisher (TJE). The electrolyte contained 10% concentrated HNO_3 (69% assay) + methanol (Fisher Scientific grade A-412). A potential of 30-40 volts was used and the electrolyte was cooled to -45°C (228 K) with liquid N_2. Sometimes, especially if the conditions stated above were not right, or the electrolyte was reused there was evidence for Ag plating out on the specimen surface, presumably from within the matrix. Consequently, a benzene cleansing agent [Leidheiser, (1980)] was tried, and this usually yielded good foils. It was found that fresh electrolyte after every polishing operation gave the best results and so, this practice was followed while preparing samples with the TJE. Figure 9(b) shows the contamination effect observed on a thin-foil of one of the samples. The thin-foils were later cleaned in a Commonwealth Scientific IMMA II ion-beam thinner or a Technics ion-beam thinner for a period of 15-20 mins. before TEM/AEM studies, at ~ 6 to 7 kV with the foil tilted at ~ 13° from the horizontal. This tends to remove any residue deposited during the TJE operation. Samples for "k-factor" determination were prepared in a different manner; the method of preparation for these specimens will be described in a later section.

F. Analytical AEM Concepts

The general principles describing the use of AEM as a technique for obtaining quantitative x-ray (microanalytical) information have been well documented; see Goldstein and Williams (1977), Goldstein et al. (1977), Romig (1979) and Goldstein (1979). Recently TEM, AEM and SEM techniques have been reviewed and compared by Williams (1980), and instrumental considerations and applications of AEM to materials science have been reviewed by Zaluzec (1979). In brief, a standardless ratio technique is usually applied to relate x-ray intensity ratios to elemental composition ratios. Consideration must be given to effects of absorption, fluorescence and spurious x-ray generation which may alter the x-ray intensities being detected (Goldstein, 1979). These factors are considered in greater detail below.

(i) The standardless-ratio technique

The basis of most AEM microanalytical procedures is the standardless ratio technique of Lorimer et al. (1971) and popularly known as the Cliff-Lorimer equation (1972). The method involves measuring the x-ray intensity ratio I_A/I_B of two elements A and B in a thin-foil simultaneously. This intensity ratio can be related directly to the ratio of their mass concentrations C_A/C_B such that

$$\frac{C_A}{C_B} = k_{AB} \frac{I_A}{I_B} \qquad (7)$$

The constant, k_{AB}, is commonly called the "k-factor", and varies with the operating voltage, and also the preferential absorption of

x-rays generated from one of the elements by another within the thin foil being analyzed. If one assumes that the analyzed film is infinitely thin, the effects of x-ray absorption and fluorescence can be neglected, and the generated x-ray intensity and the x-ray intensity leaving the specimen are identical. This assumption is known as the "thin-film criterion." Once system and specimen induced x-rays are eliminated, the x-ray spectra obtained by the energy dispersive x-ray detector can be used to give a quantitative chemical analysis. This method is often referred to as the standardless ratio method, in that pure bulk standards are not needed for analysis, unlike for the EPMA.

(ii) Determination of k_{Al-Ag}

The constant k_{AB} can be determined from thin-film standards or calculated theoretically from expressions that consider x-ray production in thin films and the characteristics of the EDS detector. In practice, most k-values are obtained from a set of well-characterized mineral standards of known composition or from single-phase homogenized alloys whose composition is accurately determined using other techniques, such as the EPMA. As no two microscopes are identical in terms of detector geometry and efficiency or contamination characteristics, k_{AB} would differ from one instrument to another. Hence it is advisable that the k-factor be determined accurately for the individual system of interest and that the microscope be used under similar conditions for analysis of the unknowns and the standard. As the k-factor is independent of the composition of the alloy, a given value of k_{AB}

can be utilized for a range of compositions of the binary alloy A-B, provided that absorption does not occur. The "k-factor" for the Al-Ag alloys under investigation was determined on the Philips EM400T using an EDAX 9100 energy dispersive analyzer. As the Al-9.395 wt% Ag alloy was prepared in the laboratory, and its composition accurately known, it was decided to utilize this alloy to determine the k-factor (k_{Al-Ag}) for the Cliff-Lorimer equation. Consequently, a 3 mm disc was punched out of the same area of the alloy analyzed for homogeneity using the EPMA. The foil was ion-beam thinned and subsequent TEM examination showed the structure to be featureless except for dislocations and similar defects observed in Fig. 9(a). The foil was then analyzed for k-factor determination using the EDAX SWTHIN program using full shell integrated counts for the Al-K and the Ag-L lines. Counting time was 100 seconds and a spot size of 10 nm was used. A total of 42 readings were taken at random points throughout the area of the sample. As no absorption correction was required (for the thickness of the foil used), it was not necessary to determine the thickness of the sample at each point. All intensities were normalized with respect to Al as base, and the concentration ratios of the elements were used to obtain appropriate values of k_{Al-Ag}.

Relative errors in the determination of the k-factors were calculated using the methods suggested by Romig (1979), following Goldstein (1975). The calculated error in k_{Al-Ag} can be estimated as:

$$\% \text{ Error} = \left[\frac{t_{99}^{n-1}}{\sqrt{n}} \cdot \sigma / k_{avg} \right] \times 100 \qquad (8)$$

where t_{99}^{n-1} is the student-t value for n readings of a 99% confidence level, σ is the standard deviation for n readings and k_{avg} is the average k_{Al-Ag} value. Taking the value of $t_{99}^{41} \simeq 2.7$ from statistical tables, TI-55 (1980), the value of k_{Al-Ag} at a 99% confidence level obtained was:

$$k_{Al-Ag} = 0.7269 \pm 0.0313.$$

Recently Wood et al.(1981) have obtained a set of k-factors on the Lehigh EM400T and an independent investigation by Wood (1981) on an Al-Ag alloy of the same composition, showed

$$k_{Al-Ag} = 0.724 \pm 0.007$$

at a 95% confidence level. As the value of k_{Al-Ag} does not vary with composition of the alloy, and as no absorption correction was necessary for the Al-16 wt% Ag alloy (see below), a value of $k_{Al-Ag} = 0.73$ was used for all AEM analyses.

(iii) Thin film criterion

It is essential while obtaining quantitative AEM data on unknown samples that the specimen meets the 'thin-film criterion', so that effects of absorption and fluorescence can be neglected. However, if this is not the case then a correction factor has to be applied to the experimentally obtained value of k_{AB}, as suggested by Goldstein et al. (1977). It is essential, therefore, for the experimenter to calculate the film thickness which would just violate the thin-film criterion. The criterion put forth by Gold-

stein et al. (1977) is that for any set of two elements, A and B, the absolute value of

$$|X_B - X_A| \cdot \frac{\rho t}{2} < 0.1 \qquad (9)$$

or an absorption correction is necessary. The term X_A is equal to $\left(\frac{\mu}{\rho}\right)^A_{spec} \cdot \text{cosec}\ \alpha$, where $\left(\frac{\mu}{\rho}\right)^A_{spec}$ is the mass absorption coefficient for the characteristic x-ray of element A in the specimen composed of elements A and B, and α is the angle between the specimen and the energy-dispersive x-ray detector, i.e., the take-off angle. The density ρ for the alloy is calculated from the relation,

$$\frac{1}{\rho} = \sum \frac{C_i}{\rho_i} \qquad (10)$$

where C_i and ρ_i are the mass concentrations and densities for the elements in the thin film.

Values of the mass-absorption coefficients were obtained from Heinrich (1966). Using a take-off angle $\alpha = 20^o$ for the Philips EM400T, and the formula given by Cullity (1978) to calculate the mass absorption coefficients of Al and Ag in the specimen:

(a) For the Al-9.395 wt% Ag alloy

$$\left(\mu/\rho\right)^{Al}_{spec} = \frac{C_{Al}}{100} \cdot \left[\mu/\rho\right]^{Al}_{Al} + \frac{C_{Ag}}{100} \left[\mu/\rho\right]^{Al}_{Ag}$$

$$= \frac{90.605}{100} \times 385.7 + \frac{9.395}{100} \times 3193$$

$$= 649.446.$$

$$\left(\mu/\rho\right)^{Ag}_{spec} = \frac{C_{Ag}}{100}\left[\mu/\rho\right]^{Ag}_{Ag} + \frac{C_{Al}}{100}\left[\mu/\rho\right]^{Ag}_{Al}$$

$$= \frac{9.395}{100} \times 521.9 + \frac{90.605}{100} \times 779.2$$

$$= 755.0267.$$

also,

$$\left[\frac{1}{\rho}\right]_{alloy} = \left[\frac{C_{Al}}{\rho_{Al}} + \frac{C_{Ag}}{\rho_{Ag}}\right]\frac{1}{100}$$

$$= \left[\frac{90.605}{2.698} + \frac{9.395}{10.49}\right] \times \frac{1}{100}$$

$$\therefore \quad \rho_{alloy} = 2.9004 \quad gms/cm^2.$$

$$\therefore \quad X_A = 755.0267 \times \text{cosec } 20^\circ = 2207.5504.$$

$$\text{and} \quad X_B = 649.446 \times \text{cosec } 20^\circ = 1898.8531$$

Using the thin-film criterion,

$$|X_A - X_B| \; \rho\frac{t}{2} < 0.1$$

and substituting the above values for X_A, X_B, and ρ, to obtain the value of the thickness beyond which an absorption correction is necessary,

$$t < 22{,}338\text{A}^\circ. \quad (\sim 2240 \text{ nm})$$

(b) Similarly for the Al-16 wt% Ag alloy, it can be shown that

$$\rho_{alloy} = 3.062$$

$$X_A = 2441.0843$$

$$\text{and } X_B = 2157.7676$$

so that $t \lesssim 2300$ nm. The values of thicknesses of thin foils obtained above for both alloy compositions indicate that absorption is not a problem in the alloys chosen for study. As these thick-

nesses represent specimens which would not be "electron transparent" at 120 kV, no further consideration is given to a correction factor for such absorption effects.

(iv) Fluorescence correction

Although it is often assumed that effects of fluorescence can be neglected in thin-foils, unlike the situation for bulk samples, Philibert and Tixier (1968) have shown that fluorescence does occur in thin-foils depending upon the values of the mass absorption coefficients, and a number of other parameters. Similar observations were made by Nockolds et al. (1980). It was decided, therefore, that effects of Ag fluorescing Al may occur and should be checked for. As a rough check for the maximum effect expected in a bulk sample, the ZAF correction program was run on the ARL microprobe at Lehigh for an alloy content of Al-16 wt% Ag for the voltage used in the Philips EM400T. The correction factors were 0.997 for Al and 1.000 for Ag, thus indicating that fluorescence corrections need not be applied.

The Al-16 wt% Ag alloy, chosen for this investigation, is an ideal alloy for AEM microanalysis, as effects of absorption and fluorescence can be neglected and can be considered to meet the Goldstein "thin-film criterion" under all operating conditions.

(v) Spatial resolution and beam broadening

A major advantage of using AEM over the EPMA is the enhanced spatial resolution made available by the AEM technique. As high accelerating voltages and thin specimens are used, minimal spreading of the focussed electron beam occurs. Therefore a very

small x-ray source is obtained, almost equal to that of the beam diameter, commonly less than 10 to 50 nm for very thin specimens. Attendant advantages of using thin foils are that effects of fluorescence and absorption can often be neglected, allowing relatively simple procedures for obtaining quantitative analyses of samples. Thus AEM x-ray microanalysis can be utilized in obtaining interphase compositions of adjoining phases, establish the presence of elements segregated or, or very close to, grain boundaries and measure the composition of very small particles and precipitates. As the electron beam diameter can be reduced to less than 5 nm in size, one might expect to obtain microanalytical information at this level of spatial resolution. However, even in thin films electrons are elastically scattered and the regions from which x-rays are generated are often much larger than the beam diameter. Figure 6 shows the interaction of the electron beam with a thin foil and a bulk sample. The severe limitation of the EPMA is immediately highlighted by the limitations in spatial resolution and it can be shown that it is impossible to accurately determine the composition of an area of submicron dimensions. Using the expression developed by Andersen and Hasler (1965) for the x-ray range and therefore the spatial resolution, as suggested by Goldstein (1975) for the matrix, Al

$$R(x) = \frac{0.064}{\rho_{Al}} (E_o^{1.68} - E_c^{1.68}) \qquad (11)$$

For an operating voltage E_o, of 20 kV, and for the K_α line of Al, E_c = 1.56 keV, with its density as 2.698 gms/cm^3, the range of

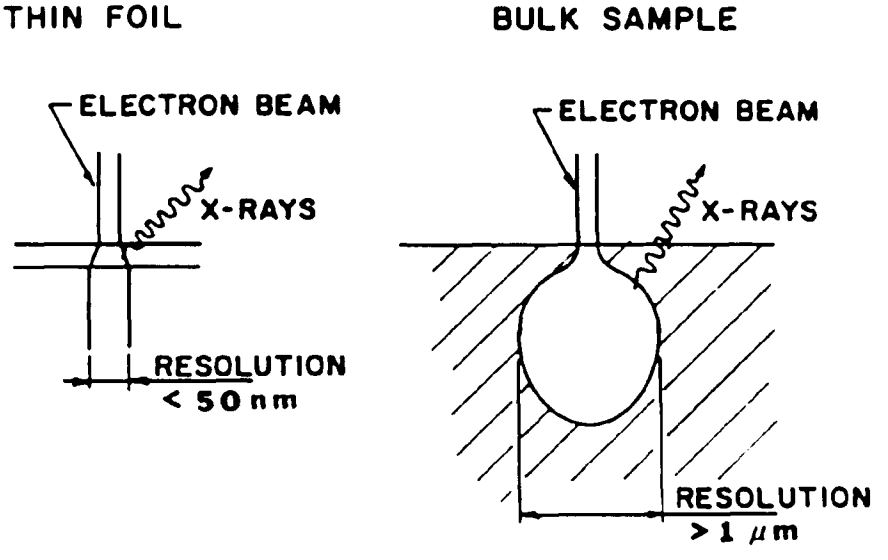

Fig. 6: Schematic depicting electron beam interactions in thin films and bulk samples. [After Romig (1979)]

production of x-rays is calculated to be 3.59 μm. To define the x-ray source size or spatial resolution, one can assume that the lateral x-ray production range is the same as R(x), the x-ray range. This assumes that the diameter of the electron beam impinging the specimen is vanishingly small. In actual practice, the beam diameter is finite ($\sim$ 0.5 μm) and is to be added to the value of R(x) obtained above. Similar calculations can be made for Ag.

The spatial resolution for chemical analysis in a thin foil can be obtained using the expression suggested by Goldstein et al. (1977), and the effects of beam broadening (b) can be calculated. In this treatment it is assumed that electron scattering occurs at the center of the thin foil. Figure 7 shows the model used to calculate b in a thin film of thickness t due to a single scattering event through an angle φ.

The equation which relates beam broadening b to the operating voltage E_o and t is,

$$b = 6.25 \times 10^5 \frac{Z}{E_o}\left(\frac{\rho}{A}\right)^{\frac{1}{2}} t^{3/2} \qquad (12)$$

where b and t are in cms, E_o is the operating voltage and Z, A and ρ are the atomic number, atomic weight and density (in gms/cm^3) of the material of the thin foil. Thus for an operating voltage of 120 kV

$$b \text{ for Al} = 21.41\ t^{3/2} \quad \text{and}$$

$$b \text{ for Ag} = 76.33\ t^{3/2}.$$

where b and t are in cms.

For a typical thin foil, i.e., 200 nm of Al or Ag observed at 120 kV, the predicted beam spreading would be ~19 nm and ~69 nm respectively. In reality, the beam will not be a point source, and will have a finite diameter. As a first approximation, R can be determined by adding the electron beam diameter, d, to the amount of beam broadening, b, predicted by the above equation, so that the situation shown in Fig. 7 should be modified to include the effect of d, and depicted as in Fig. 8. In order to obtain values of b in Al-Ag alloy studied, the weighted average values of Z, A and ρ were selected and a simple computer program was written to calculate values of b, having obtained t from the separation of contamination spots at the top and bottom of the thin-foil. For the Al-16 wt% Ag alloy, observed at 120 kV

$$Z_{avg} = Z_{Al} \times \text{wt.fraction of Al} + Z_{Ag} \times \text{wt.fraction of Ag}$$

$$= 13 \times 0.84 + 40 \times 0.16$$

$$= 18.44.$$

$$A_{avg} = A_{Al} \times \text{wt.fraction Al} + A_{Ag} \times \text{wt.fraction of Ag}$$

$$= 26.98 \times 0.84 + 107.87 \times 0.16$$

$$= 39.9224.$$

$$\rho_{avg} = 3.0619$$

$$b_{alloy} = 6.25 \times 10^5 \times \frac{18.44}{120 \times 10^3} \times \left(\frac{3.0619}{39.9226}\right)^{\frac{1}{2}} t^{3/2}$$

$$b_{alloy} = 26.598\ t^{3/2}$$

where b and t are in cm.

Thus for a 200 nm thick specimen, a 'b' value of ~24 nm is obtained.

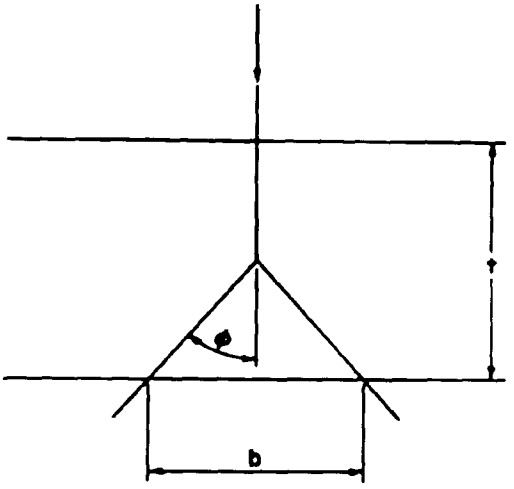

Beam Spreading in Thin Foils

Fig. 7: Schematic for electron beam broadening b in a thin film of thickness t. [From Romig (1979)]

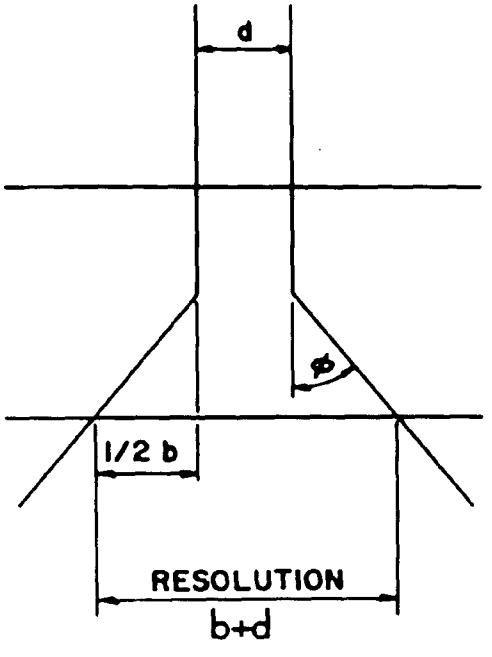

Thin Foil Spatial Resolution

Fig. 8: Simple schematic for x-ray spatial resolution in AEM. [From Romig (1979)]

(vi) X-ray microanalyses-concentration profiles

Solute concentration profiles across grain boundary PFZ were obtained using the Philips EM400T AEM and EDAX 9100 energy-dispersive x-ray analyzer in solution treated and aged Al-16 wt% Ag alloy thin-foils. It is important that the foils be "cleaned" in an ion-beam thinner before AEM examination. In most cases, care was taken to orient the grain boundary PFZ perpendicular to the electron beam, and to keep the foil at low tilt angles ($< 20^{o}$). Reasons for such precautions are discussed later. A 100 second counting time was used for each analysis point. The microscope was operated at an accelerating voltage of 120 kV and the electron beam diameter (spot size) varied, depending upon the resolution desired, between 5 nm and 10 nm. All x-ray data were converted to weight percentage using the Cliff-Lorimer equation and a k-factor value of 0.73. Sample thicknesses were measured using contamination marks or other techniques, and ranged from 100-200 nm. Hence no absorption correction was necessary to compute the absolute elemental concentrations.

Microanalysis was conducted in regions across a grain boundary away from grain boundary precipitates through the length of the WPFZ and occasionally across the GPFZ. The electron beam was moved in 50 nm to 200 nm steps across the PFZ, usually at an angle ($> 10^{o}$) to the grain boundary, so as to maximize the number of readings in the WPFZ and obtain "smooth" variations in Ag content.

Concentration profiles for the foils examined were obtained by plotting the Ag concentration (wt%) against the distance

(in nm) from the grain boundary and errors associated with microanalysis determined (see below). Profiles in overaged alloys, such as alloys with no conspicious WPFZ, as a result of excessive solute depletion by γ' and γ precipitates within the grain and at the grain boundary, were rejected. Also, profiles where contamination marks seemed to overlap were discarded. Errors involved in the determination of the Ag concentration and the spatial resolution were calculated for each point of analysis using the methods of Romig and Goldstein (1980).

As x-ray counting statistics obey Gaussian behavior during AEM operations, the relative error involved with N accumulated counts during each analysis would be $\sigma = \sqrt{N}$ [see Cullity, (1978), p. 220]. The relative standard deviation to be expected in a single measurement of N pulses is

$$\text{Relative } \sigma = \frac{\sqrt{N}}{N} \times 100.$$

At a 3σ confidence interval, the relative error would be

$$\text{Relative Error} = \frac{3\sqrt{N}}{N} \times 100.$$

As the Cliff-Lorimer equation utilizes the x-ray intensity ratio $\frac{I_{Al}}{I_{Ag}}$, the relative error involved in any microanalytical determination is the sum of the errors in I_{Al} and I_{Ag}. Values for the relative errors in I_{Al} and I_{Ag} were calculated from the total accumulated counts using the above equation in each case.

Another source of error is the uncertainty in the value of $k_{Al\text{-}Ag}$ (see this section, part ii) and a relative error of 4.3% was always added to the relative errors in I_{Al} and I_{Ag}. The

vertical error bars on the profiles thus indicate the sum of the errors in I_{Al}, I_{Ag} and $k_{Al\text{-}Ag}$.

In order to determine the extent of the x-ray generation region caused by the electron beam, i.e., the spatial resolution, the beam broadening equation (12) was used to determine b (see this section part (v)) having previously measured the foil thickness. The value of the probe size, d, was added to b. The horizontal error bars in each profile have been determined in this way. A value of < 50 nm for (b + d) was obtained for most of the profiles measured.

IV. RESULTS

A. Microstructures (TEM/AEM Investigations)

1. Structure of the supersaturated solid solution.

Figure 9(a) shows the structure of the Al-9 wt% Ag alloy which had been solution heated at 550°C (823 K) for 4 hrs. and quenched in water at room temperature. Complex dislocation networks are seen and there is no evidence for precipitation, even at the strongly diffracting thickness fringes (TF) near the edge of the foil (E). This sample was used to determine the k-factor for AEM results. Figure 9(b) shows another thin foil of the same alloy obtained by twin-jet electropolishing rather than by ion-beam thinning. As the foil was twin-jet electropolished in an electrolyte which had been used two or three times earlier, there was excessive contamination (C) of the foil. AEM investigation of these black particles showed them to be elemental--Ag or Al-Ag compounds. Methods to rectify such contamination have already been discussed.

2. Structure of aged alloys

The following sections describe the microstructures of thin foils of Al-16% Ag alloy that had been solution treated for an hour at 550°C (823 K) and quenched in water at room temperature. They were subsequently aged at 160°C (433 K), 250°C (523 K) and 325°C (598 K) for various times. Heat treatments were chosen so as to obtain optimum widths of the WPFZ for TEM/AEM examination. The period between solution treatment and ageing was usually around 4 to 5 mins. unless otherwise stated. No ageing treatments were carried out on the Al-9% Ag alloy.

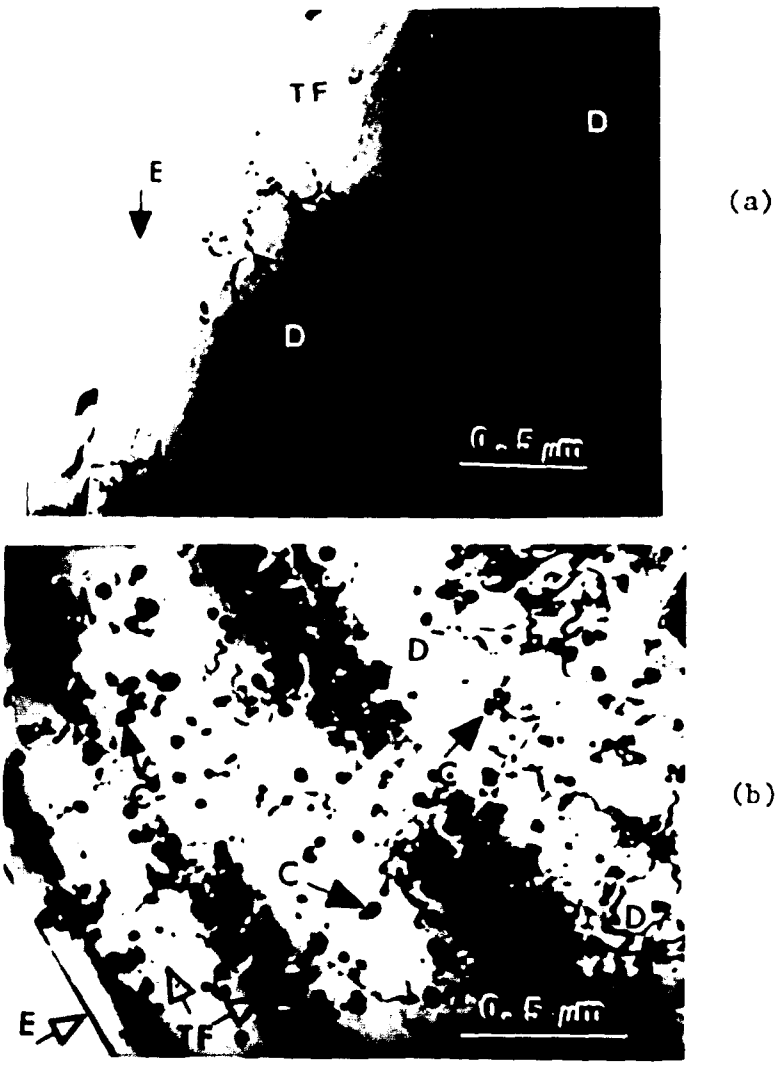

Fig. 9: (a) Al-9 wt% Ag alloy, solution treated at 550°C for 1 hr. and water quenched at room temperature and ion-beam thinned. No precipitation is seen in the microstructure even under strongly diffracting conditions such as within thickness fringes (TF) or at the edge of the foil (E). Complex dislocations (D) can be observed throughout the micrograph. (b) Same as (a) but specimen twin jet electropolished in "recycled electrolyte" caused contamination C.

i. Microstructures after ageing at 160°C (433 K)

Discs three millimeters in diameter were isothermally aged at 160°C for periods of time ranging from 4 hrs. to 87 hrs. Figure 10 shows a specimen that had been aged for 87 hrs. at this temperature. Copious precipitation of Guinier-Preston zones was observed in such samples throughout the matrix except in regions around the grain boundaries constituting the WPFZ. γ' precipitates were observed on dislocations and the figure shows the characteristic contrast (at F) exhibited by these precipitates, as described by Nicholson and Nutting (1961).

Specimens aged for shorter times (50 hrs.) showed much less γ' as seen in Figure 11 with attendant increase in the width of the GPFZ. The figure shows grain boundary γ precipitates and a wide (~ 2 μm) GPFZ. Notice the absence of γ' precipitates in areas to the right of the grain boundary near the edge of the foil (E), the GPFZ.

In these samples, it was commonly observed that there was considerable grain boundary movement, either to accommodate grain boundary allotriomorphs or due to the onset of discontinuous precipitation. This would result in asymmetric WPFZ along the grain boundary and, as shown later, an asymmetric solute concentration profile during AEM microanalysis. Figure 12 is one such example where the grain boundary has moved (solid arrows) from an original position (hollow arrows). Another example of an asymmetric WPFZ is seen in Figure 13. It was observed that such boundary movement would lead to a gradual size distribution of the

Fig. 10: γ' precipitates exhibiting characteristic fringe contrast at F. Guinier-Preston zones (GPZ) are seen in the matrix. C is specimen contamination. Sample aged at 160°C for 87 hours.

Fig. 11: Al-16 wt% Ag alloy aged at 160°C for 50 hrs. showing distinct WPFZ and GPFZ. Also seen are γ and γ' precipitates. See text for details.

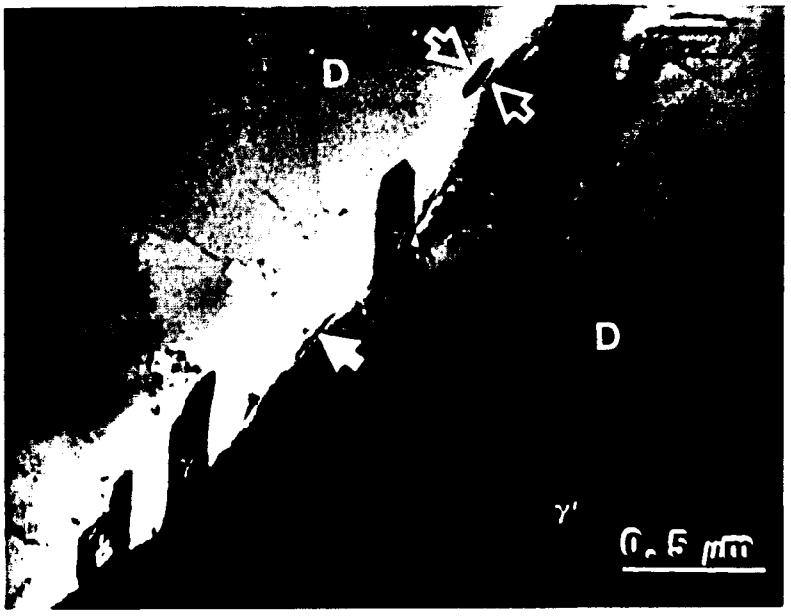

Fig. 12: Specimen aged at 160°C for 50 hrs. showing grain boundary movement to accommodate the grain boundary precipitate (γ) or account for the onset of the discontinuous precipitation reaction. Dislocations at D were probably introduced during the mechanical polishing of the sample and should not be confused with an "inherent" dislocation structure.

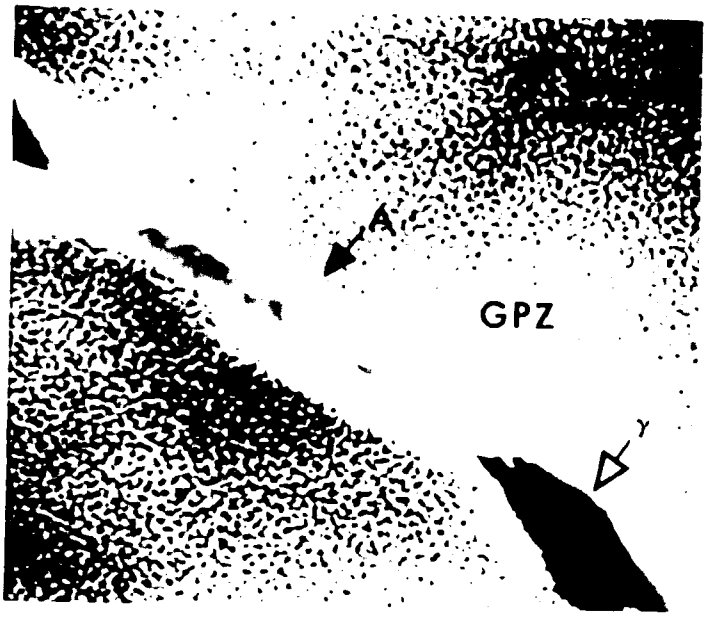

Fig. 13: An asymmetric WPFZ around a grain boundary. Note the nature of the WPFZ and size distribution of Guinier-Preston zones at B compared with region A. Corresponding AEM composition profile is Fig. 39. Aged 50 hrs. at 160°C.

Guinier-Preston zones, when looking away from the boundary towards the interior of the grain. Note the size distributions in the region around B, where the boundary has migrated, to that at A where there has been no movement of the boundary. Asymmetric WPFZ such as these also showed asymmetric solute profiles in AEM and non-uniform concentration gradients on either side of the grain boundary.

Figure 14 shows a group of γ' precipitates exhibiting characteristic plate-like structure, surrounded by spherical Guinier-Preston zones. The pointer shows a cross-section of a γ' precipitate which appears hexagonal. Figure 15(a) shows one such precipitate. Note the solute depleted region around the precipitate (SD) where the Guinier-Preston zones are absent. Figure 15(b) shows a γ' precipitate viewed perpendicular to the major plane of the precipitate.

After examination of specimens aged for shorter times at 160°C, it was decided that samples heat-treated for 50 hrs. at this temperature would be used for microanalysis. Figure 16 shows one such region where an AEM trace T was taken along the width of the GPFZ. The contamination spots serve as "tell-tale" marks which are useful to determine foil thickness and step-increment sizes during a set of readings. In order to profile across the entire GPFZ (1-2 μm at 160C/50 hrs.) with a reasonable number of readings, the step distance was increased and these were taken at low magnifications, typically 25,000X, in AEM. As the dimensions of the WPFZ are very small (40-80 nm in this case), the

Fig. 14: Specimen aged at 160°C for 50 hrs.; bright field image showing plate-like γ' precipitates surrounded by Guinier-Preston zones. The arrow points to a γ' precipitate running perpendicular to the plane of view.

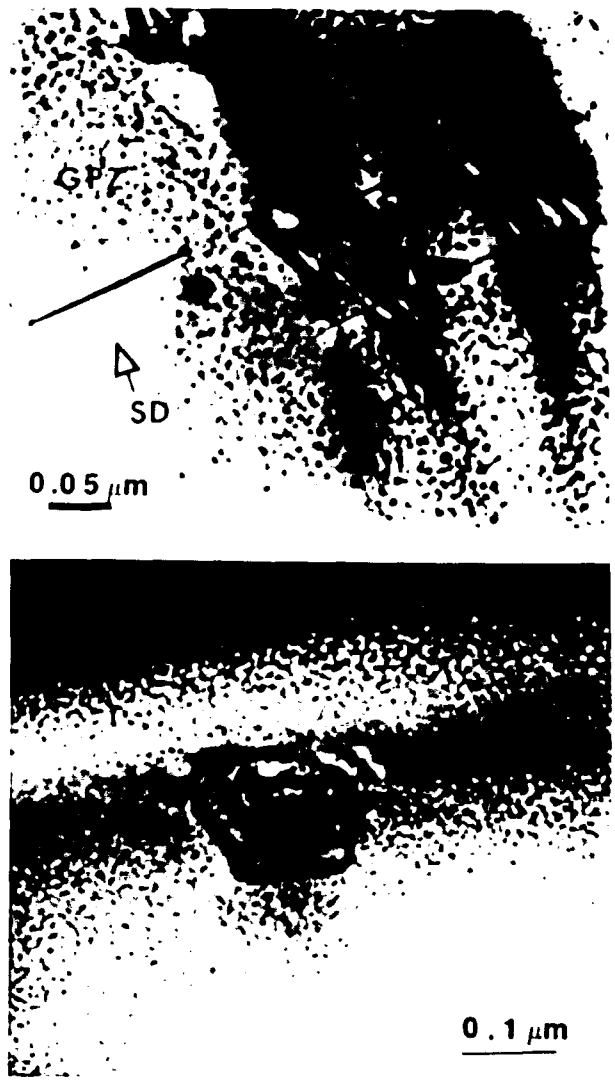

Fig. 15: (a) Specimen aged at 160°C for 50 hrs. showing a γ' precipitate. Note the absence of Guinier-Preston zones in areas such as SD where preferential dissolution of these zones has occurred to supply solute atoms to the γ' precipitates. (b) Same sample shows a γ' precipitate when observed perpendicular to its major plane.

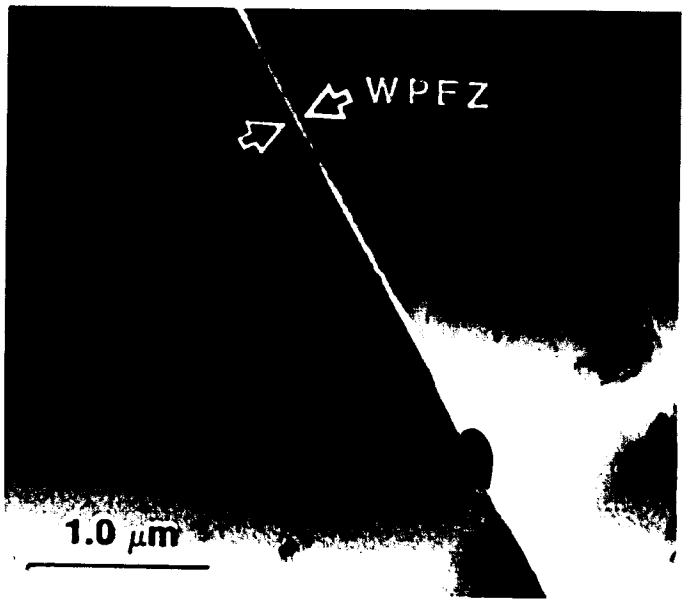

Fig. 16: Shows an AEM trace (T) across a GPFZ marked by the absence of γ' precipitates on either side of the grain boundary. Also seen is a narrow WPFZ and a γ precipitate at the grain boundary. Aged 50 hrs. at 160°C. Profile number 2896.

amount of information obtained at low magnifications is small, i.e. one single reading at the grain boundary. This is the case for Figure 16. Hence it was essential to use high magnifications (> 50,000X, typically 100,000X) in AEM, with smaller step sizes (50 nm) and smaller probe diameters (5 nm) to maximize the data from the WPFZ. Figure 17 shows an AEM micrograph of the same area as in Figure 13 and the dots show approximately the region where a trace was taken. As AEM micrographs lack the contrast offered by TEM images, no attempts were made to take AEM pictures during each analysis. This was justified as there exists a very good correlation between TEM and AEM images if the microscope is well-aligned.

ii. Microstructures after ageing at 250°C (598 K)

A similar program of optimization of WPFZ-widths was followed at 250°C by ageing for various times and examining the microstructure after each heat-treatment. Preliminary examination of foils, heat-treated for 1½ hrs. at this temperature showed a well-developed precipitate structure in the thin foils. Figure 18(a) shows a WPFZ surrounded by copious γ' and γ precipitates and Guinier-Preston zones, and Figure 18(b) shows an area in the interior of another grain. The γ' plates no longer exhibit the characteristic contrast effects seen at 160°C but have grown large so that simple distinct interfaces between the WPFZ and GPFZ are no longer seen. Streaks parallel to the <111> of the matrix are clearly seen in selected area diffraction patterns at this stage, see Figure 32(b). It is evident from Figure 18(a), where γ' and γ precipitates have overlapped as a result of encroachment of the matrix

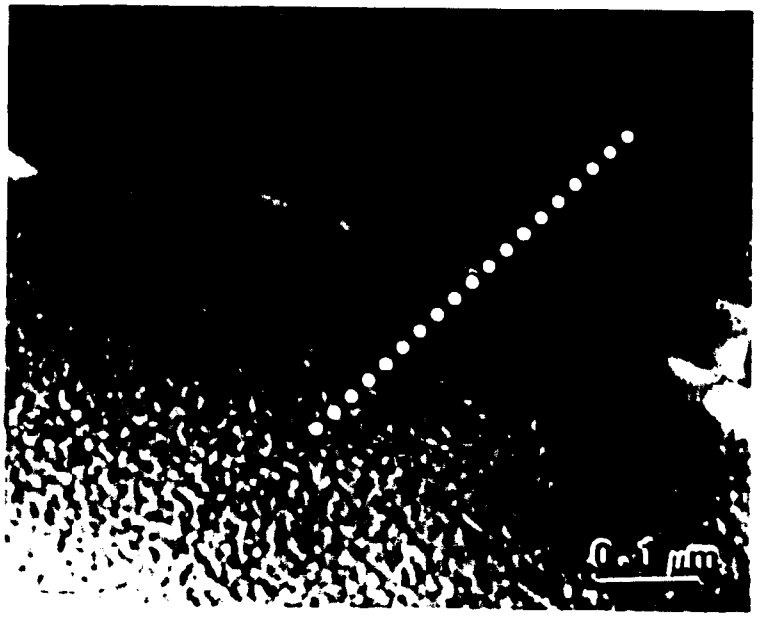

Fig. 17: AEM micrograph for the profile in Fig. 39, corresponding to the TEM image, Fig. 13. Dots show the approximate region analyzed.

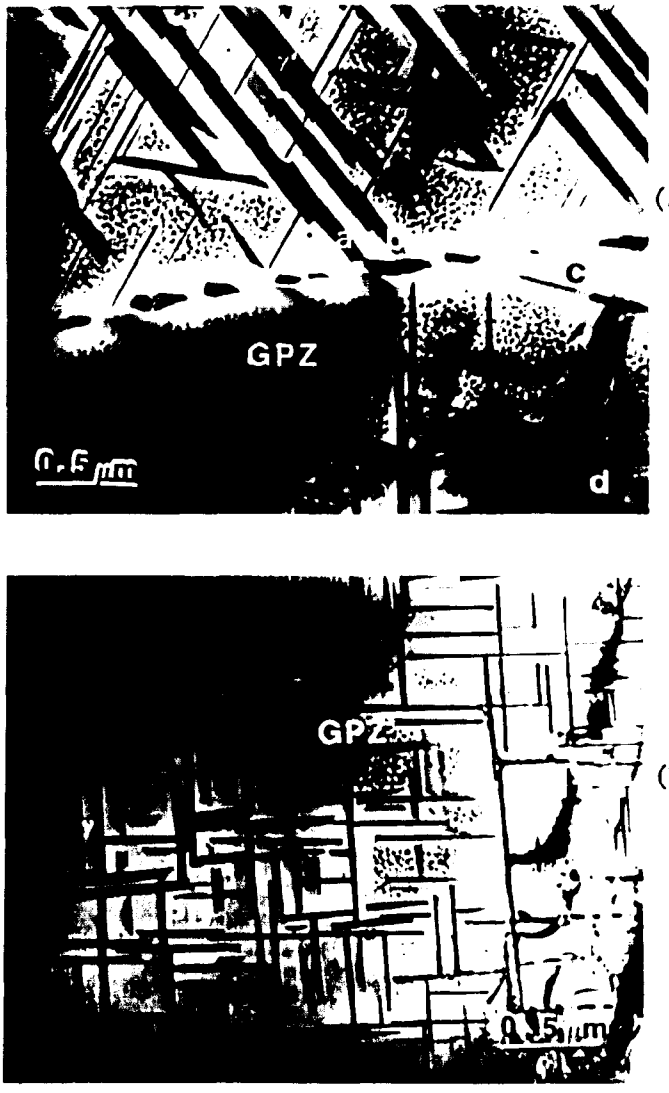

Fig. 18: (a) and (b): Alloy aged at 250°C for 1-1/4 hrs. Note the absence of a conspicuous GPFZ. For an explanation of the symbols, see text. γ' and Guinier-Preston zones are seen within the matrix and γ at the grain boundary.

precipitates into the WPFZ. It was thought necessary to avoid microanalysis of such regions or similar heat-treated specimens. The precipitates which had crossed the WPFZ "boundary" (as at a and b), would draw more solute during the course of the heat-treatment from the already impoverished WPFZ and interact with the solute-depletion fields of the grain-boundary γ precipitates. This is emphasized in region c, where a severe solute depletion region is noticed. Also note the regions d (Figure 18(a)) and PD (Figure 18(b)) where preferential dissolution of the Guinier-Preston zones has occurred in favor of the γ' and γ precipitates. The discontinuous reaction is also present at this temperature as shown in Figure 19. Isolated γ plates are in equilibrium with the α-matrix, while the boundary migrates forward. Copious precipitation of lenticular γ' and spherical Guinier-Preston zones occurs within the interior of the grains.

As suggested earlier, the microstructures of the alloy, heat-treated for 1½ hrs. showed them to be slightly over-aged. Hence it was decided to reduce the ageing time to one-half hour. Figure 20(a) shows a typical microstructure where an AEM trace (T) was taken across the WPFZ. A well defined GPFZ existed in these specimens, as shown in the micrograph. Figure 20(b) is an enlarged view of the inset in Figure 20(a). Figures 21 and 22 show similar AEM traces taken across WPFZ in the same sample.

It was observed in these samples that a size distribution of Guinier-Preston zones existed at the edge of the WPFZ.

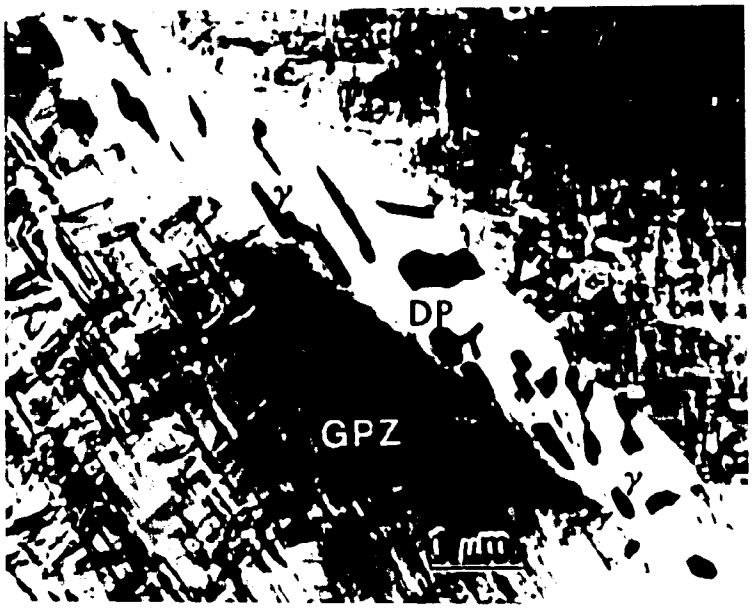

Fig. 19: Microstructure of a sample aged for 1-1/4 hr. at 250°C showing the discontinuous precipitation reaction. Isolated "islands" of γ precipitates are seen within the α-matrix. γ' precipitates and Guinier-Preston zones are seen in the interior of the grains.

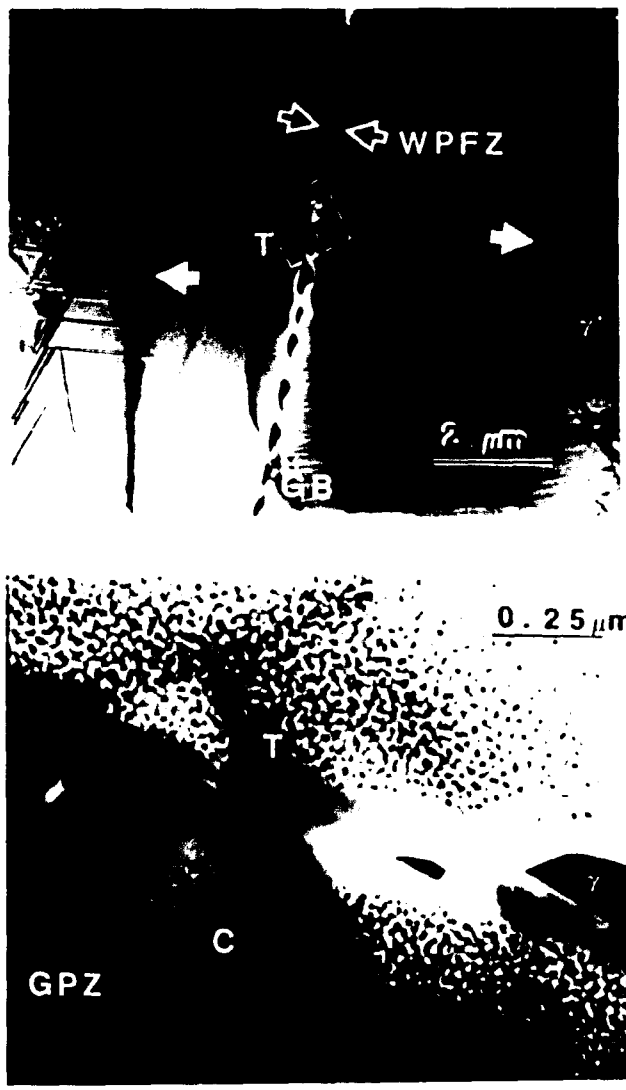

(a)

(b)

Fig. 20: (a) Specimen aged at 250°C for 1/2 hr, shows well-defined GPFZ and WPFZ. Note the decrease in the size of the γ' precipitates as compared to those seen in Fig. 18 (a), and a wide GPFZ (solid arrows). AEM trace (T) taken between grain boundary (GB) γ precipitates across WPFZ (hollow arrows) as shown in inset is enlarged in (b). C is the contamination spot used to determine the thickness of the foil.

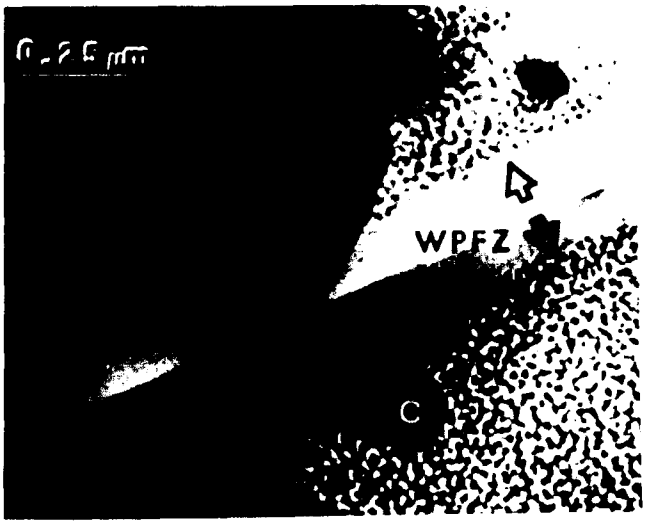

Fig. 21

Fig. 22

Figs. 21 and 22: Same sample as in Fig. 20 showing additional AEM traces (T) across grain boundary (GB). WPFZ between γ precipitates. C is the contamination spot used to measure the foil thickness, the cone caused by tilting the specimen is clearly seen in Fig. 22.

A double ageing treatment, due to excessive heating in the ion-beam thinner shows a much finer distribution of precipitates within the original WPFZ, see Fig. 23, indicating that there is a competitive growth and dissolution process in deciding the boundary of the WPFZ. An explanation for this reprecipitation has been developed and will be discussed later.

Figure 24 shows a WPFZ in a sample aged at 250°C for ½ hr.; much narrower WPFZ are observed in this case as compared with those seen in micrographs of specimens aged for longer times at the same temperature.

iii. Microstructures after ageing at 325°C (598 K)

Heat-treatments were carried out on samples aged at 325°C (598 K) for times from 4 mins. to 47 hrs. Micrographs of the alloy aged for 47 hrs. showed no conspicuous GPFZ and there was excessive intrusion of the matrix γ and γ' precipitates into regions adjoining the grain boundary resulting in difficulty to delineate a WPFZ. Ageing for such long times also caused Guinier-Preston zones to dissolve preferentially and these were seen only in a few regions of the specimen. Figure 25 shows one such microstructure of the alloy heat-treated for 46½ hrs.

Samples that had been aged for very short periods (4 to 10 mins.) at this temperature were found to be suitable for microanalysis of the WPFZ. The alloy also undergoes the discontinuous precipitation reaction at this temperature, as shown in Figure 26. For samples aged at 325°C for 4 minutes, the WPFZ was conspicuous, as shown in the composite Figure 27 although at

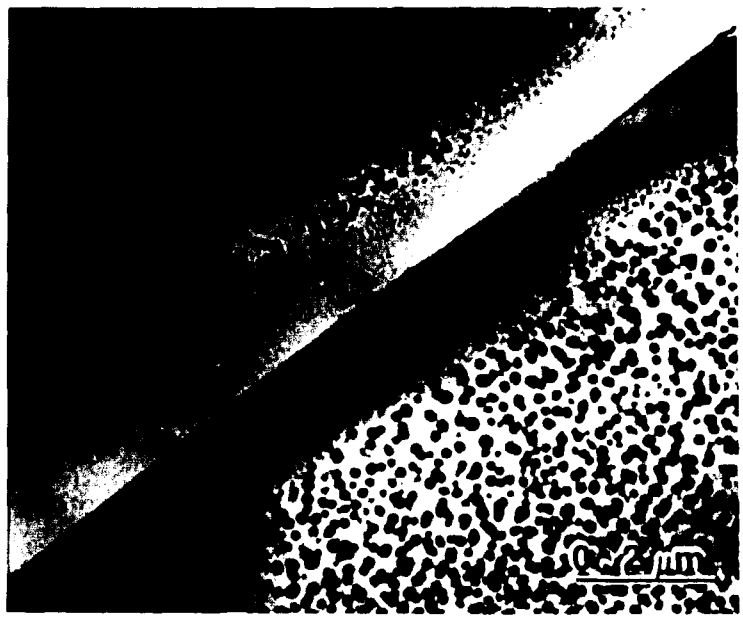

Fig. 23: Reprecipitation (inner arrows) within the original WPFZ (outer arrows) due to excessive heating of the specimen during ion beam thinning. Aged at 250°C for ½ hr.

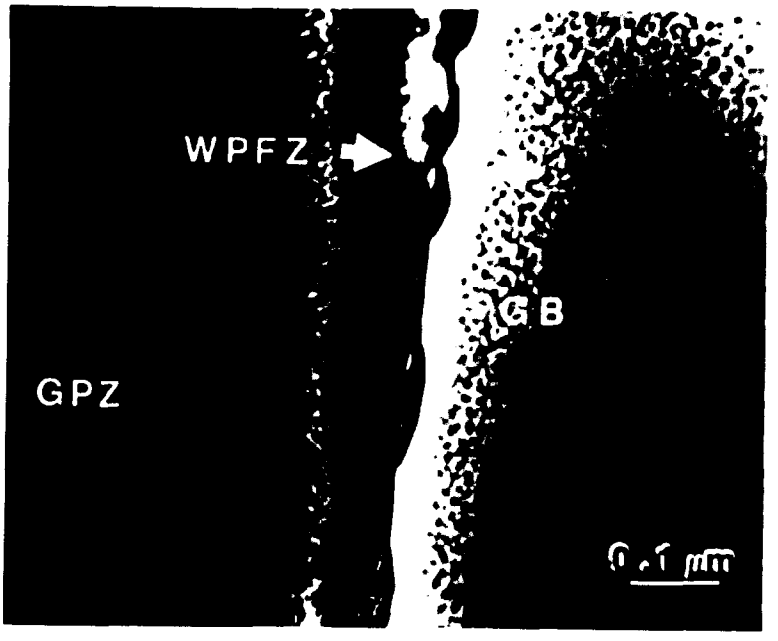

Fig. 24: Microstructure of a sample aged at 250°C for 1/4 hr., showing a narrow WPFZ as a result of a shorter ageing treatment (compared with Figs. 21 and 22). Grain boundary (GB) γ precipitates and Guinier-Preston zones (GPZ) within the matrix are clearly seen.

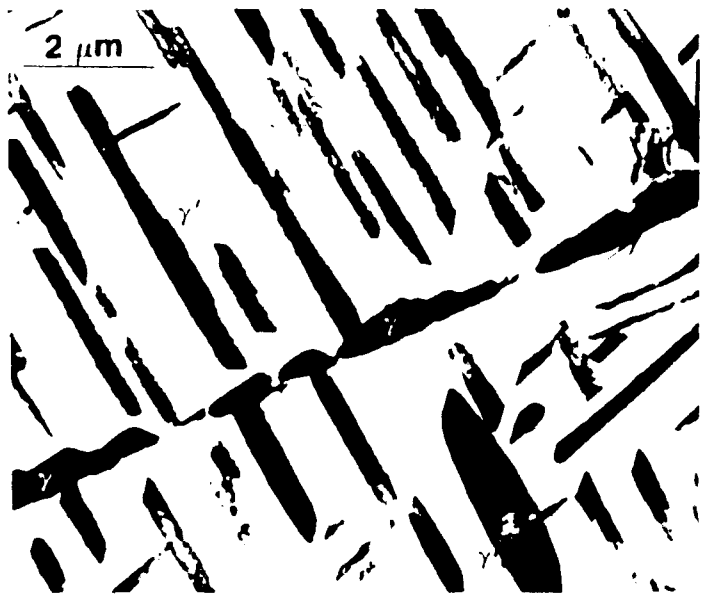

Fig. 25: Microstructure of a sample aged at 325°C for 46½ hrs. showing an area near the grain boundary devoid of a delineating WPFZ due to the absence of Guinier-Preston zones and highly overaged matrix precipitates.

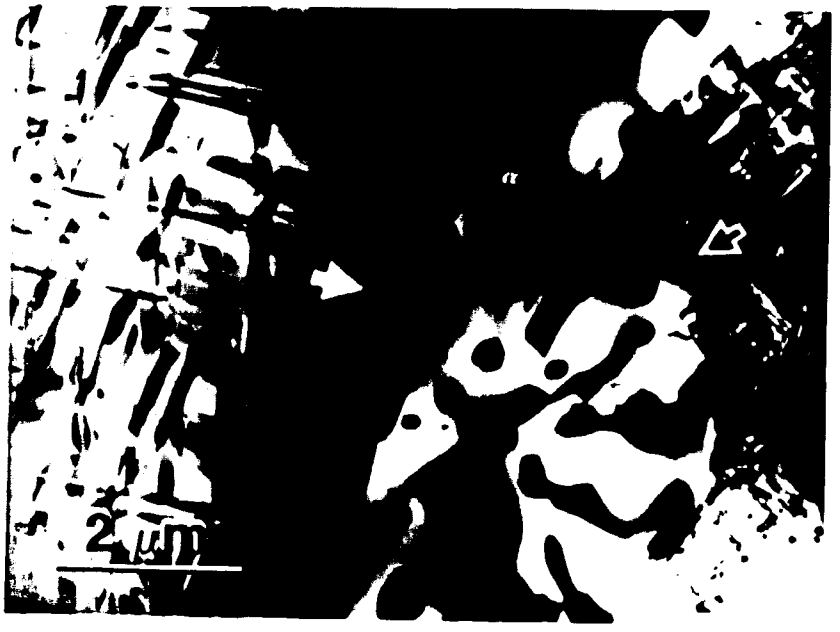

Fig. 26: Specimen aged at 325°C for 10 mins. shows the presence of the discontinuous precipitation reaction. Note the migration of the boundary (hollow arrow) with attendant formation of γ precipitates within the α-matrix. The reaction is about to occur on the other side also (solid arrow). γ' precipitates are seen within the grains.

Fig. 27: A composite picture of regions around a grain boundary of a sample aged at 325°C for 4 mins. Note the WPFZ, γ precipitates at the grain boundary and γ' precipitates within the grains with a dislocation structure on their periphery. As γ' has grown into the WPFZ, it may interfere with the solute distribution within the WPFZ and such regions were not analyzed.

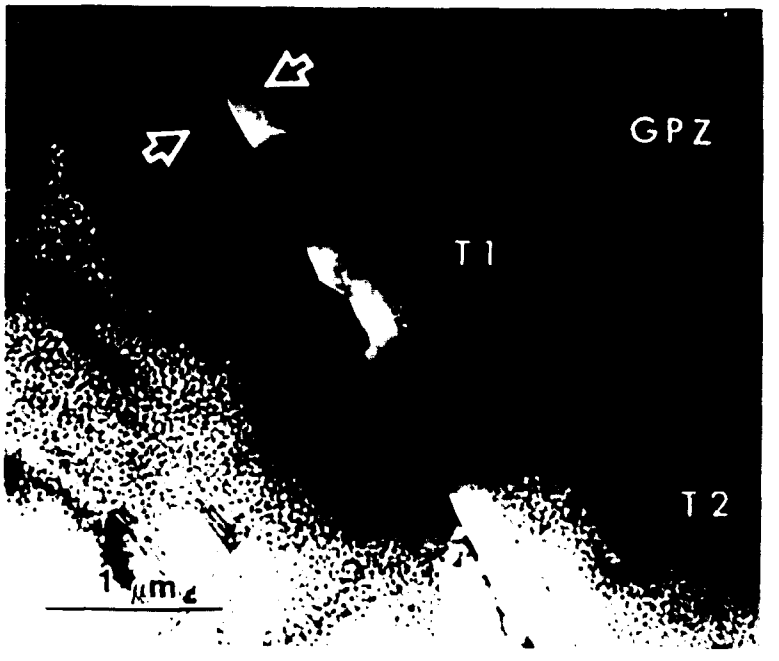

Fig. 28: Same sample as in Fig. 27 but a different grain boundary. AEM traces were obtained in regions free of the γ' phase, across the WPFZ (T_1) and the GPFZ (T_2).

certain regions, the γ' precipitates from the matrix would tend to encroach into the solute depletion regions. AEM microanalysis was not carried out in such regions, but in areas such as shown in Figure 28. In this case, AEM traces were taken across the WPFZ (shown by arrows, T1) and also the GPFZ (T2).

iv. General observations on the precipitation reactions in aged Al-Ag alloys

- Guinier-Preston zones: The Guinier-Preston zones are Ag-rich aggregates within the matrix and are distinguished by their small, dark and roughly spherical nature. These zones seem to grow continuously with time and temperature. At 160°C, a size distribution in the range of 5-10 nm diameter was observed while high-magnification pictures for alloys aged at 325°C for 10 mins. showed a size distribution of 10-25 nm. During ageing, the zones decrease in diameter, first in regions close to growing γ' plates, as seen in Figure 29(a), or around grain boundaries, Figures 21 and 22, producing a visible gradient of sizes. Thus, the zones do not disappear altogether, but preferentially dissolve in regions where Ag atoms are taken up by growing γ' or γ precipitates. As there is very small misfit between the Ag and Al atoms due to similar lattice spacings [Hill and Axon, (1955)] contrast effects due to strains, as observed in Al-Cu or Al-Li alloys [Edington, (1976)] are not seen in Al-Ag alloys. In alloys aged at shorter times and lower temperatures (e.g., 4 hrs. at 160°C), it becomes increasingly difficult to distinguish the Guinier-Preston zones from the "mottled" background of the specimens caused by

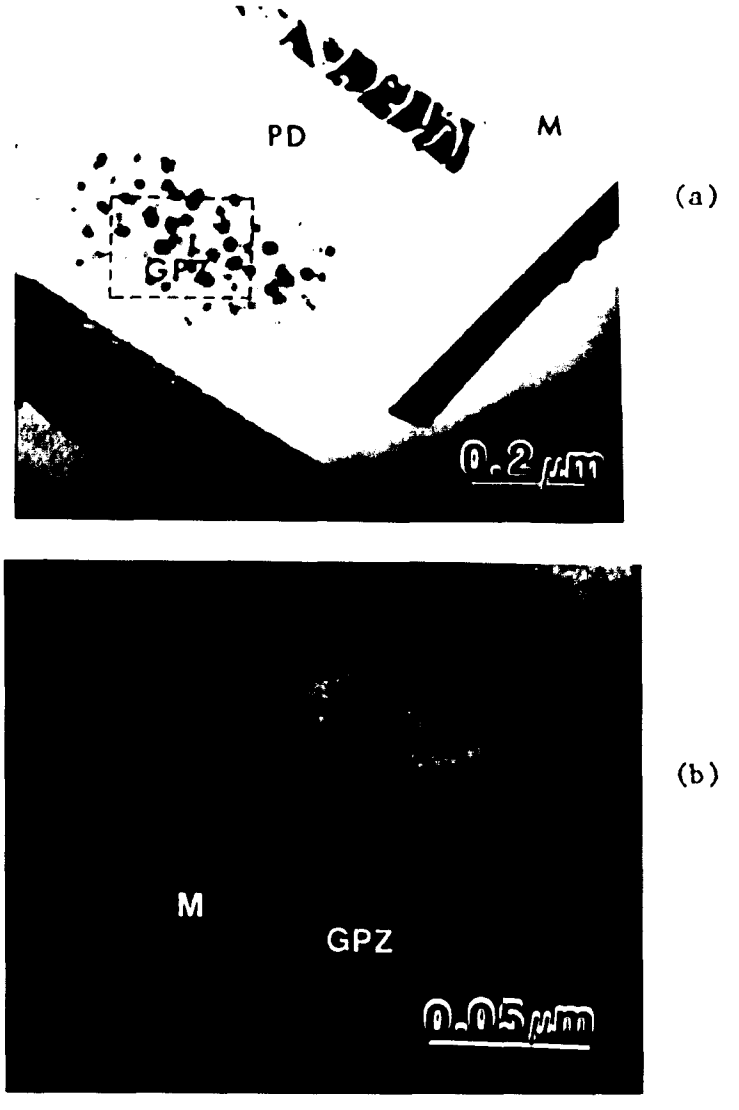

Fig. 29: (a) Preferential dissolution of the Guinier-Preston zones in regions around growing γ' precipitates in a sample aged at 325°C for 10 minutes. (b) High magnification picture of inset area in (a) showing the presence of facets on the Guinier-Preston zones (see region marked GPZ) contained in the matrix M.

twin-jet electropolishing. Strong Bragg reflections do help to distinguish Guinier-Preston zones in such cases, when imaged near bend contours ($\bar{s}$, slightly positive). Although Gragg and Cohen (1971) have suggested a change in shape from octahedral to spherical above 170°C, Figure 29(b) shows a high magnification TEM picture of Guinier-Preston zones in an alloy aged at 325°C for 10 mins., where the zones seem to be nearly spherical but appear faceted in certain cases. Pictures such as these are very difficult to obtain and require extremely good alignment of the microscope. Lack of contrast in such pictures makes imaging very difficult. No Ag-depleted haloes around the Guinier-Preston zones were detected, as claimed by Guinier (1956), and Walker and Guinier (1953), probably due to lack of contrast. Similarly, it was not possible to detect the very small (~ 1.6 nm diam.) Guinier-Preston zones found by Walker and Guinier (1953) in quenched alloys.

- γ' and γ precipitates: A major problem encountered for alloys aged at high temperatures and longer times, is the ability to distinguish between the γ and γ' precipitates. Both phases are h.c.p. and have very similar lattice spacings (for γ': a = 0.2558 nm, c = 0.4607 nm and c/a = 1.612. and γ: a = 0.2879 nm, c = 0.4573 and c/a = 1.588. Thus, distinguishing between an individual precipitate plate as being γ or γ' by means of selected area diffraction patterns is virtually precluded. This problem is particularly acute when determining the nature of the precipitating phase within the matrix. Examination of the grain boundary is less of a problem since γ' does not form at the grain

boundary and γ always precipitates at the grain boundary or forms by the discontinuous precipitation reaction. Laird and Aaronson (1967) have used the technique of imaging Moiré patterns formed by combining the transmitted beam with a beam that is diffracted by the matrix and the precipitate, i.e., a double diffracted beam. The lattice parameters of γ are such that they cause Moiré fringes whereas those of γ' do not. This technique is very tedious and was not followed during the course of this investigation. Hence more rapid methods to determine the identity of the plates were sought. Krause and Laird (1967/68) suggested that as γ forms from γ' as a result of acquisition of misfit dislocations, the observation of dislocations on the broad faces of plates would mean that they were γ plates. However Laird and Aaronson (1967) had observed dislocation arrays on the broad faces of γ' plates (Figures 14a,b of their paper) and so this method of distinguishing between them was also rejected. Fujime et al. (1964) used the variation in c/a ratios between γ' and γ to distinguish between them through selected area diffraction patterns. However their specimens were aged for very long times (30 to 200 days) at 170^{o}C and contained well-developed γ' and γ plates, a condition not found in microstructures in this investigation where ageing times were short. Therefore, for alloys aged at 325^{o}C, the TTT curve constructed by Laird and Aaronson (1967) for the in-situ $\gamma' \rightarrow \gamma$ transformation was followed; for lower temperatures, a comparison of microstructures was made with those obtained by previous workers for similar compositions and heat treatments [Nicholson (1960), Nicholson and

Nutting (1961), Hren and Thomas (1963), Clark (1964), Aaronson and Clark (1967) and Laird and Aaronson (1967, 1969) and Nemoz (1973)].

For alloys aged at shorter times and lower temperatures (e.g., 50 hrs. at 160°C), careful tilting experiments showed displacement-fringe contrast characteristics of γ' precipitates. The observation of this "stacking-fault" type of contrast helped Nicholson and Nutting (1961) to explain the mechanism of formation of γ' precipitates and has been discussed in great detail in their paper. Figures 30 and 31 show γ' precipitates exhibiting this contrast. Figure 31 shows parallel "bands" of γ' precipitate, somewhat similar to Figure 11 of Nicholson and Nutting's paper where γ' has probably formed on parallel sets of dislocations. (See Section II C for an explanation for the formation of γ' precipitates.) Figure 32(a) and its selected area diffraction pattern, Figure 32(b) show streaks along 111 spots indicating their habit plane.

No evidence was obtained to show that γ' nucleated at Guinier-Preston zones, as had been believed earlier before the work of Nicholson and Nutting (1961). No elastic strain fields were observed near the γ' precipitates, although the γ' phase has a different crystal structure, and is never completely coherent with the matrix. There must exist a net of partial dislocations at the periphery of the precipitate to accommodate the small lattice misfit and this was confirmed in overaged micrographs.

Fig. 30: Specimen aged at 160°C for 50 hrs. showing a displacement-fringe contrast characteristic of γ' precipitates.

Fig. 31: Parallel "bands" of γ' precipitates are seen probably nucleated at parallel dislocations during the early stages of ageing. Note the characteristic fringe contrast. Specimen aged for 50 hrs. at 160°C.

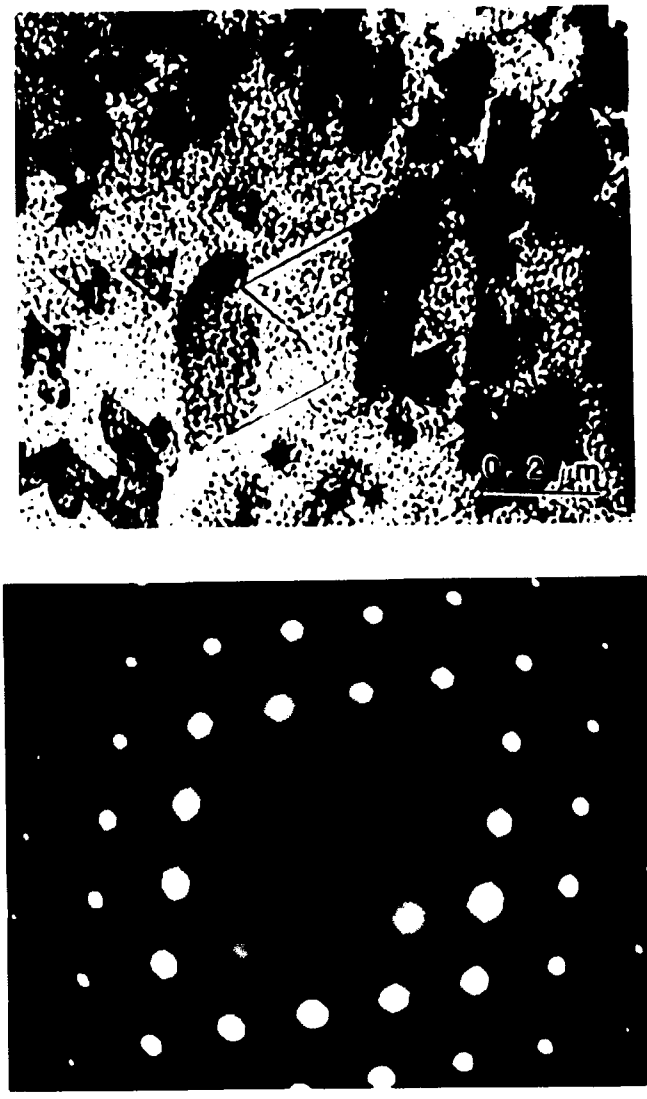

Fig. 32: (a) Micrograph shows γ' precipitates and the associated diffraction pattern (b) with streaks along the 111 spots, indicating their habit plane. Zone axis of SADP: [110]. Sample aged for 50 hrs. at 160°C.

B. Deformation Experiments

A forty percent deformation followed by a three hour ageing treatment on a few samples that had been previously aged for 50 hrs. at 160°C showed a dramatic increase in the rate of γ' formation. The γ' plates are more numerous in such samples as compared to conventionally aged material, and this is interpreted as due to easier nucleation of γ' on dislocations introduced by deformation. The γ' plates were observed to be much smaller (see Figure 33 and compare with Figure 30). The discontinuous precipitation reaction and the formation of γ' is drastically accelerated in such deformed alloys (see Figure 34 and 35) with the microstructure consisting of "isometric" γ (von Heimendahl and Schneider, 1970) i.e, having a shape approximately equally extended in all three dimensions (nearly equiaxed) or lamellar, due to the discontinuous reaction.

The well-defined GPFZ which existed in the aged but undeformed material were not observed in deformed samples because of the drastic change in microstructure. Consequently it was decided to decrease the amount of deformation and the ageing time.

Samples that had been deformed 10% at room temperature and aged 2 hrs. at 160°C showed reprecipitation of γ' within the original GPFZ. The γ' plates were much smaller in size and more numerous compared to the conventionally aged material. See Figure 36(a) and (b) and compare with Figure 33. The amount of discontinuous precipitation had also increased and Guinier-Preston zones in most areas were seen to have preferentially dissolved to provide

Fig. 33: Heterogeneous nucleation of γ' precipitates as a result of a 40% deformation and 3 hr. ageing treatment at 160°C on a sample that had been previously aged at 160°C for 50 hrs. γ' plates more numerous and much smaller than conventionally aged material, see Fig. 30.

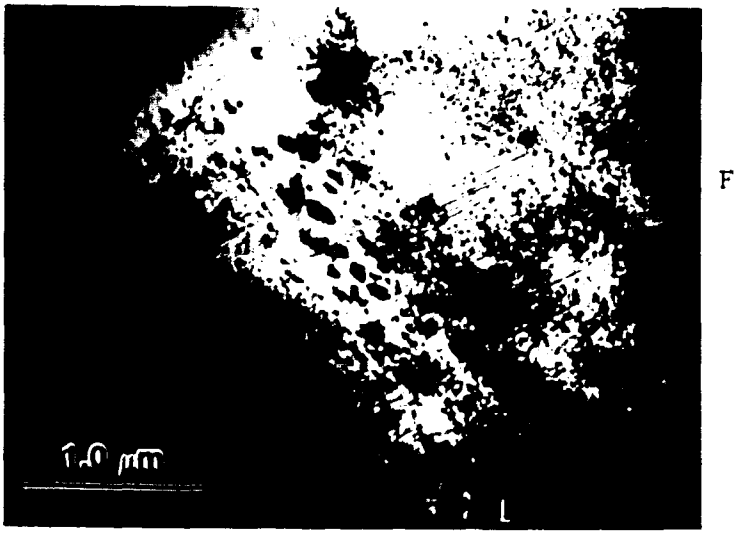

Fig. 34

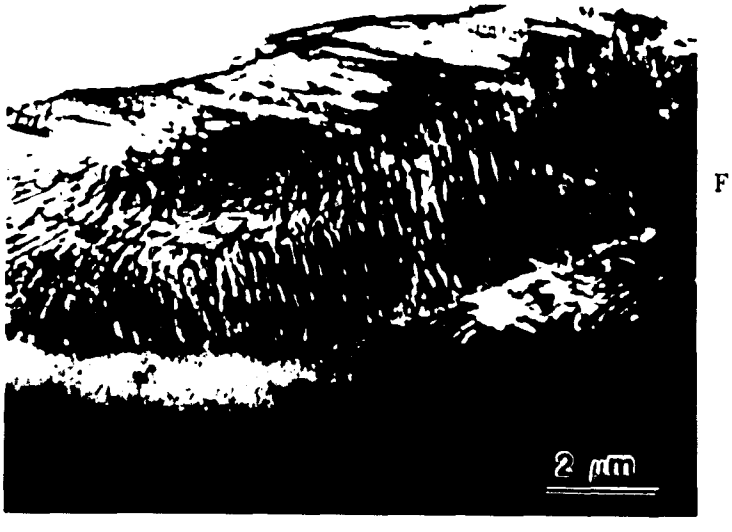

Fig. 35

Figs. 34 and 35: Drastic acceleration in the rate of the discontinuous precipitation reaction in the same sample as shown in Fig. 33. Microstructure consists of "isometric" or equiaxed (Fig. 34) and lamellar (L) γ precipitates more clearly seen in Fig. 35.

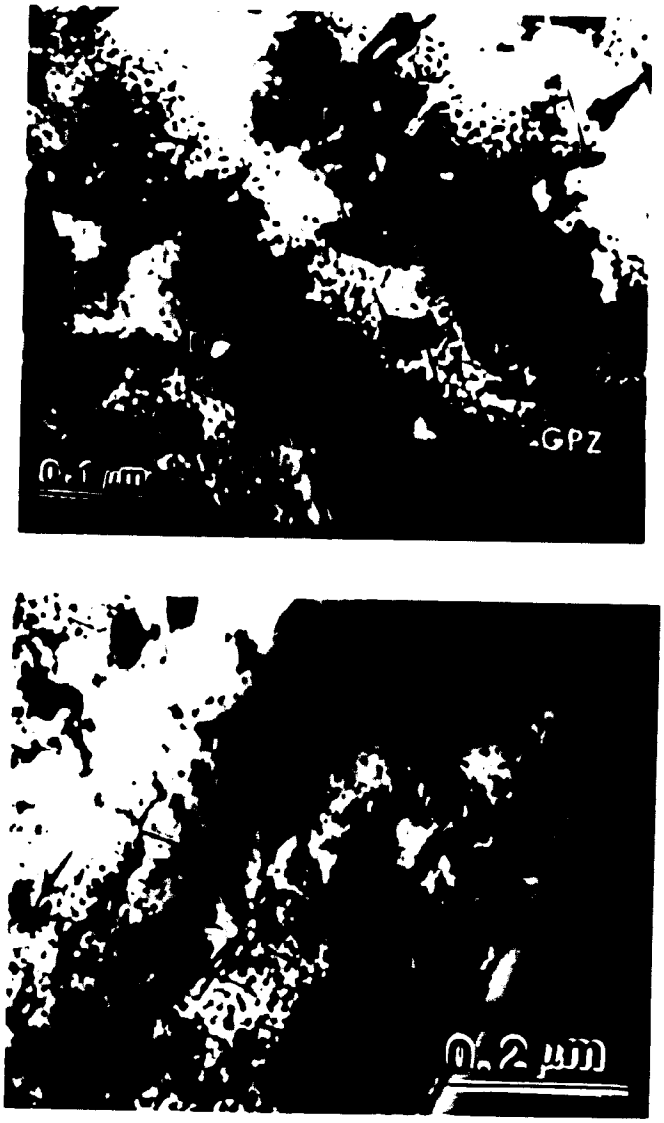

(a)

(b)

Fig. 36: Sample deformed 10% and aged 2 hrs. at 160°C after an initial ageing treatment of 50 hrs. at 160°C. (a) The strain contrast is evident from the presence of dislocations at D caused by deformation. Preferential dissolution of the Guinier-Preston zones for γ' precipitates is also observed. (b) Same specimen, region near a grain boundary.

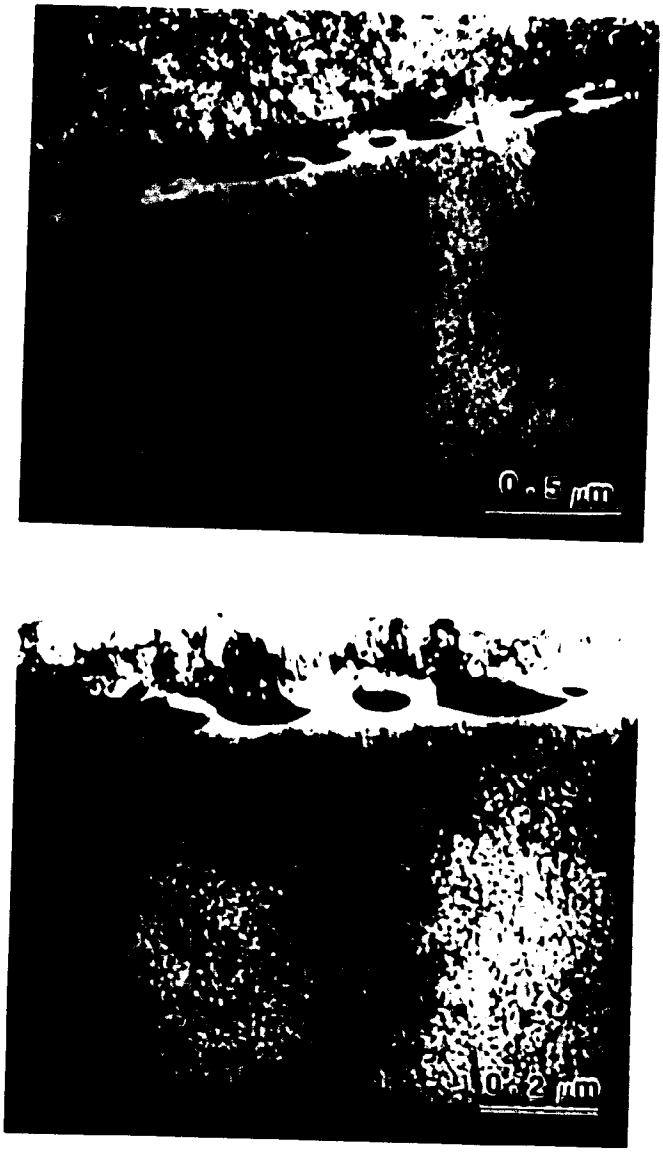

(a)

(b)

Fig. 37: (a) Micrograph shows fine precipitation of γ' within the original GPFZ (as delineated by the coarse γ' precipitates in the foreground) upon a 10% deformation and reageing for 2 hrs. at 160°C for a sample aged earlier for 50 hrs. at 160°C to form PFZ. (b) Area of inset in (a). Note that there is no nucleation of γ' within the WPFZ.

solute atoms for the growth of newly formed γ' plates on dislocations and defects introduced by deformation, see Figure 36.

Figure 37(a) shows the presence of γ' precipitates in the material given the 10% deformation and second ageing treatment. The limits of the original GPFZ are evident from the large γ' plates, $\sim$ 1 μm away from the grain boundary. γ' plates have nucleated right up to the WPFZ. This fact is highlighted in Figure 37(b) which is the area marked by the inset in Figure 37(a).

C. AEM profiles across PFZ

At least four concentration profiles across grain boundaries were obtained for each of the ageing temperatures. Some of these were taken across the GPFZ to ascertain the variation in Ag concentration within them. Selected, but typical profiles, representative of the results obtained are given in Figures 38 through 43. The concentration of Ag across the GPFZ remained constant within statistical limits. Concentration profiles were obtained mainly across WPFZ and the minimum composition of the grain boundary noted. Table V gives a summary of the TEM/AEM data obtained from PFZ at various ageing times and temperatures.

The half-widths of the WPFZ in aged alloys were used to calculate the diffusivity values and activation energy for diffusion of Ag in Al. The equilibrium 2-phase solvus and the Guinier-Preston zone metastable solvus were also determined (see Sections IV E(i) and (ii) for a detailed discussion). The profiles shown in Figures 40(a) and 40(b) are taken across the WPFZ and GPFZ on the same grain boundary but with different probe sizes and at

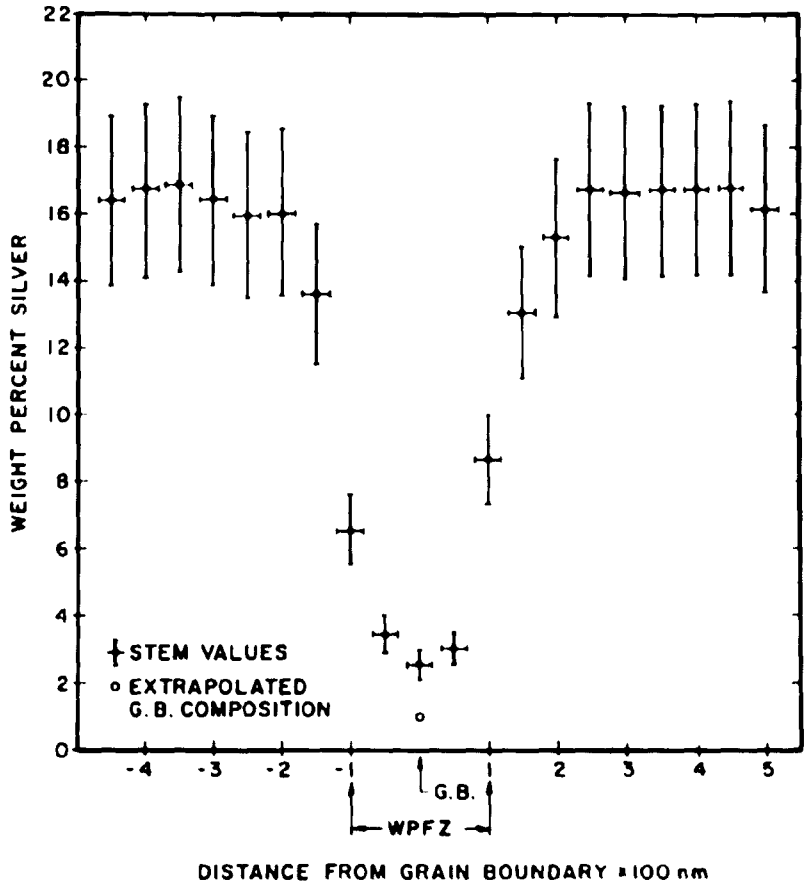

Fig. 38: AEM concentration profile across a grain boundary WPFZ in a specimen aged for 50 hrs. at 160°C. Note the effects of solute depletion around the grain boundary (GB). The terminal extrapolated composition used to determine the equilibrium solvus line is also indicated. Corresponding profile number 3036.

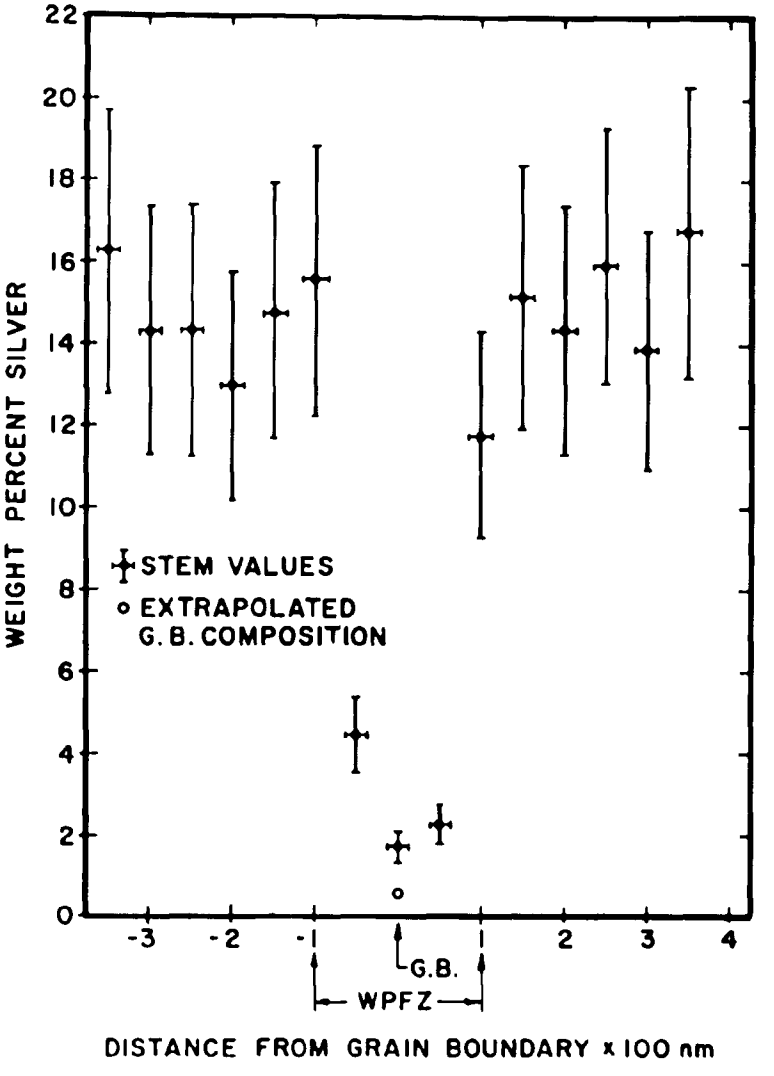

Fig. 39: AEM concentration profile across the region shown in Figs. 13 and 17. Note the solute depletion in the WPFZ and the relatively constant solute content in regions beyond the limits of the WPFZ, namely within the GPFZ. Specimen aged for 50 hrs. at 160°C. Profile number 2883.

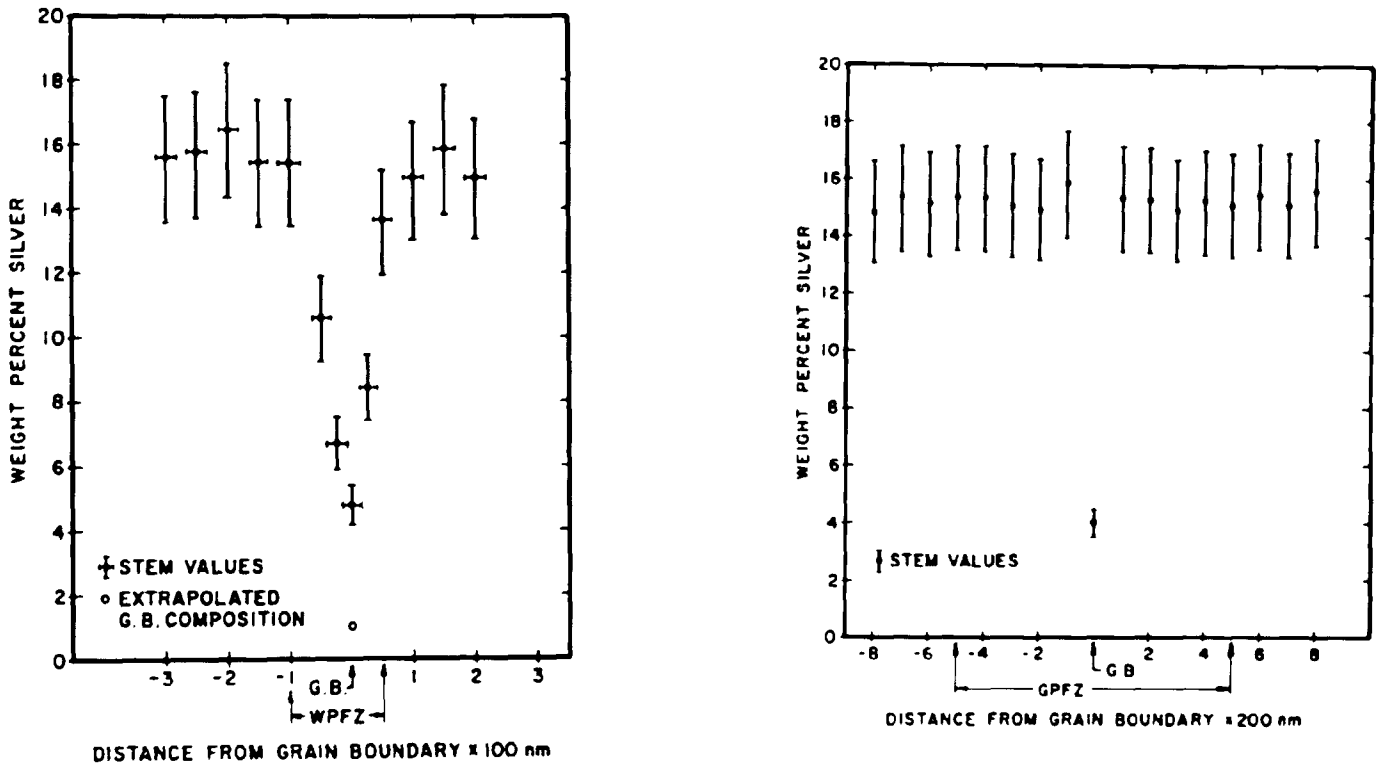

(a) (b)

Fig. 40: (a) AEM concentration profile across a grain boundary WPFZ for a sample aged at 160°C for 50 hrs. The effects of marked solute depletion are evident. (b) AEM concentration profile across the grain boundary region of (a). Note the relatively constant solute concentration within the GPFZ. The V-shape of the solute distribution in (a) is clearly seen. Corresponding profile numbers are 2888W and 2888G.

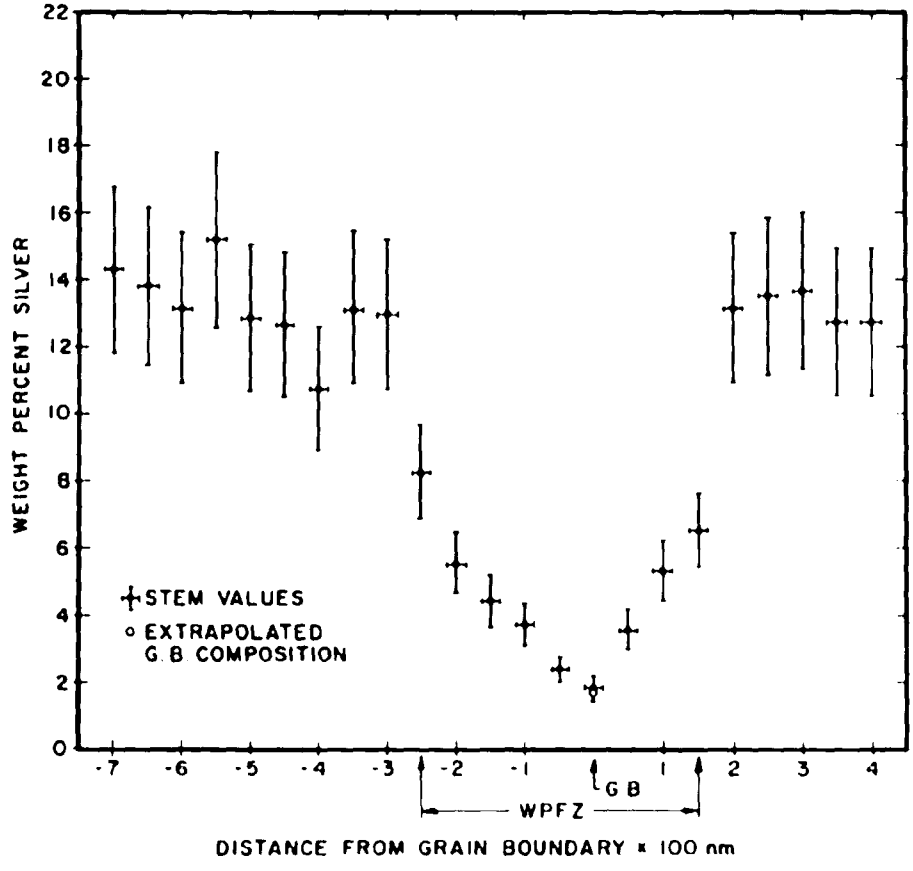

Fig. 41: AEM concentration profile across a grain boundary WPFZ for a sample aged at 250°C for 30 mins. Note the asymmetric nature of the profile caused by the asymmetric WPFZ and its increased width as compared to samples aged at 160°C, see Figs. 38 to 40. Profile number 3380.

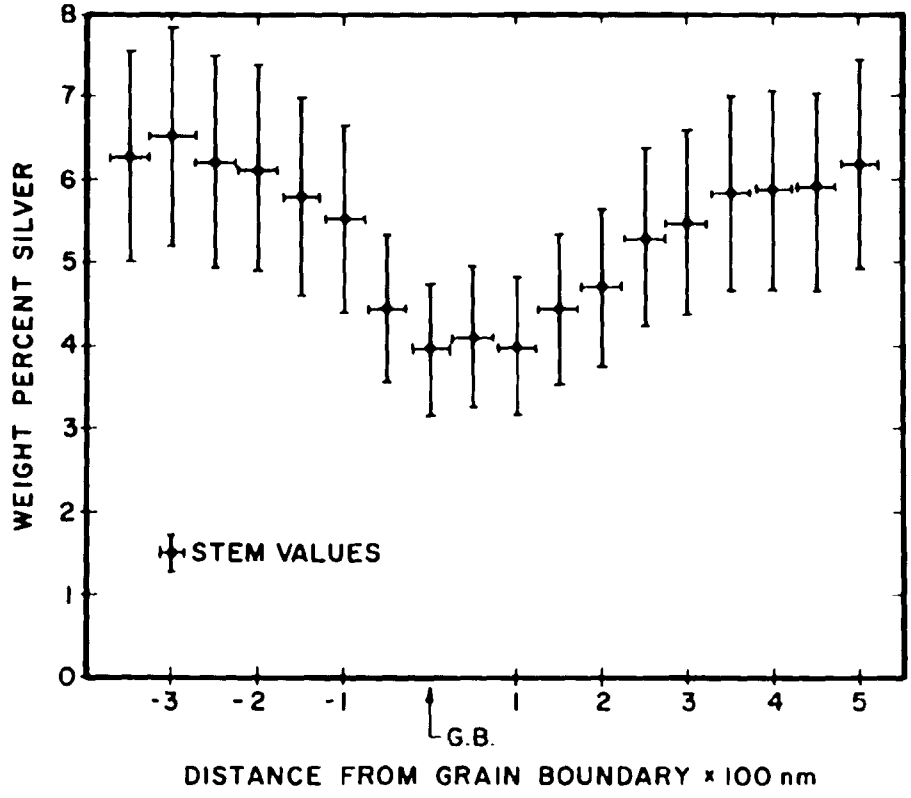

Fig. 42: An AEM concentration profile across a grain boundary in a sample aged at 325°C for 10 mins. The flat bottom nature of the profile is in marked contrast with the steep V-shaped solute distribution characteristic of low ageing temperatures, see Fig. 40. No conspicuous WPFZ was observed in this sample on account of encroaching γ' precipitates. Profile number 3756.

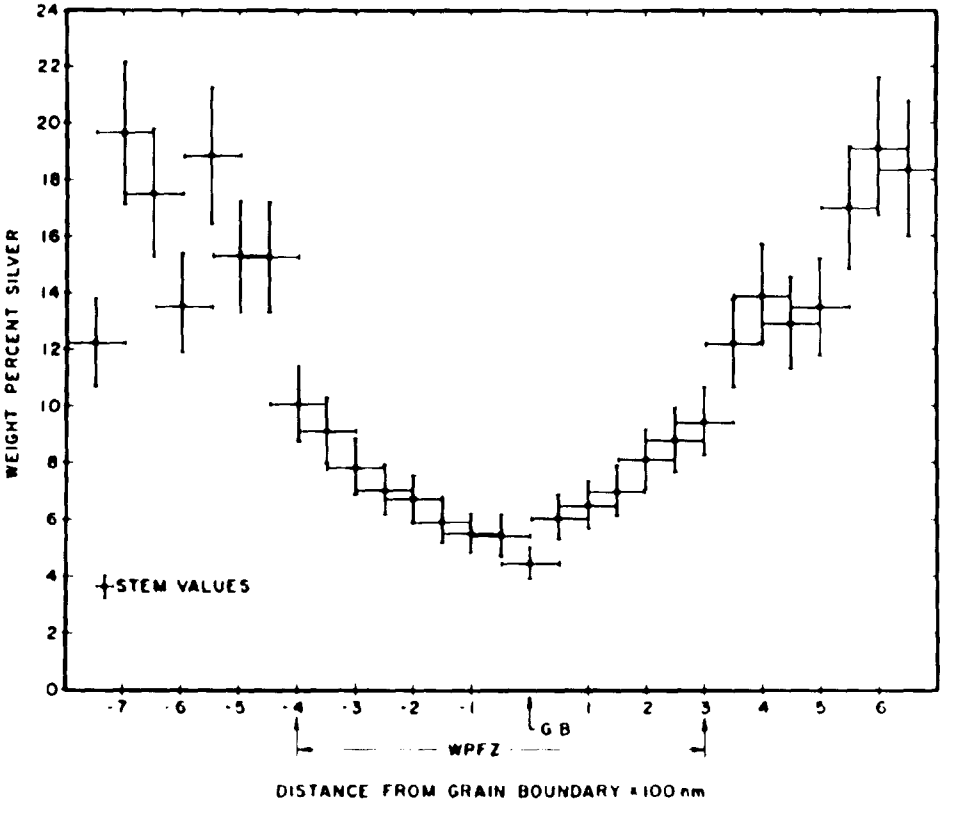

Fig. 43: A concentration profile obtained across the WPFZ in a sample aged at 325°C for a short ageing time of 4 mins. The WPFZ could easily be delineated; a representative TEM micrograph is shown in Fig. 28. Profile number 3894.

TABLE V

List of AEM Concentration Profiles Across PFZ and Their Minimum Compositions at Various Ageing Times and Temperatures

Temp.	Profile Number	Figure Number	Ageing time (secs)	WPFZ Width (nm)	Minimum composition at grain boundary (Wt. Pct.)	(At. Pct.)
160°C	3036	38	180,000	137	2.57 ± 0.4	0.66 ± 0.1
(433 K)	3025	-	180,000	82	2.24 ± 0.63	0.57 ± 0.16
	2896	-	180,000	80	4.16 ± 0.44	1.07 ± 0.11
	2890	-	180,000	80	4.43 ± 0.52	1.15 ± 0.13
	2888G	40(b)	180,000	150	4.01 ± 0.49	1.03 ± 0.12
	2888W	40(a)	180,000	80	4.79 ± 0.61	1.24 ± 0.15
	2883	39	180,000	140	1.73 ± 0.37+	0.44 ± 0.09
	4172	-	180,000	80	3.32 ± 0.14	0.85 ± 0.04
250°C	027356@	18(a)	4,500	250	-	-
(523 K)	3380	41	1,800	220	1.88 ± 0.33+	0.48 ± 0.08
	3248	-	1,800	216	4.16 ± 0.5	1.08 ± 0.13
	3319	-	1,800	280	-	-
	3374	-	1,800	240	3.74 ± 0.68	0.96 ± 0.17
	24M	-	900	170	1.99 ± 0.39	0.51 ± 0.1
	3144	-	900	130	4.61 ± 0.6	1.2 ± 0.15
325°C	3493*	-	600	-	3.7 ± 0.85+	0.95 ± 0.21
(598 K)	3756*	42	600	-	3.95 ± 0.81	1.02 ± 0.2
	3894	43	240	600	4.48 ± 0.57	1.16 ± 0.14
	3989	-	240	444	9.15 ± 1.66	2.46 ± 0.42
	3990	-	240	450	6.65 ± 1.25	1.75 ± 0.31

*In samples where γ' precipitates were encroaching into the WPFZ.

+Minimum composition analyzed at grain boundary using AEM (without extrapolation).

@TEM only.

different magnifications for reasons described in the experimental section. The specimen was aged at 160°C for 50 hours. The profile in Figure 41 was taken across a WPFZ in a sample aged at 250°C for 30 minutes, and the profile shown in Figure 42 was taken across the WPFZ in a sample aged at 325°C for 10 mins.; since γ' precipitates had encroached into the regions around the grain boundary, there was no conspicuous WPFZ in these samples. Therefore profiles were also obtained across a WPFZ in a sample aged at 325°C for 4 minutes, see Figure 43.

Composition profiles obtained across the regions where reprecipitation of γ' precipitates had occurred (i.e., the GPFZ) in deformed and aged specimens did not show any significant variation in concentration as compared to specimens aged at 160°C for 50 hrs. No attempts were made to take readings across the WPFZ in deformed specimens.

D. Diffusivity Values

As discussed in the previous section, the PFZ are caused both by vacancy depletion and solute depletion. As there is copious precipitation within the matrix, for all the heat-treatments carried out on the Al-16% Ag alloy, the Grube analysis, as suggested by Doig and Edington (1974) cannot be used in such a situation. As the WPFZ has been shown to be caused only by effects of solute depletion and, moreover, the solute atoms travel only towards the grain boundary, an estimate of the diffusion coefficient, of Ag in Al, D_{Ag}, corresponding to different values of the ageing parameters (time and temperature) has been obtained. By equating

the half-width of the solute depleted PFZ to the diffusion distance perpendicular to the grain boundary, Y, the value of the volume diffusion coefficient of Ag in Al, D_{Ag} can be determined if the ageing time t at a particular temperature is known, from the following equation:

$$Y = 2\sqrt{D_{Ag} \cdot t}$$

The values of Y have been obtained from TEM/AEM micrographs which were subsequently corrected using magnification calibration data. In cases where the WPFZ was asymmetric, an average value of Y has been reported. Cases where the grain boundary had migrated as a result of discontinuous precipitation were ignored.

An average value of D_{Ag} was obtained, see Table VI, and used to obtain a plot of ($\ln$ D vs. 1/T) in order to determine the activation energy for diffusion of Ag in Al at the three ageing temperatures, T (in Kelvin) as shown in Figure 44. The error bars represent the scatter associated with the values of D_{Ag} about the mean, at each temperature. The slope of the linear plot yields a value of Q = 30.08 $\pm$ 1 kcals/mole (1.3 $\pm$ 0.04 eV). Also included in the figure is the extrapolated high-temperature diffusion data of Heumann and Dittrich (1957) and Hren and Thomas (1963), see Section II D and Table VII(a). The present data is in close agreement with the investigation of the previous workers [Figure 45 and Table VII(b)].on alloys of similar compositions.

TABLE VI

Determination of the Solute Diffusion Coefficient, D_{Ag}, in Al from PFZ widths; $Y = 2\sqrt{D_{Ag}t}$

Temp.	Time secs.	Profile number	Average Half-width of PFZ Y (nm)	$D_{Ag}^{Al} = \left(\frac{Y^2}{4} \cdot \frac{1}{t}\right)$ $cm^2/sec.$	ln D_{Ag}
160°C	180,000	3036	68.5	6.52×10^{-17}	-37.27
(433 K)	180,000	3025	41	2.33×10^{-17}	-38.30
	180,000	2896	40	2.22×10^{-17}	-38.35
	180,000	2890	40	2.22×10^{-17}	-38.35
	180,000	2888	75	7.81×10^{-17}	-37.09
	180,000	2888	40	2.22×10^{-17}	-38.35
	180,000	2883	70	6.81×10^{-17}	-37.23
			$\bar{D}_{Ag}$ =	4.30×10^{-17}	-37.69
250°C	4,500	027356	125	8.68×10^{-15}	-32.38
(523 K)	1,800	3380	110	1.68×10^{-14}	-31.72
	1,800	3248	108	1.62×10^{-14}	-31.75
	1,800	3319	140	2.72×10^{-14}	-31.23
	1,800	3374	120	2.0×10^{-14}	-31.54
	900	24 M	85	2.01×10^{-14}	-31.54
	900	3144	65	1.17×10^{-14}	-32.08
			$\bar{D}_{Ag}$ =	1.72×10^{-14}	-31.70
325°C	240	3894	300	9.38×10^{-13}	-27.70
(598 K)	240	3989	222	5.14×10^{-13}	-28.30
	240	3990	225	5.27×10^{-13}	-28.27
			$\bar{D}_{Ag}$ =	6.6×10^{-13}	-28.04

TABLE VII (a)

Comparison of D_{Ag} and Q Values Obtained in the Present Study with Extrapolated High Temperature Data of Other Workers

Temperature (°C)	Hren and Thomas (1963) D_{Ag} (cm^2/sec)	Heumann and Dittrich (1957) D_{Ag} (cm^2/sec)	This Study D_{Ag} (cm^2/sec)
325	1.7×10^{-13}	8.98×10^{-13}	6.6×10^{-13}
250	1.8×10^{-15}	1.32×10^{-14}	1.72×10^{-14}
160	1.0×10^{-18}	1.2×10^{-17}	4.30×10^{-17}
	Q kcals/mole	Q kcals/mole	Q kcals/mole
-	37.5 ± 4	35.0	30.08 ± 1

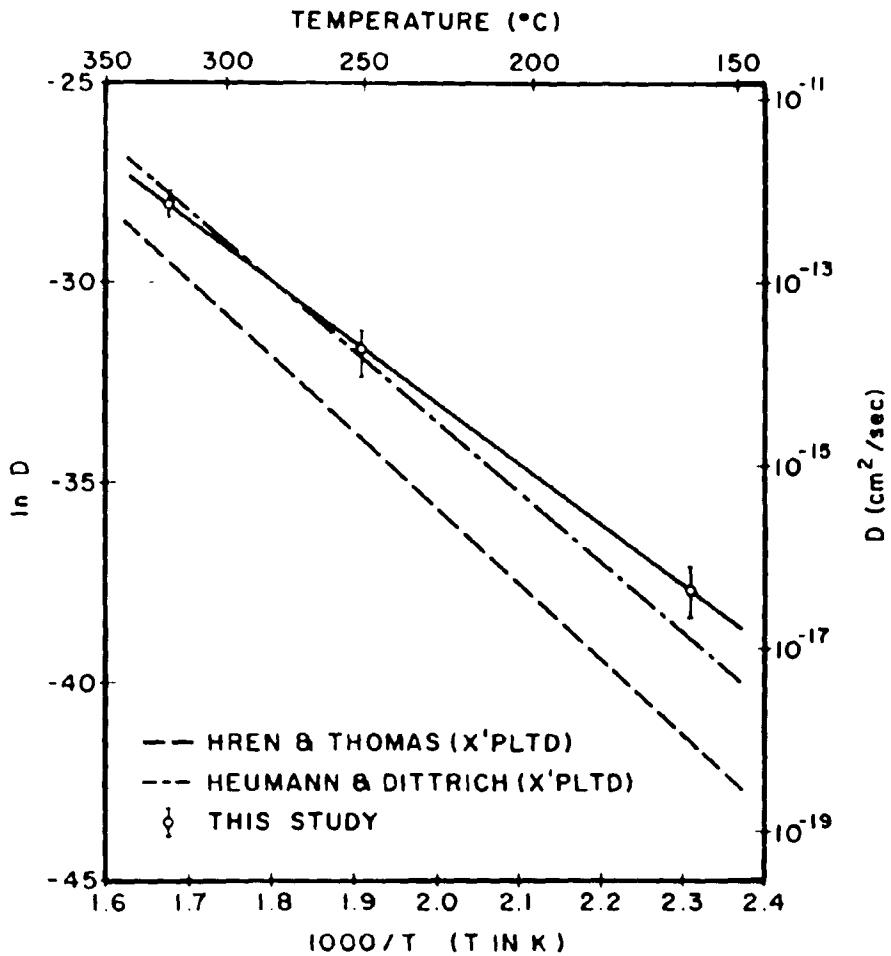

Fig. 44: Plot of $\ell n\ D_{Ag}$ vs. $^{1}/T$ to obtain the value of the activation energy for the diffusion of Ag in Al. Also shown is the extrapolated high-temperature diffusion data of Hren and Thomas (1963) and Heumann and Dittrich (1957), see Table VII (a).

TABLE VII (b)

Comparison of Values of D_{Ag} Obtained From Previous Investigations as a Function of Temperature and This Study

Investigator	$T^{o}C$	1000/T K($\times 10^{3}$)	D_{Ag} (cm^{2}/sec)	$\ell n\ D_{Ag}$ (- negative)
Hren & Thomas (1963)	450	1.383	4×10^{-11}	23.94
	460	1.364	5×10^{-11}	23.72
	475	1.337	1.1×10^{-10}	22.93
	500	1.294	1.2×10^{-9}	20.54
Heumann & Dittrich	500	1.294	0.7×10^{-9}	21.08
(1957)	535	1.238	1.66×10^{-9}	20.21
Anand & Agarwala	550	1.215	4.24×10^{-9}	19.28
(1967)	500	1.294	1.24×10^{-9}	20.51
	450	1.383	3.96×10^{-10}	21.65
	425	1.432	1.63×10^{-10}	22.54
	400	1.486	5.62×10^{-11}	23.60
Abbott & Haworth	393	1.502	0.5×10^{-10}	23.72
(1972)	406	1.473	0.8×10^{-10}	23.25
	419	1.445	1×10^{-10}	23.03
	433	1.416	2×10^{-10}	22.33
This study	325	1.672	6.6×10^{-13}	28.04
	250	1.912	1.72×10^{-14}	31.70
	160	2.31	4.3×10^{-17}	37.69

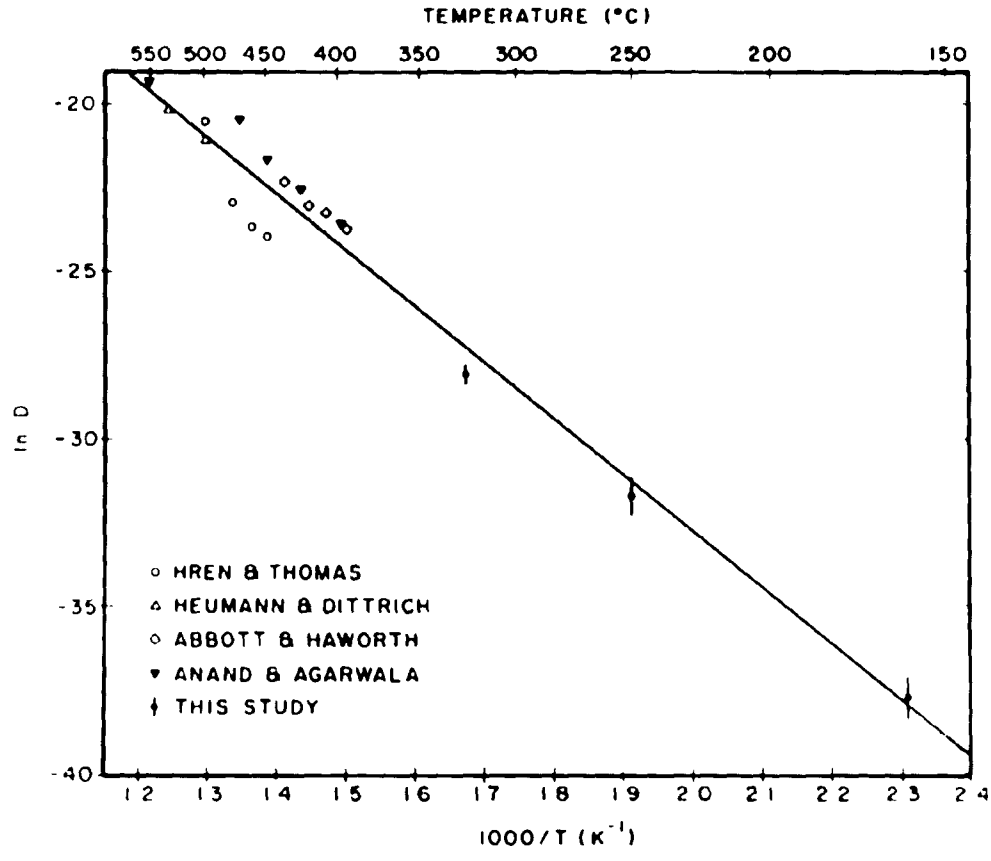

Fig. 45: Arrhenius plot for the measured diffusion coefficients from TEM/AEM investigations (solid circles). The extrapolation from previous high temperature investigations is also shown. See Table VII(b) for details.

E. Phase Boundary Determination

(i) The equilibrium solvus line.

The AEM concentration profiles analyzed across WPFZ in specimens aged at 160°C, 250°C and 325°C were used to determine the solid solubility limit of Ag in Al. For reasons discussed later [Section V D(i)], an extrapolation technique was necessary to determine the solid solubility limit. Extrapolation was performed by fitting the profile shape to a straight line and extrapolating this line to the observed grain boundary interface plane. In all cases, the concentration value corresponding to the intersection is the value reported.

The data is presented in a number of different formats. Table VIII lists the Ag concentrations obtained as a result of such a terminal extrapolation at the grain boundary. Asymmetric profiles, and profiles where readings had not been taken across the WPFZ but only across the GPFZ were not considered at all. Table X compares these readings with the values of the solid solubility limit of Ag in Al reported in the literature for the various temperatures. Figure 46 shows the equilibrium solvus line for Ag in Al where a comparison has been made between the extrapolated Ag concentrations and the solid solubility limits determined using Williams and Easton's (1974) theoretical expression and Elliott and Shunk's (1980) phase diagram study, see Table IX. The error bars represent the errors evaluated using a student t distribution at a 95% confidence level about the mean.

TABLE VIII

Values of the Solute Content Obtained from AEM Concentration Profiles Upon Terminal Extrapolation at the Grain Boundary

Temperature	Profile No.	Terminal Composition Upon Extrapolation wt% Ag	Solid Solubility of of Ag in Al wt%/(at%) Ag*
160°C (433 K)	3036	1.0	
	3025	Asymmetric PFZ	
	2896	GPFZ only	
	2890	GPFZ only	
	2888G	GPFZ only	
	2888W	1.0	
	2883	0.5	0.88 ± 0.4
	4172	1.0	(0.22 ± 0.1)
250°C (523 K)	027356	TEM only	
	3380	1.7	
	3248	---	
	24M	1.99	
	3319	---	
	3374	---	1.9 ± 0.43
	3144	2.0	(0.48 ± 0.11)
325°C (598 K)	3493	3.7	
	3756	3.95	
	3894	4.48	
	3989	---	4.04 ± 0.97
	3990	Asymmetric PFZ	(1.04 ± 0.24)

*Errors determined using a student t distribution at a 95% confidence level about the mean.

TABLE IX

Values of the Solid Solubility Limit of Ag in Al, Calculated for Temperatures Less Than 300°C (573 K) from the Expression Suggested by Williams and Easton (1974). Also listed are the values obtained from Elliott and Shunk (1980)

Temp. °C	Temp. K	Solid Solubility Limit of Ag in Al			
		Williams and Easton[1]		Elliott and Shunk[2]	
		at%	wt%	at%	wt%
325	598	0.95	3.42*	4.5	1.16
300	573	0.73	2.84	3.5	0.9
275	548	0.59	2.32	2.5	0.64
250	523	0.47	1.84	2.0	0.51
225	498	0.36	1.42	1.5	0.38
200	473	0.28	1.09	1.0	0.25
160	433	0.17	0.65	-	-
150	423	0.14	0.57	-	-
100	373	0.06	0.25	-	-

*Experimental.

(1)Theoretical expression: x (at% Ag) = exp [4.261 - 2625.42 /T] (T in K)

(2)From the bulletin of Alloy Phase Diagrams, ASM Provisional.

TABLE X

Values of the Solid Solubility Limit of Ag in Al Obtained by Extrapolation From AEM Concentration Profiles (Table VIII) and Compared with Data in the Literature for Various Temperatures

All compositions are in wt.% Ag

Solid Solubility Limit of Ag in Al			
Temperature (°C)	Williams & Easton (1974)	Elliott and Shunk (1980)	This Investigation
160	0.65	--	0.88 ± 0.4
250	1.84	2.0	1.89 ± 0.43
325	3.42*	4.5	4.04 ± 0.97

*Experimental

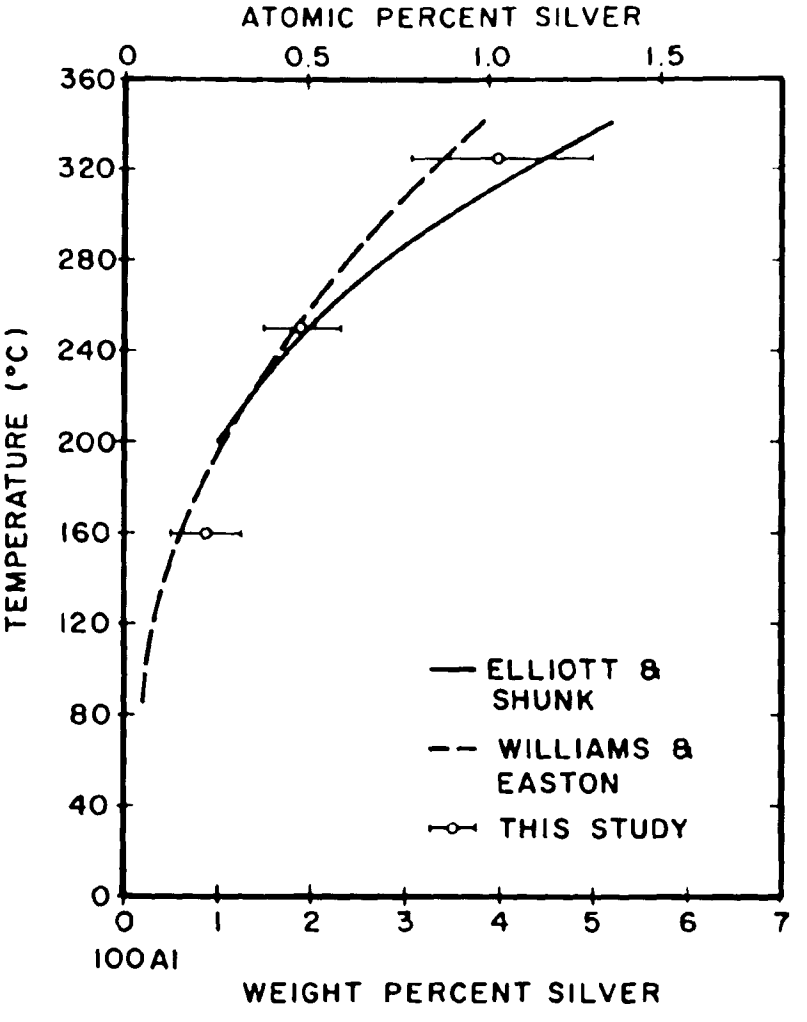

Fig. 46: Comparison of the solid solubility limit of Ag in Al obtained by terminal extrapolation at the grain boundary with previous investigations.

Figure 47 is similar to Figure 46 except that the single actually measured (using AEM) minimum composition obtained at each temperature is compared with the extrapolated value at the same temperature. It may be seen, that for the two highest temperatures, there is no significant difference between the two values, while at the lower temperature, there is one.

(ii) The metastable Guinier-Preston zone solvus line.

It was explained earlier (Section II B(ii)) that during the course of the investigation of the solute distribution within the WPFZ, it may be possible to obtain an estimate of the Guinier-Preston zone metastable solvus. This is a result of the hypothesis that the composition limit at the boundary of the WPFZ would be dictated by the composition given by the intersection of the solute depletion profile and the critical composition necessary for the formation of Guinier-Preston zones, i.e., the GPFZ. This is by definition the metastable solvus line. Thus, the TEM/AEM micrographs were used to determine the physical (spatial) limits of Guinier-Preston zone formation, and this was then compared to the AEM profiles to obtain the composition at that distance.

There is some error involved in this technique, especially if a gradation in the Guinier-Preston zone sizes exists at the edge of the WPFZ. Therefore, in almost all cases the limits were taken as the region where the last Guinier-Preston zones were observed. Errors due to beam broadening and interference from large diameter ($\sim$ 25 nm) and high-Ag content parti-

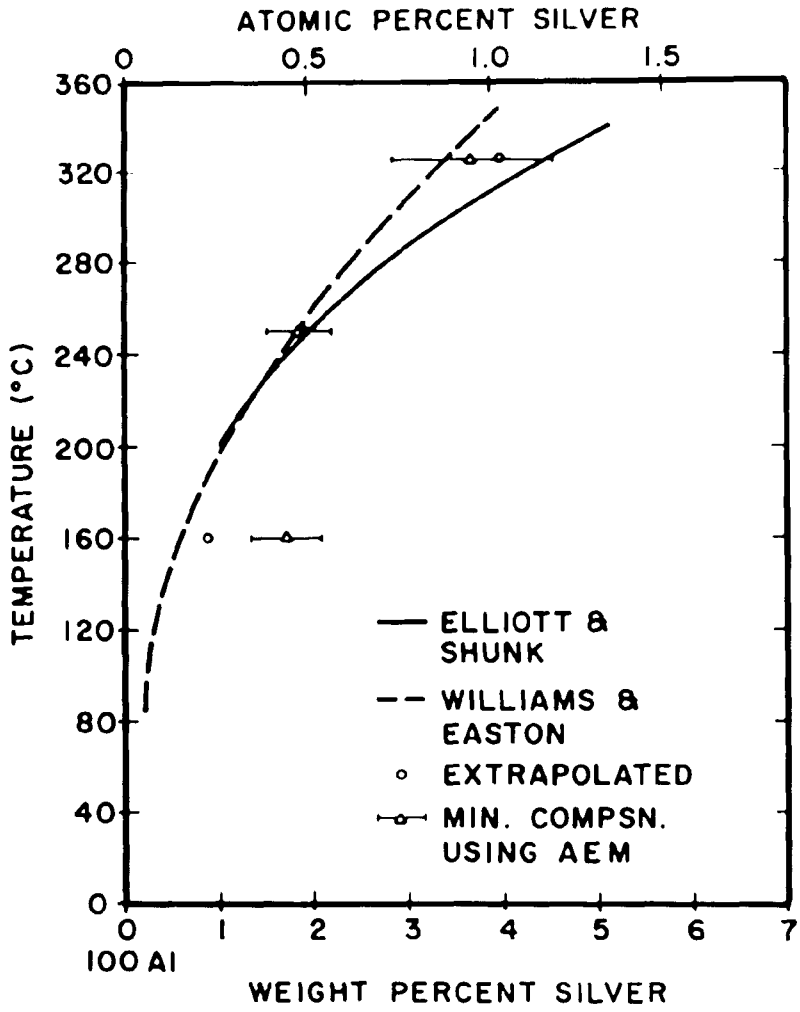

Fig. 47: Same as Fig. 46 but a further comparison is made with a single actually measured (using AEM) minimum composition obtained at each ageing temperature.

cles [~ 90 wt% Ag as per Gragg and Cohen (1971)], would also occur, but cannot be avoided (see Section V A). Asymmetric and steep concentration profiles were disregarded. Occasionally, if two different concentrations were obtained on either side of the grain boundary, an average value has been reported. At least three compositions were determined at each ageing temperature, and an average value determined. Table XI shows these results, and also gives the errors associated with each point determined using a student t distribution within a 95% confidence interval.

Table XII shows a comparison of the values obtained during this investigation with those of Baur and Gerold (1962), the values of Borelius [as reported by Baur and Gerold (1962)] and the results given by Gerold (1963) are also tabulated. These results have been plotted in Figure 48(a) and (b).

TABLE XI

Determination of the Metastable Guinier-Preston Zone Solvus Line from AEM Concentration Profiles at the Edge of the WPFZ in Aged Al-Ag Alloys

Temperature	Profile Number	Solute Composition at Edge of WPFZ, wt% Ag	Guinier-Preston Zone Solvus Limit wt%/(at%) Ag*
160°C (433 K)	3036	—	
	3025	Asymmetric PFZ	
	2896	4.5	
	2890	4.5	
	2888G	--	
	2888W	--	
	2883	4.5	4.83 ± 1.43
	4172	"Steep" profile	(1.25 ± 0.36)
250°C (523 K)	3380	6.5	
	3374	9.0	
	3319	8.0	
	3248	--	
	24M	7.0	8.7 ± 3.2
	3144	13.0	(2.33 ± 0.82)
325°C (598 K)	3493	--	
	3356	--	
	3894	9.75	
	3989	11.0	10.58 ± 1.79
	3990	11.0	(2.87 ± 0.45)

*Errors determined using a student t distribution at a 95% confidence interval about the mean.

TABLE XII

Comparison of Results Obtained From the Determination of the Metastable Guinier-Preston Zone Solvus Line with Data of Other Investigators for Al-Ag Alloys

Investigator	Temperature (°C)	Silver Concentration at%	wt%
Baur & Gerold (1962)	23	0.2 ± 0.35	0.8 ± 1.38
	100	0.68 ± 0.33	2.66 ± 1.31
	140	0.71 ± 0.04	2.78 ± 0.16
	175	1.07 ± 0.60	4.14 ± 2.36
	226	0.83 ± 0.15	3.24 ± 0.6
	300	1.33 ± 1.30	5.11 ± 5.0
Borelius as per Baur & Gerold (1962)	312	3.0	11.0
	350	4.0	14.28
	380	6.5	21.75
Gerold (1963)	100	0.04	0.16
	140	0.22	0.87
	175	0.88	3.43
	225	1.2	4.63
	300	2.16	8.11
This Study	160	1.25 ± 0.36	4.83 ± 1.43
	250	2.33 ± 0.82	8.7 ± 3.2
	325	2.87 ± 0.45	10.58 ± 0.45

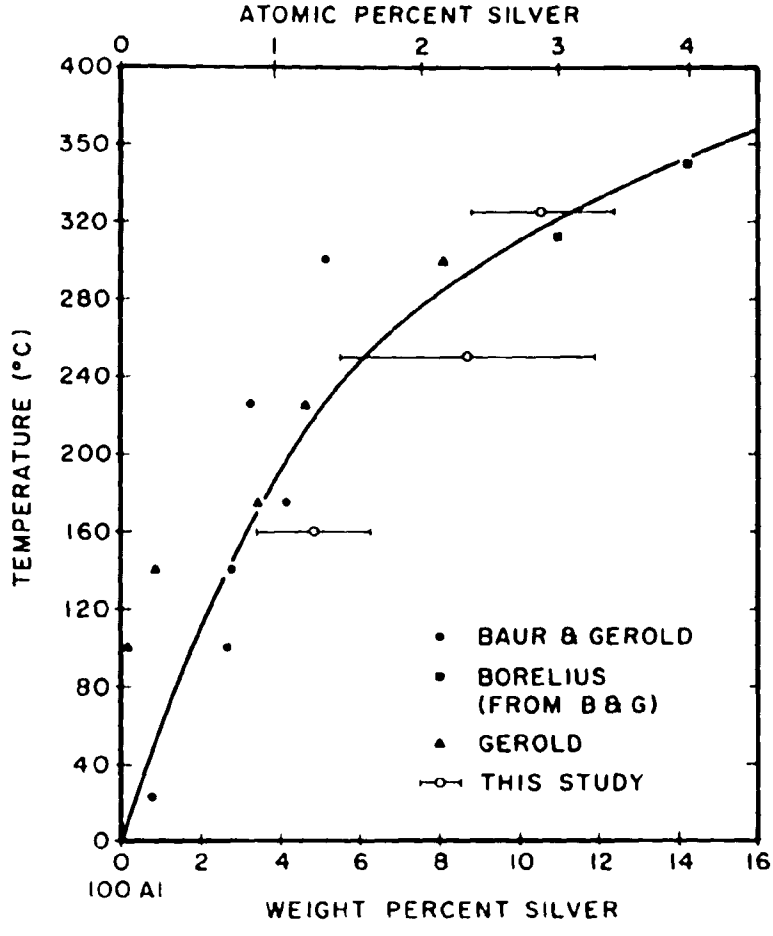

Fig. 48(a): Comparison of the metastable Guinier-Preston zone solvus line with previous investigations.

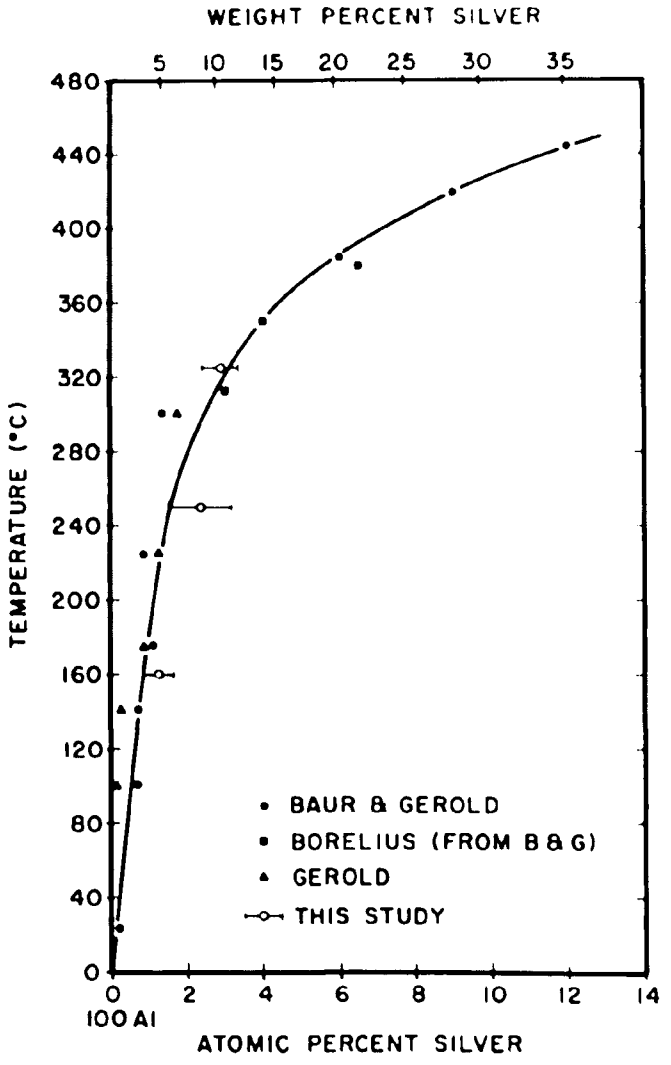

Fig. 48(b): Same as Fig. 48(a), however on a different scale.

V. DISCUSSION

A. AEM Profiles

AEM microanalysis across grain boundary PFZ showed, that in aged Al-Ag alloys, the composition of thin foils in regions far away from the boundaries is, within experimental error, the composition of the bulk alloy, as determined using the EPMA. This is true for concentration profiles taken both in the "matrix" region as well as across the GPFZ. As the grain boundary was approached, there was a reduction in solute content, within the regions corresponding to the WPFZ, to a value at the grain boundary which corresponds to that given by the equilibrium phase diagram. This is a clear indication, as proposed by Clark (1964), that the GPFZ would be solute rich, but precipitate-free, and that the WPFZ would be solute depleted, as a result of a concentration gradient set up near the grain boundary.

One of the major problems associated with AEM microanalysis is that of defining the exact region of generation of x-rays detected by the energy-dispersive x-ray analyzer (EDAX) within the thin-foil; this has been pointed out in Section III F (v). It is mandatory that the foil be kept perfectly normal to the electron beam during analysis. However, this was not always the case, as the specimen had to be tilted in order to make the boundary parallel to left-hand traverse of the microscope ('normal to the electron beam'), or to make the grain boundary fringes disappear or converge to a single fringe. The effect of specimen tilt on the uncertainty in-

volved in the accuracy of microanalytical data has been considered qualitatively by Williams (1980). The problem is associated with the generation of continuum x-rays during microanalysis from within the thin-foil. With increasing tilt from the normal position (perpendicular to the electron beam) regions of the specimen away from the area of interest may be fluoresced. This effect is shown schematically in Figure 49. Increasing the angle of tilt would increase the effect, especially as the thin-foil is wedge-shaped, such that fluorescence will occur in the thick regions of the foil adjacent to the thin area of interest.

Although very small probe diameters (5-10 nm) were commonly used during microanalysis, effects of beam broadening do not restrict x-ray generation to that extent. Commonly, depending on the thickness of the area analyzed, microchemical information was obtained from regions as large as 50 nm, i.e., the extent to spatial resolution.

Figure 50 shows a schematic illustration of this effect with superimposed effects of beam broadening. Depending upon the specific specimen volume being analyzed and hence the volume fraction of the Guinier-Preston zones intersected by the beam, the intensity of x-rays detected within the excited volume could be higher than that corresponding to the actual value of the average solute concentration in the bulk alloy. A theoretical analysis of this problem has been considered by Zaluzec et al. (1980) in which a correction is applied to account for interference from matrix precipitates.

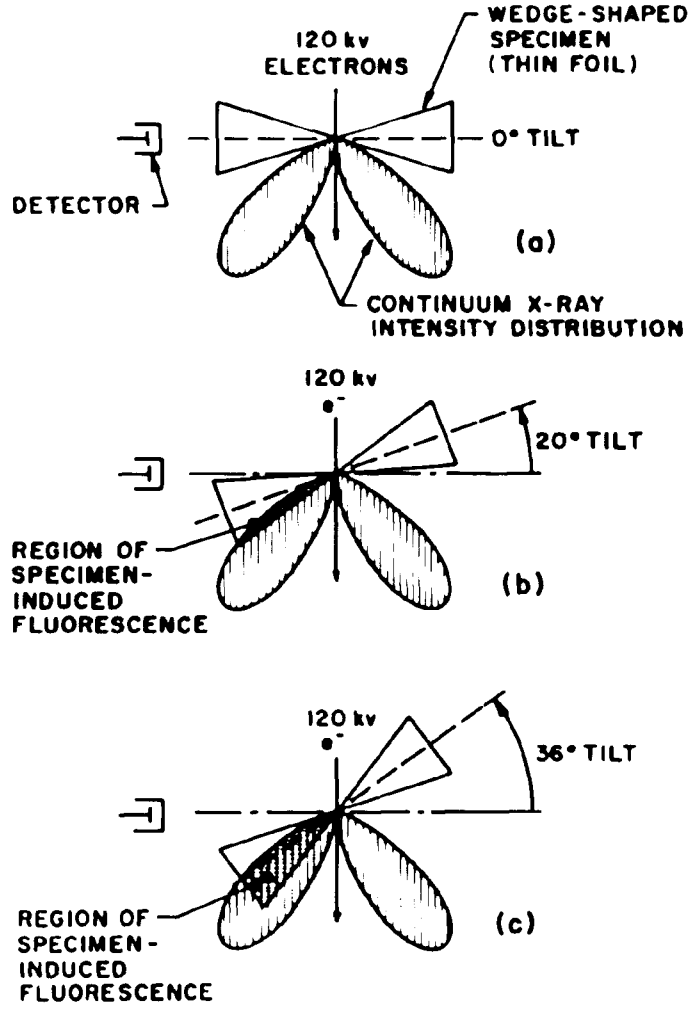

Fig. 49: Schematic indicating the effects of specimen induced fluorescence by continuum x-ray generation from within the thin foil at 120 kV. [After Williams (1980)].

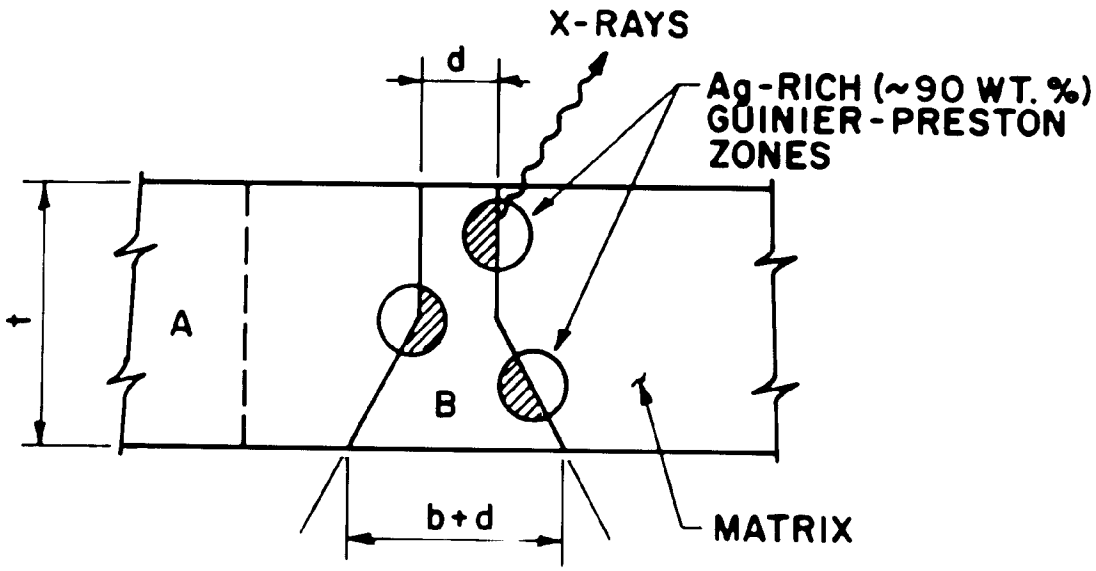

Fig. 50: Schematic diagram illustrating interference from the Ag-rich Guinier-Preston zones during microanalysis with superimposed effects of beam broadening. Region B registers a higher Ag content than region A where the zones are absent.

The type of correction outlined by Zaluzec cannot however be applied in this study as there is always copious precipitation of Guinier-Preston zones present within the matrix. This effect was most pronounced in some of the profiles taken across the GPFZ in alloys aged at 325°C. The relatively large (10-25 nm) Ag-rich (~ 90 wt%) Guinier-Preston zones present in the matrix would then interfere with the quantitative analysis of the area within the GPFZ, giving a much higher-than-average composition.

Other factors which might affect AEM microanalysis are specimen contamination due to deposition of hydrocarbons used in the vacuum system of the microscope, specimen drift, specimen quality, spurious x-rays from the specimen holder or microscope column and the alignment of the microscope.

B. Interpretation of Deformation Experiments

Deformation experiments were performed using samples that had been aged at 160°C for 50 hrs. and were known to contain well-defined GPFZ about 1-3 μm wide (as seen in micrographs of thin-foils of the same heat-treated batch of specimens). The results of examination of foils which had been deformed, then given a 2 hr. ageing treatment at 160°C clearly indicated the enhanced rate of γ' precipitation presumably on heterogeneities introduced by deformation. The original GPFZ could be easily delineated by the large γ' precipitates formed during the first ageing treatment and the second thermo-mechanical cycle caused precipitation of γ' right up to the edge of the WPFZ. Conversely, this result indicates that precipitation of γ' within the GPFZ is normally pre-

vented because of the lack of heterogeneous nucleation sites. This could be due to the rapid migration of excess vacancies to the grain boundary such that the diminished vacancy concentration near the grain boundary precludes the formation of vacancy clusters and helical dislocations necessary for the nucleation of γ' phase. Deformation treatments tend to introduce dislocations and point defects and the subsequent ageing treatment causes considerable solute atom/vacancy redistribution so that precipitation of γ' can be induced. The γ' plates form by the usual mechanism (see Section II(c)). The solute atoms may be provided by the concomittant dissolution of Guinier-Preston zones in the vicinity of the newly formed γ' plates, within the GPFZ.

B. Proposed Model for PFZ Formation

Two distinct regions (zones) free of γ' precipitates, were observed by TEM/AEM investigation to be present in all specimens that had been solution treated, water-quenched, and aged at elevated temperatures (below the Guinier-Preston zone solvus). These regions consist of a narrow "white" zone $\sim$ 50 - 240 nm wide, immediately adjacent to the grain boundary and a surrounding "grey" zone 1 - 3 μm wide. In all cases studied, the width of the WPFZ is strongly dependent upon the ageing time and temperature. The solution treatment temperature and the time between the water-quench and ageing was kept almost constant so that these variables were not investigated.

No grain boundary precipitation was observed in samples that had been freshly quenched. An AEM concentration profile across a grain boundary in such a sample did not indicate any appreciable solute segregation or depletion. It was also observed that the limits of the WPFZ on either side of the grain boundary were well-defined in underaged alloys (alloys aged to less than the γ' peak hardness, e.g., 50 hrs. at 160^{o}C), although a size distribution of the Guinier-Preston zones was observed in certain cases at higher temperatures. The limits of the GPFZ were not always well-defined and isolated γ' precipitates were observed within the GPFZ in some specimens.

Although the widths of the PFZ were found to be a function of the misorientation between the two grains, no attempts were made to study this effect.

AEM concentration profiles clearly showed that considerable solute depletion had occurred within the WPFZ, immediately adjacent to the grain boundary and hence, it may be concluded that the WPFZ is caused by effects of lack of solute. The GPFZ, or the region between the outer limits of the WPFZ and the area where γ' precipitates are observed, see Figure 51, possesses an approximately constant solute concentration, equal to that in the bulk of the alloy. On the basis of the above observations, a model is proposed to explain the mechanism of formation of these PFZ:

During homogenization, solute atoms and vacancies are presumed to be randomly distributed in the substitutional solid solution.

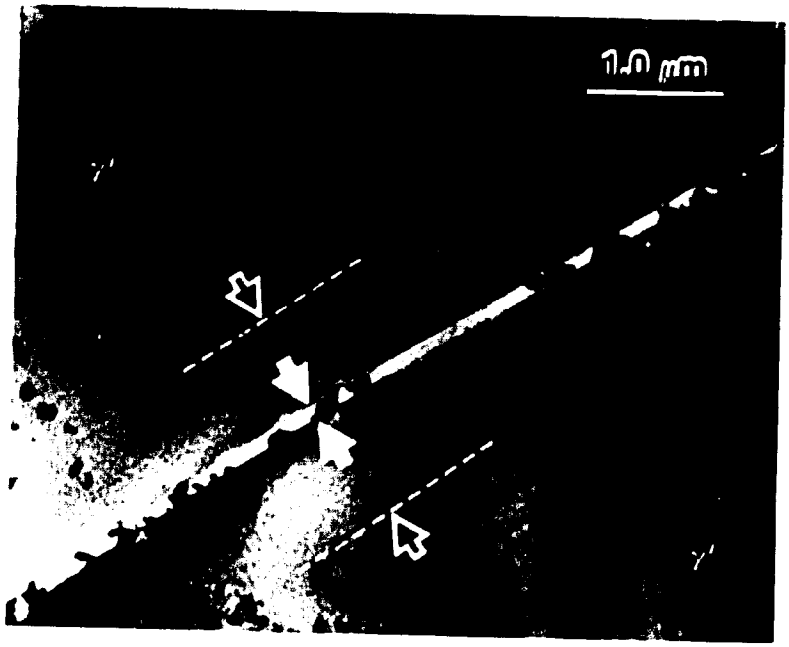

Fig. 51: A typical microstructure of a sample aged at 160°C for 50 hrs. Note the two distinct PFZ around the grain boundary, the WPFZ (inner arrows) and the GPFZ (outer arrows) free of γ' but containing Guinier-Preston zones.

MODEL FOR FORMATION OF PFZ IN AGED AL-AG ALLOYS

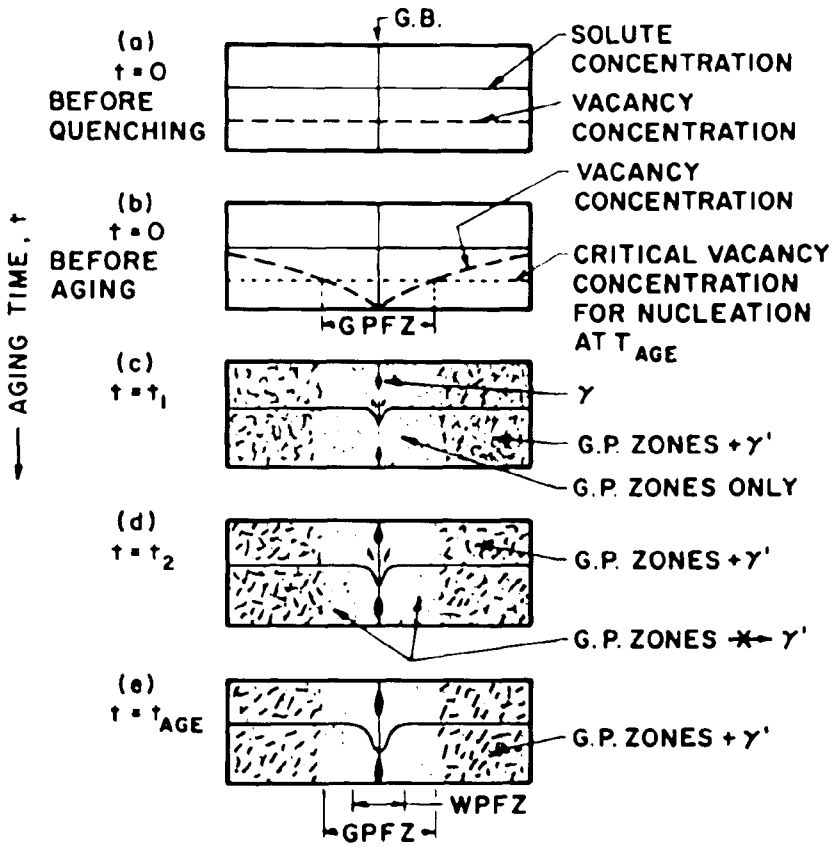

Fig. 52: Model for formation of PFZ in aged Al-Ag alloys.

Both an equilibrium solute concentration and a vacancy concentration are established such that, at the nominal composition of the alloy, the solute concentration is greater than the vacancy concentration (Figure 52(a)). Immediately upon quenching from the solution heat-treatment temperature or during the early stages of ageing, the supersaturated solid solution will tend to eject excess vacancies and solute atoms. Two clustering reactions may take place [Katz and Ryum (1981)]: clustering of solute atoms, i.e., the process of "preprecipitation" [Walker and Guinier (1953), Guinier (1956), Guinier (1959)] occurs, and concurrently the aggregation of vacancies may take place to form vacancy clusters [Smallman et al. (1959/60)]. The solute clusters continue to grow until they are large enough to be identified as matrix-coherent and solute-rich Guinier-Preston zones. As the temperature is drastically lowered during the quench, the vacancy concentration should decrease in order to maintain equilibrium. The excess vacancies condense to form dislocation loops or migrate to dislocations causing climb. Others may be eliminated at the grain boundary, so that a diminishing vacancy concentration gradient is set-up adjacent to it [Figure 52(a)].

The quenching and ageing temperatures used in the present study were carefully chosen with respect to previous investigations. The quenching temperature used in this investigation is less than both, the Guinier-Preston zone solvus temperature ["Thermodynamic model," Lorimer and Nicholson (1966) and Unwin et al., (1969)] and the critical temperature necessary for homogeneous nucleation with-

out the help of excess vacancies ["Kinetic Model," Jacobs and Pashley (1969)], and the ageing temperatures used in this study were all below the Guinier-Preston zone solvus temperature for the composition of the alloy [Borelius, as per Baur and Gerold (1962)].

Upon ageing, nucleation of the Guinier-Preston zones will take place homogeneously [possibly by spinodal decomposition, see Ohta and co-workers (1978)] throughout the matrix and (since solute depletion has not yet occurred) right up to the grain boundary. It is believed, following Turnbull and coworkers (1957, 1960) that the clustering reaction and the rate of Guinier-Preston zone formation would be enhanced in the presence of the quenched-in vacancies. The Guinier-Preston zones adjacent to the grain boundary will draw solute atoms from the matrix, as will the Guinier-Preston zones inside the grain. Hence some "localized" solute depletion will occur in the immediate vicinity of the grain boundary. The growth of these Guinier-Preston zones would be highly competitive, with concomittant dissolution of the smaller ones. The Ag atoms leaving such zones would then immediately begin to reform or redeposit on pre-existing clusters.

During the same period, the γ-phase nucleates at the grain boundary. As it is the equilibrium phase, it is stable with respect to the Guinier-Preston zones and grows by draining solute atoms from the matrix, i.e., from the immediate vicinity of the grain boundary. Solute atoms would then diffuse to the grain

boundary by volume diffusional-controlled processes and then travel along the grain boundary at higher diffusion rates, viz. the "collector-plate" mechanism can be presumed to be operative. See Figure 52(c). Thereafter, in the immediate vicinity of the grain boundary the WPFZ will begin to be established, devoid of excess solute. The grain boundary precipitates will continuously "pull-in" solute atoms from within the WPFZ. The nature of the solute concentration profile might possibly depend upon the structure and misorientation of the grain boundary due to the influence of these parameters on the nucleation of grain boundary precipitates. The WPFZ is caused only by effects of solute depletion and therefore solute atoms will migrate only towards the grain boundary, since the WPFZ is depleted with respect to the Guinier-Preston zones but supersaturated with respect to the equilibrium γ phase present at the grain boundary. Consequently, as suggested by Clark (1964), the spatial extent of solute depletion is indicated roughly by the limit of Guinier-Preston zone formation; this composition corresponds to the composition of the metastable solvus line at the ageing temperature. The composition within the WPFZ will decrease from the value at its outer boundaries to the equilibrium (solid) solubility limit of Ag in Al at the grain boundary.

The Guinier-Preston zones will compete for survival during the early stages of ageing. As competition amongst these zones would cause the smallest zones to preferentially dissolve in favor of

larger ones, this can explain the narrow gradation in sizes observed in some specimens. This effect appears more pronounced at higher temperatures.

Figure 23 can be used to demonstrate that the limits of the WPFZ are given by the Guinier-Preston zone metastable solvus line and that competitive growth of these Guinier-Preston zones occurs in these regions. The micrograph shows a grain boundary WPFZ formed during an ageing treatment of one-half hour at 250^{o}C (523 K), (outer arrows). Excessive heating (for about 20 mins.) in the ion-beam thinner has caused reprecipitation within the original WPFZ and a gradual gradation in sizes is clearly observed. Reprecipitation, such as seen in Figure 23 has been studied in Al-Li alloys by Njegic and Williams (1979) when temperatures in excess of 140^{o}C (413 K) have been deduced to have been reached during ion-beam thinning. This is equivalent to a second ageing treatment at a lower temperature. Applying the same interpretation to the Al-Ag system, the composition of the matrix in metastable equilibrium with the Guinier-Preston zones at the second ageing temperature (say > 140^{o}C) is higher in Al than that at the first ageing temperature, i.e., at T_1 (C_1) there is excess Ag over the composition at temperature T_2 (C_2). The excess Ag will be ejected and reprecipitation occurs (inner arrows) within the original WPFZ, see Figure 53.

AEM microanalysis of the GPFZ indicated that no significant solute depletion occurred during ageing. This zone is therefore in all probability caused by effects of vacancy depletion. This can be explained on the basis that the grain boundary acts as an effi-

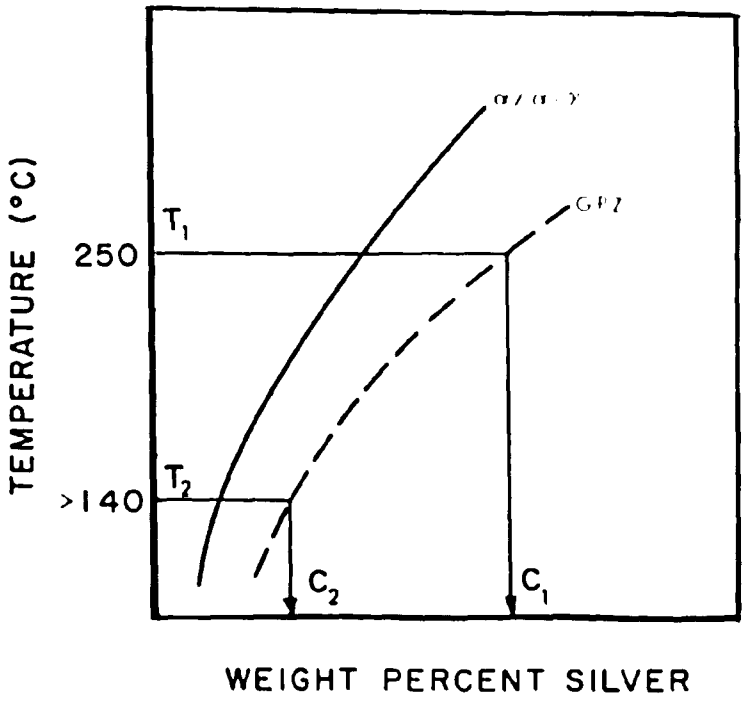

Fig. 53: Schematic diagram to illustrate reprecipitation of the Guinier-Preston zones due to excessive heating in the ion-beam thinner in a WPFZ (Fig. 23). The $\alpha/\alpha+\gamma$ solvus and the Guinier-Preston zones metastable solvus (GPZ) are shown. See text for details.

cient vacancy sink and that during the quench from the solution heat-treatment temperature, "quenched-in" excess vacancies, in the regions adjacent to the grain boundaries would migrate to them, see Greenwood (1976). These regions would have a lower vacancy concentration than the balance of the grain, setting up a vacancy concentration gradient. The limits of the GPFZ are then given by the intersection of the diminishing vacancy concentration gradient and the horizontal used to describe a critical vacancy concentration necessary for the formation of vacancy clusters or nucleation sites for γ' precipitates [see Figure 52(c)]. Upon examination of TEM/AEM micrographs, it was found that the GPFZ does contain Guinier-Preston zones; this is not inconsistent with the concept of vacancy depletion because homogeneous nucleation of Guinier-Preston zones is possible even in the absence of excess vacancies, as the quenching and ageing temperatures are below the "critical temperature" defined by the kinetic model of Jacobs and Pashley (1969). Although the GPFZ is thought to be vacancy depleted, considerable vacancy movement must still occur, during and after the quench to allow diffusion of Ag atoms to form these Guinier-Preston zones.

Detailed examination of the microstructures of quenched and aged alloys indicated that the GPFZ are devoid of clustered vacancy defects such as dislocation loops, helical dislocations and similar defects necessary for the heterogeneous nucleation of γ'. Such an effect is clearly seen in Figure 51 where the limits of the GPFZ are shown by dotted lines. It must be realized, however, that

quenching strains or non-uniform localized vacancy concentrations may give rise to a few defect clusters or dislocations within the GPFZ, but outside the WPFZ, as may be evident in the same figure. Such dislocation loop-free regions have been observed in thin foils of pure Al by Hirsch et al. (1958). Smallman et al. (1959/60) have observed the reduced tendency for spiral dislocations, vacancy clusters and dislocation loops to be present in the immediate vicinity of grain boundaries in aged Al-Ag alloys. A similar study of dislocation loop-free regions around grain boundaries has been made by Frank and co-workers (1961). Both groups of workers have discussed the importance of such heterogeneities in the nucleation of precipitates. It is proposed that the absence of these heterogeneous sites prevents the nucleation of γ' precipitates within the GPFZ. Also, as γ' precipitates do not nucleate on the Guinier-Preston zones [following Nicholson and Nutting (1961)], no γ' precipitates can form within the GPFZ. It can be concluded therefore the GPFZ is caused essentially by the absence of vacancy clusters such as dislocation loops and helical dislocations which serve as nucleating sites for the γ' precipitates. This occurs as a result of a decrease in vacancy supersaturation around grain boundaries and is due to the migration of excess vacancies to such sinks. Thus the GPFZ may be described as solute-rich, but precipitate-free (of γ' only), as postulated by Clark (1964).

As the extent of solute depletion will increase with increasing ageing times and temperatures, the width of the WPFZ will consequently increase [Figure 52(c)-(e)]. The final microstructure

and solute concentration profile for the ageing time investigated will appear as shown in Figure 52(e). Ageing the sample for longer times and over peak γ' hardness will cause an extension or smearing out of the WPFZ. Compare the profile shown in Figure 42 to that in Figure 43.

In short, both the solute depletion and vacancy depletion mechanisms contribute to the formation of the PFZ in aged Al-Ag alloys. The effect of each mechanism is used to explain the formation of the two distinct PFZ seen during the early stages of ageing. With increasing ageing time and temperature, solute depletion effects will be more pronounced, so that the GPFZ will eventually disappear as a result of the lengthening and thickening of γ' precipitates near the grain boundary. Dissolution of the Guinier-Preston zones will occur in favor of the growing γ' precipitates, eventually providing a situation such that they are lost as characteristic microstructural features which are used to delineate the limits of the WPFZ.

Finally the formation of asymmetric PFZ (WPFZ in particular) can be explained in terms of the precipitation at the grain boundaries. The microstructural evidence indicates that the discontinuous precipitation reaction leads to migration of the grain boundary at all three temperatures investigated. At 160^{o}C, however, the reaction is not very pronounced, giving the impression that the boundary has migrated to accommodate the grain boundary allotriomorphs. At high temperatures, the grain boundaries are mobile and

any movement causes a sweeping effect whereby solute atoms diffuse to the grain boundary allotriomorph from the grain into which the boundary migrates. The most common effect is a migration in a single direction, with the width of the WPFZ on the other side unchanged. However evidence for discontinuous precipitation causing asymmetric PFZ on either side is also observed. The net result is an asymmetric solute concentration distribution.

The possibility of the discontinuous precipitation reaction influencing the solute distribution (or concentration profile) and vice versa, should therefore, not be ruled out and needs further examination.

A similar observation to support the above model has been made by Ryum (1981). He has indicated that based on the composition of the alloy investigated, the relative amounts of solute and vacancies would be such that no PFZ could be formed in freshly quenched samples of Al-Ag. With increasing times at a given ageing temperature the width of the PFZ would increase on account of solute depletion by grain boundary precipitates.

(i) Re-examination of Clark's model

The results of the present investigation are similar to the description of PFZ formation in aged Al-Ag alloys suggested by Clark (1964). Thus the contribution of both, the solute depletion and vacancy depletion mechanisms to give rise to co-existing solute-rich and solute-impoverished areas around the grain boundary was confirmed. However Clark's belief that the vacancy deple-

tion mechanism would be dominant at lower temperatures and solute depletion would cause the PFZ at higher temperatures, is not perfectly correct. Clark suggested the co-existence of both effects for samples aged at 160°C. Since his specimens at 325°C were aged for 144 hours, these were clearly in an overaged condition and he was therefore only able to detect a WPFZ which he attributed to a solute depletion effect. In such overaged specimens, considerable solute redistribution occurs near the grain boundary as well as within the grains. The γ' or γ precipitates within the matrix lengthen and cause concomittant dissolution of nearby Guinier-Preston zones. Hence because of the long ageing treatment no conclusions can be drawn regarding the absence of vacancy depletion effects in this case.

Had the 325°C sample been aged for much shorter times ($\lesssim$ 5 minutes), a solute-rich GPFZ, similar to the one he observed at 160°C would be seen. As no TEM micrographs have been included in Clark's paper for the 144 hours ageing treatment or 325°C no further comments can be made about the extent of the WPFZ.

Clark has observed that considerable growth of the intragranular γ' precipitates occurs upon ageing for longer times at 160°C (1200 hours versus 120 hours). This growth occurs by the extension of the γ' precipitates into what would be defined as the γ'-free zone into specimens aged at 120 hours. Therefore, rather than concluding that solute depletion effects are responsible for causing PFZ at higher temperatures, Clark should have examined

alloys aged for various times at 325^{o}C. Hence the effects of vacancy depletion should always be considered while studying PFZ formation, because a diminishing vacancy concentration gradient will always be established near a grain boundary, during or immediately after the quench from the solution heat treatment temperature, irrespective of the final ageing temperature.

However, Clark's idea that the limits of the WPFZ would be dictated by the composition of the miscibility gap for Guinier-Preston zone formation, was confirmed using AEM and was utilized to determine the Guinier-Preston zone metastable solvus line.

(ii) Re-examination of Raghavan's model

Raghavan (1980) has suggested two separate and different models for PFZ formation in aged Al-Zn-Mg and Cu-Ni-Nb alloys. The grain boundary PFZ are primarily caused by the vacancy concentration gradient in the Al-Zn-Mg alloys and a solute depletion mechanism in the Cu-Ni-Nb alloys. Effects of a solute diffusion flux were used to explain the coarsening of PFZ boundary precipitates in Al-Zn-Mg alloys. In Cu-Ni-Nb alloys, the solute flux is directed only towards the grain boundary and hence no preferential coarsening of precipitates at the edge of the PFZ occurs. These effects have been explained in terms of the differences in solid solubility between the precipitates at the grain boundary and within the matrix. When this difference is large, as in the case of Cu-Ni-Nb alloys, coarsening of the PFZ boundary precipitates does

not occur. In case of the Al-Zn-Mg system, a superimposed vacancy concentration gradient would create a situation where solute atoms can move in two directions.

Preferential coarsening of either the γ' precipitates at the edges of the GPFZ or the Guinier-Preston zones at the edges of the WPFZ was not observed to occur in aged Al-Ag alloys; this is clearly illustrated in micrographs included in the text. Clark's study also makes no mention of a coarsening effect. The lack of coarsening of the Guinier-Preston zones can be explained in terms of a unidirectional flow of solute atoms to form the grain boundary γ precipitates. This causes a solute depleted WPFZ, and a γ'-free but solute rich GPFZ due to lack of nucleation sites, an effect of a diminishing vacancy concentration gradient. Vacancies travel only towards the grain boundary, from a distance of ~ 1 to 3 μm around it.

The two models suggested by Raghavan cannot be applied to explain the formation of PFZ in aged Al-Ag alloys, because of the presence of two distinct regions, free of precipitates, a WPFZ caused by solute depletion effects and free of the Guinier-Preston zones and a GPFZ due to lack of γ' formation. Such well-defined, simultaneously co-existing PFZ do not form in either the Al-Zn-Mg or the Cu-Ni-Nb alloys studied by Raghavan.

The PFZ widths in aged Al-Zn-Mg alloys are defined by the vacancy concentration gradient during the early stages of ageing and a diminishing solute supersaturation with continued ageing. In aged Al-Ag alloys, the PFZ are caused by both effects, the diminishing

vacancy concentration gradient defines only the GPFZ and has no effect on the WPFZ; the WPFZ is caused entirely by solute depletion effects due to grain boundary precipitation. The formation of the WPFZ in aged Al-Ag alloys may roughly be compared to PFZ in aged Cu-Ni-Nb alloys while the GPFZ in aged Al-Ag alloys may be compared with Raghavan's model for aged Al-Zn-Mg alloys but without the effects of solute depletion. It therefore appears that a reasonable model to describe the formation of PFZ in aged Al-Ag alloys can be obtained by a combination of parts of both models suggested by Raghavan.

(iii) Re-examination of models by other workers

A very systematic study of PFZ formation in aged Al-Zn-Mg alloys was performed by Nicholson and co-workers [see Embury and Nicholson (1963, 1965), Lorimer and Nicholson (1966) and Unwin, Lorimer and Nicholson (1969)]. They presented a qualitative explanation for the formation of PFZ by assuming that at a given ageing temperature, a critical vacancy concentration was necessary for the nucleation of a precipitate. In addition to a certain vacancy supersaturation, a certain solute supersaturation was also necessary in order that the precipitate might form. The boundary of the PFZ would then be given by the intersection of the vacancy concentration gradient at the grain boundary and a critical vacancy concentration required (and therefore also the solute supersaturation, as they are complimentary) for the nucleation of precipitates. Therefore precipitation would occur in the grain where vacancies in excess of the equilibrium value would be available for nucleation.

An experiment performed by the investigators consisted of ageing a specimen above the Guinier-Preston zone solvus temperature after quenching it into water from the homogenization temperature. A further ageing treatment for a longer period below the Guinier-Preston zone solvus caused copious nucleation of precipitates within the original PFZ from the previous ageing treatment. The investigators indicated that the copious precipitation after the second ageing treatment is not related to decreasing solid solubility. But rather, they concluded that this can be explained in terms of the high stability of the vacancy concentration gradient, as a consequence of a high (~ 0.3 eV) binding energy between the vacancy and the solute atom. Vacancies and solute atoms that were not active nuclei at the higher ageing temperature (first ageing treatment) reform large clusters and act as nuclei when the ageing temperature is lowered (during the second ageing treatment). The binding energy causes the solute atom/vacancy pairs to migrate slowly after the quench. Reprecipitation would then occur because of the availability of such pairs and increased solute supersaturation.

Nicholson and co-workers cite Polmear's work (1960/61) on the addition of Ag to Al-Zn-Mg alloys, so that Ag atoms stabilize the solute atom/vacancy clusters in the matrix and prevent vacancy flow to the grain boundaries. Thus the addition of Ag eliminates the PFZ around the grain boundary and available vacancies reduce the critical nucleus size for precipitation, creating a fine dispersion of precipitates. They indicated that the width of the PFZ

depends on a solute atom/vacancy flux and the ageing temperature when compared with the Guinier-Preston zone metastable solvus temperature for a given alloy composition. In the follow-up paper on their previous work Unwin et al. (1969) recognized the fact that solute depletion would occur around grain boundaries due to grain boundary precipitation. A solute concentration profile must thus be superimposed upon a vacancy concentration gradient, if solute depleted PFZ are formed.

Based on the hypothesis of Nicholson and co-workers, a simple qualitative model could possibly be used to describe the formation of PFZ in the Al-Ag system. Immediately after the quench and during the early stages of ageing, the nucleation of Guinier-Preston zones would occur throughout the grain except in the immediate vicinity of the grain boundary which acts as a vacancy sink. Assuming that the Guinier-Preston zone in this system is a complex solute atom/vacancy cluster, a critical vacancy concentration would be required for the precipitation of Guinier-Preston zones. This, critical vacancy concentration together with the superimposed vacancy concentration gradient, would decide the width of the WPFZ. By a similar argument, the GPFZ is defined by a critical vacancy concentration necessary for the heterogeneous nucleation of γ' precipitates on vacancy clusters. In addition, a superimposed solute depletion gradient, created as a result of grain boundary γ precipitates must be considered causing an impoverishment of solute atoms within the WPFZ. The extent of the WPFZ will increase with increasing ageing times and temperatures because

of enhanced diffusion. This may be used to explain the gradation in Guinier-Preston zone sizes at the edge of the WPFZ, especially at high temperatures. The limits of the WPFZ would then be given by the limits of Guinier-Preston zone formation.

As described above, this alternate model for the formation of PFZ in aged Al-Ag alloys is based upon the hypothesis of Nicholson and co-workers. The use of this alternate model therefore depends upon the assumption of both a high solute atom/vacancy binding energy as well as the need for an excess vacancy concentration. Nicholson and Nutting (1961) have proposed that the finite binding energy cannot be explained by the presence of elastic forces, because the atomic diameters of Ag and Al are nearly the same, but there may be an electrical interaction as proposed by Cottrell et al., (1953) or a chemical interaction as proposed by Hart (1958). Jacobs and Pashley (1969) have indicated that excess vacancies are not required for the homogeneous nucleation of Gunier-Preston zones as the quenching and ageing temperatures are below the "critical temperature" defined in their kinetic model. That excess vacancies may not be necessary for the homogeneous nucleation of Guinier-Preston zones, has also been proposed for the Al-Zn-Mg system by Abe et al. (1972) and Asano and co-workers (1976). Therefore the nucleation of Guinier-Preston zones cannot be adequately explained by the thermodynamic model of Nicholson and co-workers.

Nicholson and Nutting (1961) used the concept of a finite binding energy between a solute atom and vacancy to explain the formation of γ' precipitates (see Section II, C). A similar mechanism was proposed by Hren and Thomas (1963) who assumed that the binding energy (E_B) would have a maximum value of ~ 0.4 eV. It was postulated that immediately after the quench or during the early stages of ageing, solute atom/vacancy pairs would migrate to vacancy sinks such as the free surface, dislocations and grain boundaries. This would cause annihilation of the vacancies and precipitation as a result of an aggregation of solute atoms. Hren and Thomas (1963) did not observe any preferential precipitation on the free surface and proposed that the vacancies were entrapped within the Guinier-Preston zones. Careful experimental studies by Wert et al. (1979) did not show any PFZ on the exterior surfaces of samples in aged Fe-Nb alloys. Hence it must be concluded that excess vacancies must migrate to cluster or annihilate at dislocations or migrate to grain boundaries. As mentioned above, annihilation of vacancies at dislocations has already been considered in the formation of the γ' precipitate. Vacancy clusters are dislocation loops, or collapsed discs of vacancies, so that they could act as nucleating sites for the γ' phase. The limits of the GPFZ would then be consequently defined on the limits for the available nucleation sites for γ' precipitates. Hence attention needs to be focused upon segregation of Ag atoms at the grain boundary.

Hanneman and Anthony (1969) have presented a model by which a coupled flow of solute atoms and vacancies could give rise

to solute enrichment or depletion at grain boundaries for non-equilibrium conditions of rapid cooling and quench ageing. Non-equilibrium segregation or solute enrichment would occur at grain boundaries, as a result of the vacancy flux, if the binding energy between the vacancy and solute atom (E_B) is larger than kT where k is the Boltzmann constant and T is the absolute homogenization temperature.

Lomer (1958) had postulated that the vacancy concentration in a binary alloy system is given by the following:

$$x' = A \exp\left(\frac{-E_f}{kT}\right) \cdot \left[1 - 12\ c + 12\ c \exp\left(\frac{E_B}{kT}\right)\right] \qquad (13)$$

where E_f is the vacancy formation energy in the solvent and c is the atomic fraction of the solute atoms. A is a constant. If $x = A \exp\left(\frac{-E_f}{kT}\right)$ and A is tentatively assumed to be equal to unity, with E_f = 0.76 eV, [see Thomas and Willens (1964)], the ratio $\frac{x'}{x}$ can be used to estimate E_B, since

$$\exp\left(\frac{E_B}{kT}\right) = \left\{\left(\frac{x'}{x} - 1\right) + 12\ c\right\} / 12\ c \qquad (14)$$

$$E_B = \left\{\ln\left[\left(\frac{x'}{x} - 1\right) + 12\ c / 12c\right]\right\} \cdot kT \qquad (15)$$

Nicholson and Nutting (1961) using TEM studies, have reported a vacancy concentration of $\sim 10^{-4}$ in a freshly quenched sample from a homogenization treatment temperature of 520°C (793 K) in an alloy containing 15.6 wt% (4.419 at%) Ag, balance Al.

Using E_f = 0.76 eV, k = 8.625×10^{-5} eV/K T = 793 K

$$x = \exp\left(-\frac{0.76}{8.625 \times 10^{-5} \times 793}\right) = 1.5 \times 10^{-5}.$$

As $x' = 1 \times 10^{-4}$, $\frac{x'}{x} = 6.67$

$$E_B = \left| \ln \left(\frac{(6.67 - 1) + 12 \times 0.04419}{12 \times 0.04419} \right) \right| \cdot (8.625 \times 10^{-5} \times 793)$$

or $E_B = 0.17$ eV.

A similar TEM study made by Smallman et al. (1959/60) for an Al-20 wt% (5.58 at%) Ag alloy quenched from 525°C (798 K) showed $x' = 2 \times 10^{-4}$. Using a similar argument, $E_B \simeq 0.2$ eV.

The values of kT can be compared with E_B and are shown below:

Investigators	T°C	kT(eV)	E_B (ev)	E_B/kT
Nicholson & Nutting (1961)	520°C	0.068	0.17	~ 2.5
Smallman et al. (1959/60)	525°C	0.069	0.2	~ 2.9

The values for E_B calculated above agree with the values of 0.13 eV obtained by Murty and Vasu (1969/70) using resistometric techniques, and 0.25 eV reported by Hashimoto (1965) using resistivity measurements. Baur and Gerold (1961) used small angle x-ray scattering in a binary Al-Ag alloy and estimated the binding energy to be less than 0.4 eV. A significantly lower value of 0.08 eV has been reported by Beaman, Ballufi and Simmons (1964), using differential length and lattice parameter measurements.

It is therefore evident that values for E_B measured by the TEM technique is greater than kT and some effects of non-equilibrium segregation must be considered at grain boundaries and vacancy sinks immediately after quenching or during the early stages of ageing. A study of this nature has been carried out in Al-Zn-Mg alloys by Chen et al., (1977) using Auger electron spec-

troscopy. They showed the segregation of Mg atoms at grain boundaries even in overaged alloys, whereas studies by Doig and Edington (1973, 1974) using AEM showed marked solute depletion. An AEM concentration profile across a grain boundary in an Al-Ag thin-foil freshly quenched from the homogenization temperature did not show any significant variation in solute content. In spite of the AEM results, it could be postulated in terms of the E_B versus kT argument that some solute segregation could occur during the quench at the grain boundary, resulting in a few atomic (or perhaps monoatomic) layer(s) of solute.

Based on the preceding discussion, it appears that both the concept of the need for excess vacancies for nucleation and the requirement for a high solute atom/vacancy binding energy are in doubt. The highly diverse values for the binding energy reported in the literature makes the latter condition more uncertain. It is for these reasons, that the first model (Section V.C and Figure 52) based upon the suggestions of Raghavan (1980) and Clark (1964), is favored in order to explain the formation of PFZ in the Al-Ag system.

D. Diffusivity Values

The errors involved in the determination of D_{Ag} in Al by measurement of the half-widths of the solute depleted PFZ may be considerable. The greatest error in the determination of D_{Ag}-values would be in the measurement of the half-width, Y. Almost all the Y values considered were obtained in regions used for AEM analysis, but this was not always the case. Some widths were

measured from TEM micrographs. The thin-foil was not always normal to the beam but slightly tilted in order to bring the Guinier-Preston zones or precipitates on either side of the PFZ in contrast, so that Y could be measured. This does introduce a certain error in Y. Corrections have however been made for errors due to magnification calibration in the microscopes. The values of D_{Ag} in Al agree well with those obtained from extrapolation of high temperature data of Hren and Thomas (1963) and Heumann and Dittrich (1958). Such an extrapolation was necessary because of the lack of low temperature D_{Ag} values and diffusion data in the literature. The activation energy value of Q = 30.08 $\pm$ 1 kcals/mole appears in good agreement with that reported by Heumann and Bohmer (1968) with Q = 28.9 kcals/mole, Anand and Agarwala (1967) with Q = 29.0 kcals/mole, for Ag^{110} diffusion in Al and von Koster and Sperner's (1953) theoretical expression where Q = 30.06 kcals/mole.

E. Phase Diagram Limits

(i) The equilibrium solvus line

AEM concentration profiles across WPFZ were used to determine the solid solubility limit of Ag in Al (or the equilibrium solvus line) at three ageing temperatures of 160°C, 250°C and 325°C.

It was observed that at high temperatures, particularly at 325°C, that ageing for longer times (15 mins. in this case) caused the solute concentration profile within the WPFZ to level off to a gradual flat-bottomed profile rather than a fairly sharp V-shaped profile, as at 160° (compare Figs. 42 and 40). It was also

noted that even after ageing for 50 hrs. at 160°C, the concentration profile remained very steep and V-shaped. The Ag concentration at the grain boundary was well above the solid solubility limit as given by the theoretical expression of Williams and Easton (1974). In one case however, Figure 39 profile 2883, the grain boundary composition reached to a value of 1.725 $\pm$ 0.37 wt%. This indicated that the steep concentration gradients involved at low temperatures, together with shorter ageing times (all alloys were aged to times below γ' peak hardness values) and the narrow dimensions of the WPFZ necessitates the extrapolation technique used. It might be pointed out that because of increased solute diffusion rates at 325°C, where the WPFZ are three to four times wider than those formed at 160°C, such an extrapolation is not required. The broad widths of WPFZ at 325°C permit more readings to be taken across it than at 160°C. It may be pointed out, however, that if the specimens had been aged for longer times (say 1200 hrs. at 160°C following Clark (1964)), much wider WPFZ would have been obtained and such an extrapolation might not have been necessary. Also, it must be realized that an averaging effect must occur when measuring concentrations at the grain boundary due to effects of beam broadening. Regions adjoining the grain boundary possess a higher Ag content than the boundary itself, and so a higher solute content is registered at the grain boundary than is actually present. These effects are more pronounced if during microanalysis, the grain boundary is not perfectly parallel to the

incident beam, or the specimen was tilted at large angles (>10°) to the horizontal.

It was decided therefore to extrapolate all symmetric U-shaped or nearly V-shaped profiles to a terminal composition. Another justification for this extrapolation is the very low solid solubility of Ag in Al at 160°C (0.65 to 0.75 wt%) which is very close to the mass detectability limits of the technique. The extrapolated values are shown in concentration profiles illustrated in the text, and have been included in Table VIII, for those profiles that have not been included, but which were used to determine the solid solubility limit.

(ii) The Guinier-Preston zone metastable solvus line

AEM concentration profiles across WPFZ were also used to determine the composition limits of Guinier-Preston zone formation at the three ageing temperatures of 160°C, 250°C and 325°C (433 K, 523 K and 598 K).

The composition limits of Guinier-Preston zone formation are given by the composition limits of the WPFZ around the grain boundary. There was some difficulty in obtaining the concentration of the matrix in metastable equilibrium with the Guinier-Preston zones at high temperatures, where the limits of the WPFZ are not well-defined due to enhanced solute diffusion compared to that at 160°C. Considerable error is therefore involved in determining the exact composition.

The rate of discontinuous precipitation is greatly enhanced at the high temperatures and causes considerable boundary movement. This sometimes results in a gradation in sizes and hence errors in determining the limits of the WPFZ. Other errors have already been mentioned in Section V. A.

VI. CONCLUSIONS

1. In an aged Al-16 wt% Ag alloy, two distinct regions free of the metastable γ' precipitates are observed, viz. a narrow WPFZ immediately adjacent to the grain boundary and a surrounding GPFZ. The WPFZ is observed to be free of the Guinier-Preston zones as well as the γ' precipitate.
2. Solute depletion occurs within the WPFZ and is caused by the lowering of solute concentration near grain boundaries as a result of grain boundary precipitation.
3. Deformation and subsequent ageing of previously aged samples shows the heterogeneous nucleation of γ' within the original GPFZ, confirming the presence therein of excess solute.
4. Solute depletion is primarily responsible for the formation of the WPFZ. Vacancy depletion effects which lead to the absence of heterogeneous nucleation sites is responsible for the formation of the GPFZ in aged Al-Ag alloys.
5. An estimate of the diffusion coefficient of Ag in Al obtained by equating the half-width of the solute depleted WPFZ in aged alloys, shows good agreement with diffusivity values extrapolated from high temperature. The activation energy for solute diffusion is consistent with a bulk diffusion-controlled mechanism to form grain boundary precipitates.
6. Measurement of the solute content at the grain boundary indicates good agreement with literature data for the equilibrium $\alpha/\alpha + \gamma$ solvus line, indicating local equilibrium to have been obtained at the grain boundary, as well as

demonstrating the utility of the analytical electron microscopy to determine phase boundaries.

7. The Guinier-Preston zone metastable solvus line was determined from the Ag concentration present at the edge of the WPFZ and is in good agreement with previous investigations in the Al-Ag system.
8. The spatial resolution of analytical electron microscopy makes it an appropriate and powerful quantitative technique for the study of the formation of precipitate-free zones in aged alloys.

REFERENCES

Aaron, H. B. and Aaronson, H. I. (1968), "Growth of Grain Boundary Precipitates in Al-4% Cu by Interfacial Diffusion," Acta Metall. vol. 16, p. 789.

Aaronson, H. I. in Decomposition of Austenite by Diffusional Processes, Zackay, V. F. and Aaronson, H. I. (eds.) New York: J. Wiley & Sons, p. 387, 1962.

Aaronson, H. I. and Clark, J. B. (1967), "Influence of Continuous Precipitation Upon the Growth Kinetics of the Cellular Reaction in an Al-Ag Alloy," Sci. Res. Staff, Ford Motor Co. Report No. SL67-44, 16 May 1967.

Abbott, K. and Haworth, C. W. (1972), "The Dissolution of γ Phase in Al-Ag Alloys," Acta Metall. vol. 21, p. 951.

Abe, M., Asano, K. and Fujiwara, A. (1972), "Studies on the Precipitate Free Zone in an Al-Zn-Mg Alloy," J. Jap. Inst. Metals, vol. 36(6), p. 597.

Alm, S. and Kiessling, R. (1962/63), "Cr Depletion Around Grain-Boundary Precipitates in Austenitic Stainless Steel," J. Inst. Metals, vol. 91, p. 190.

Anand, M. S. and Agarwala, R. P. (1967), "Diffusion of Pd, Ag, Cd, In and Sn in Al," TMS-AIME, vol. 239, p. 1848.

Andersen, C. A. and Hasler, M. F. (1965) in X-ray Optics and Microanalysis, IV Intl. Congr. on X-ray Optics and Microanalysis, Orsay, 1965, Castaing, R., Deschamps, P. and Philibert, J. (eds.) Paris: Hermann, p. 310, 1966.

Asano, K., Abe, M. and Fujiwara, A. (1976), "Nucleation of Precipitates in Al-Zn-Mg Alloys," Materials Sci. & Engg., vol. 22, p. 61.

Barrett, C. S., Geisler, A. H. and Mehl, R. K. (1941), "Mechanism of Precipitation from the Solid Solution of Ag in Al," TMS-AIME, vol. 143, p. 134.

Baur, R. and Gerold, V. (1961), "Segregation in the System Al-Ag," Zeit. Metall., vol. 52, p. 671.

Baur, R. and Gerold, V. (1962), "The Exsistence of a Metastable Miscibility Gap in Al-Ag Alloys," Acta Metall., vol. 10, p. 637.

Beaman, D. R., Balluffi, R. W. and Simmons, R. O. (1964), "Measurement of Equilibrium Vacancy Concentrations in Dilute Al-Ag Alloys," Phys. Rev., vol. 134(28), p.A532.

Beerwald, A. (1939), "Diffusion of Various Metals in Al," Zeit. Elektrochemie, vol. 45, p. 789.

Borelius, G. and Larsson, L. E. (1956), "Resistometric and Calorimetric Studies on the Precipitation in Al-Ag Alloys," Arkiv. för Fysik, vol. 11, p. 137.

Chen, J. M., Sun, T. S., Viswanadham, R. K. and Green, J. A. S. (1977), "Grain Boundary Segregation of an Al-Zn-Mg Ternary Alloy," Met. Trans., vol. 8A, p. 1935.

Clark, J. B. (1964), "Electron Probe Test of Two Theories of "Denuded Zone" Formation in Aged Alloys," Acta Metall., vol. 12, p. 1197.

Cliff, G. and Lorimer, G. W. (1972), "Quantitative Analysis of Thin Metal Foils Using EMMA-4, the Ratio Technique," Proc. Fifth Europ. Conf. on Electron Microscopy, Institute of Physics, London, 1972, p. 140.

Cottrell, A. H. (1958) in Vacancies and Other Point Defects in Metals and Alloys, London: Institute of Metals, p. 1.

Cottrell, A. H., Hunter, S. C. and Nabarro, F. R. N. (1953), "Electrical Interaction of a Dislocation and a Solute Atom," Phil. Mag., vol. 44, p. 1064.

Crepaz, E. (1930), "The System Aluminum-Silver," Congress Internationaux de Chimie Industrielle, Comptes Rendue, Brussells, vol. III, p. 371.

Cullity, B. D. (1978) Elements of X-ray Diffraction, 2nd Edition, Reading, MA: Addison Wesley Pub. Co., p. 13.

Dix, E. H., Jr. (1940),"Acceleration of the Rate of Corrosion by High Constant Stresses," Trans. Am. Inst. Mining Met. Engrs., vol. 137, p. 11.

Dobromyslov, A. V. (1972), "Formation Mechanism of γ' Phase in Al-Ag Alloy,", Fiz. Metall. Metalloved., vol. 34(4), p. 729.

Doig, P. and Edington, J. W. (1973), "Low Temperature Diffusion in Al-7 wt% Mg and Al-4 wt% Cu Alloys," Phil. Mag., vol. 28, p. 961.

Doig, P. and Edington, J. W. (1974), "The Influence of Solute Segregation to Grain Boundaries on the Stress Corrosion Susceptibility of Al Alloys," Proc. Fourth Bolton Landing Conf., p. 461.

Doig, P. and Edington, J. W. (1975), "The Influence of Quenching on the Segregation of Mg to the Grain Boundaries in an Al-5.9 wt% Zn-3.2 wt% Mg alloy," Met. Trans., vol. 6A, p. 943.

Doig, P., Edington, J. W. and Hibbert, G. (1973), "Measurement of Mg Supersaturations Within Precipitate Free Zones in Al-Zn-Mg Alloys," Phil. Mag., vol. 28, p. 971

Edington, J. W. (1976) in Practical Electron Microscopy in Materials Science, New York: Van Nostrand Reinhold.

Elliott, R. P. and Shunk, F. A. (1980), "The Ag-Al System," Bull. Alloy Phase Diagrams, vol. 1, p. 36 and 91.

Embury, J. D. and Nicholson, R. B. (1963), "The Effect of Vacancy Concentration on the Distribution of Precipitates in an Al-Zn-Mg Alloy," J. Australian Inst. Metals, vol. 8, p. 76.

Embury, J. D. and Nicholson, R. B. (1965), "The Nucleation of Precipitates: The System Al-Zn-Mg," Acta Metall., vol. 13, p. 403.

Federighi, T. and Passari, L. (1959), "Anamolous increase of Resistivity During Ageing of Al-Ag Alloys," Acta Metall., vol. 7, p. 422.

Fleetwood, M. J. (1961/62), "The Distribution of Cr Around Grain-Boundary Carbides in Nimonic 80A," J. Inst. Metals, vol. 90, p. 429.

Frank, G. R., Robinson, D. L. and Thomas, G. (1961), "Precipitation Sites in Al Alloys," J. Appd. Physics, vol. 32(9), p. 1763.

Fujime, S. Watanabe, D. and Ogawa, S. (1964), "On the {0001} Spots in Electron Diffraction Patterns from the Precipitates of an

Al-20% Ag Alloys," Jour. Japan. Physics Society, Vol. 19(12), p. 2292.

Geisler, A. H. (1951), "Precipitation from Solid Solutions of Melts," in Phase Transformations in Solids, New York: John Wiley & Sons, p. 387.

Gerold, V. (1963), "Physical Properties of Solid Solutions Containing Spherical Guinier-Preston Zones," in Metallic Solid Solutions: A symposium on their electronic and atomic structure, Friedel, J. and Guinier, A. (eds.), New York: Benjamin, p.XL-1.

Goldstein, J. I. (1975) in Practical Scanning Electron Microscopy, Goldstein, J. I. and Yakowitz, H. (eds.) New York: Plenum Press, p. 49.

Goldstein, J. I. (1979), "Principles of Thin Film X-ray Microanalysis," in Introduction to Analytical Electron Microscopy Hren, J. J., Goldstein, J. I. and Joy, D. C. (eds.), New York: Plenum Press, p. 83.

Goldstein, J. I., Costley, J. L. Lorimer, G. W. and Reed, S. J. B. (1977), 'Quantitative X-ray Analysis in the Electron Microscope," SEM/1977, vol. I, Johari, O. (ed.), Chicago: IITRI, p. 315.

Goldstein, J. I. and Williams, D. B. (1977), "X-ray Analysis in the TEM/STEM," SEM/1977, vol. I, Johari, O. (ed.) Chicago: IITRI, p. 651.

Gragg, J. E., Jr. and Cohen, J. B. (1971), "The Structure of Guinier-Preston Zones in Al-5 at% Ag," Acta Metall., vol. 19 p. 507.

Greenwood, G. W. (1976), "Grain Boundaries as Vacancy Sources and Sinks," in Vacancies 1976, London: The Metals Society, mono. no. 186, p. 141.

Guinier, A. (1952), "Data on the Diffusion of Small-angle X-rays by the Structure of Age Hardened Alloys. Case of Al-Ag Alloys," Zeit. Metall., vol. 43, p. 217.

Guinier, A. (1956), "Precipitation Phenomena in Supersaturated Solid Solutions," J. of Metals, vol.8, p. 673.

Guinier, A. (1959), "Heterogeneities in Solid Solutions," Solid State Physics. Advances in Research and Applications, vol. 9, p. 293.

Hanneman, R. E. and Anthony, T. R. (1969), "Effects of Non-equilibrium Segregation on Near-Surface Diffusion," Acta Metall. vol. 17, p. 1133.

Hansen, M. (1928), "Structure of Al-rich Ag-Al alloys," Zeit. Metall., vol. 20, p. 217; "Hardening of Aged Al-Ag alloys," Naturwissenschaften, vol. 16, p. 417.

Hart, E. W. (1958), "On the Role of Point Defects in Some low Temperature Reactions," Acta Metall., vol. 6, p. 553.

Hashimoto, F. (1965), "Interaction Between a Vacancy and a Silver Atom in Al," J. Phys. Soc. of Japan, vol. 20(3), p. 336.

Heinrich, K. F. J. (1966) in The Electron Microprobe, McKinley, T. D., Heinrich, K. F. J. and Wittry, D. B. (eds.) New York: John Wiley & Sons, p. 296.

Heumann, Th. and Bohmer, H. (1968), "Diffusion of Ag in Al," J. Phys. Chem. of Solids, vol. 29, p. 237.

Heumann, Th. and Dittrich, S. (1957), "On the Diffusion in Ag-Al Alloys," Zeit. for Elektrochemie, vol. 61, p. 1138.

Hill, R. B. and Axon, H. J. (1955), "The Lattice Spacings of Al-rich, Al-Ag Solid Solutions," Research Corresp., vol. 8, p. 52.

Hirano, Ken-ichi (1967), "Metastable State in Al-Ag Alloys Formed During Quenching," Nippon Kinzoku Gakkaishi, Trans., vol. 10(2), p. 132.

Hirsch, P. B., Howie, A., Nicholson, R. B., Pashley, D. W. and Whelan, M. J. (1965) in Electron Microscopy of Thin Crystals, London: Butterworths, p. 420.

Hirsch, P. B., Silcox, J., Smallman, R. E. and Westmacott, K. H. (1958), "Dislocation Loops in Quenched Al," Phil. Mag., vol. 3, p. 897.

Hopkinson, B. E. and Carroll, K. G. (1959), "Cr Distribution Around Grain Boundary Carbides Found in Austenitic Stainless Steel," Nature, vol. 184, p. 1479, 7 Nov. 1959.

Hren, J. and Thomas, G. (1963), "Direct Observations of Precipitation in Thin Foils of Al-20% Ag Alloy," TMS-AIME, vol. 227, p. 308.

Jacobs, M. H. and Pashley, D. W. (1969), "The Factors Controlling the Width of Precipitate-Free Zones in Grain Boundaries in Al-Zn," in The Mechanism of Phase Transformations in Crystalline Solids, London: Inst. of Metals, monograph no. 33, p. 43.

Kahkonen, H. and Syrjanen, E. (1970), "Kirkendall Effect and Diffusion in the Al-Ag System," Let. to Ed., J. Mater. Sc. vol. 5, p. 710.

Katz, Z. and Ryum, N. (1981), "Precipitation Kinetics in Al-Alloys," Scripta Metall., vol. 15, p. 265.

Kelly, A. and Nicholson, R. B. (1963), "Precipitation Hardening," Progress in Materials Science, vol. 10, p. 151.

Koda, S. and Takeyama, T. (1952), "Electron Microscopic Studies of an Al-Ag Alloy," Hokkaido Daigaku Kogakuba Kenkyu Hokoku (Bull. of the Faculty of Engg., Hokkaido Univ., Japan), vol. 7, p. 250.

Koda, S. and Takeyama, T. (1953), "Electron Microscopic Studies on recipitation from an Al-Ag alloy," Journal of Electron Microscopy (Japan), vol. 1(1), p. 39.

Krause, A. R. and Laird, C. (1967/68), "A Critical Investigation of the Factors Controlling the Long-Life Fatigue Properties of Al-alloys," Mater. Sci. Eng., vol. 2, p. 330.

Kuhlmann-Wilsdorf, D. (1958), "On the Origin of Dislocations," Phil. Mag., vol. 3, p. 125.

Laird, C. and Aaronson, H. I. (1967), "The Dislocation Structures of the Broad Faces of the Widmanstatten γ Plates in an Al-15% Ag Alloy," Acta Metall., vol. 15, p. 73.

Laird, C. and Aaronson, H. I. (1969), "The Growth of γ Plates in an Al-15% Ag Alloy," Acta Metall., vol. 17, p. 505.

Leidheiser, H. (1980), Lehigh University, private communication.

Lomer, W. M. (1958), "Point Defects and Diffusion in Metals and Alloys," in Vacancies and Other Point Defects in Metals and Alloys, London: Institute of Metals, mono. no. 23, p. 79.

Lorimer, G. W. (1978), "Precipitation in Aluminium alloys," in Precipitation Processes in Solids, Russell, K. C. and Aaronson, H. I. (eds.), Warrendale, Pa: TMS-AIME, p. 87.

Lorimer, G. W., Nasir, M. J., Nicholson, R. B., Nuttall, K., Ward, D. E. and Webb, J. R. (1971), "The Use of an AEM (EMMA-4) to Investigate Solute Concentrations in Thin Metal Foils," in Electron Microscopy and Structure of Materials, Thomas, G., Fulrath, R. and Fisher, R. M. (eds.), Berkeley: Univ. of Calif. Press, p. 222.

Lorimer, G. W. and Nicholson, R. B. (1966), "Further Results on the Nucleation of Precipitates in the Al-Zn-Mg System," Let. to Ed., Acta Metall., vol. 14, p. 1009.

Mehl, R. F. and Barrett, C. S. (1931), "Studies upon the Widmanstatten Structure, I.--Introduction. The Al-Ag System and the Cu-Si system," TMS-AIME, vol. 93, p. 78.

Mehl, R. F., Rhines, F. N., von Steinen, K. A. (1941), "Diffusion in α-Solid Solutions of Al," Metals and Alloys, vol. 13, p. 41.

Murty, K. N. and Vasu, K. I. (1969), "Clustering Kinetics in Al-Ag Alloys," Mater. Sci. Eng., vol. 5, p. 251.

Murty, K. N. and Vasu, K. I. (1971), "Formation and Reversion of Guinier-Preston Zones in Al-1.3 at% Ag Alloy," J. Mater. Sc. vol. 6, p. 39.

Nemoto, M. and Koda, S. (1964/65), "Observation of Extended Dislocation Nodes in an Al-5.5% Ag Alloy," J. Inst. Metals, vol. 93, p. 164.

Nemoz, A. (1973), "Effect of Cellular Precipitation on the Superconducting Properties of Al-16.7 at% Ag Alloy," Phil. Mag., vol. 28, p. 867.

Nicholson, R. B. (1960), "The Interaction of Solute Atoms and Dislocations in Al Alloy," Proc. Europ. Reg. Confrn. on Elec. Microscopy, Delft (1960), The Netherlands, p. 375.

Nicholson, R. B. and Nutting, J. (1961), "The Metallography of Precipitation in an Al-16% Ag Alloy," Acta Metall., vol. 9, p. 332.

Njegic, A. and Williams, D. B. (1979), Lehigh University, to be published.

Nockolds, C. Nasir, M. J., Cliff, G. and Lorimer, G. W. (1979), "X-ray Fluorescence Correction in Thin Foil Analysis and Direct Methods for Foil Thickness Determination," Intl. Phys. Confrn. Series No. 52, p. 417.

Ohta, M., Kanadani, T., Yamada, M. and Sakakibara, A. (1978), "Ageing and Reversion of Dilute Al-Ag Alloy," Keikinzoku (J. Jap. Inst. Light Metals), vol. 28, p. 406.

Pande, C. S., Suenaga, M., Vyas, B., Isaacs, H. S. and Harling, D. F. (1977), "Direct Evidence of Cr Depletion Near the Grain Boundaries in Sensitized Stainless Steels," Scripta Metall., vol. 11, p. 681.

Passoja, D. E. and Ansell, G. S. (1971), "Heterogeneous Nucleation of γ' in Al-Ag and Al-Ag (Cd or Cu) Alloys," Acta Metall., vol. 19, p. 1253.

Philibert, J. and Tixier, R. (1968), "Electron Penetration and the Atomic Number Correction in Electron Probe Microanalysis," Brit. Jour. Appd. Phys. (J. Phys. D) Ser. 2, vol. 1, p. 685.

Picraux, S. T. (1974), "Mass Transport Between Two Metal Layers as Studied by Ion-Scattering," Proc. Sixth Intl. Vacuum Congr., 1974, Japan J. Appl. Phys., Suppl. 2, Pt. 1, p. 617.

Polmear, I. J. (1960/61), "The Properties of Commerical Al-Zn-Mg Alloys: Practical Implications of Trace Additions of Ag," J. Inst. Metals, vol. 89, p. 193.

Raghavan, M. (1977), "Precipitation in a Cu-30 Ni-1 Nb Alloy," Met. Trans., vol. 8A, p. 1071.

Raghavan, M. (1980), "Microanalysis of Precipitate-Free Zones (PFZ) in Al-Zn-Mg and Cu-Ni-Nb Alloys," Met. Trans., vol. 11A, p. 993.

Raynor, G. V. and Wakeman, D. W. (1949), "The Primary Solid Solution of Ag in Al," Phil. Mag., vol. 40, p. 404.

Read, W. T. Jr. (1953) Dislocations in Crystals, New York: McGraw-Hill Book Co.

Romig, A. D. Jr. (1979), Ph.D. Thesis, Lehigh University.

Romig, A. D. Jr. and Goldstein, J. I. (1980), "Determination of the Fe-Ni and Fe-Ni-P Phase Diagrams at Low Temperatures (700 to 300°C)," Met. Trans., vol. 11A, p. 1151.

Rosenbaum, H. S. and Turnbull, D. (1958), "On the Precipitation of Si out of a Supersaturated Al-Si Solid Solution," Acta Metall., vol. 6, p. 653.

Rosenbaum, H. S. and Turnbull, D. (1959), "Metallographic Investigation of Precipitation of Si from Al," Acta Metall., vol. 7, p. 664.

Rotherham, L. and Larke, L. W. (1952/53), "The Solid Solubility of Ag in Al," J. Inst. Metals, vol. 81, p. 67.

Ryum, N. (1981), Inst. Physical Met., NTH-Trondheim, Norway, private communication.

Smallman, R. E. (1976), Modern Physical Metallurgy, 3rd edition, London: Butterworths, p. 116.

Smallman, R. E., Westmacott, K. H. and Coiley, J. H. (1959/60), "Clustered Vacancy Defects in Some FCC Metals and Alloys," J. Inst. Metals, vol. 88, p. 127.

Smith, W. F. and Grant, N. J. (1969), "Mechanism of Formation of Precipitate Free Zones in an Al-4.7% Zn-3.9% Mg Alloy," Trans. Amer. Soc. Metals, vol. 62, p. 724.

Sperry, P. R. (1970), "Discussion of 'Mechanism of Formation of PFZ in an Al-4.7% Zn-3.9% Mg Alloy,'" Met. Trans. vol. 1, p. 2650.

Starke, E. A. Jr. (1970), "The Causes and Effects of 'denuded' or 'Precipitate Free Zones' at Grain Boundaries in Al-base Alloys," J. Metals, vol. 22, p. 54.

Subramanya, B. S. (1968), "An Observation of the Precipitate-Free Zone in an Al-Mg-Ag Alloy," J. Inst. Metals, vol. 96, p. 288.

Suzuki, H. (1952), "Chemical Interaction of Solute Atoms with Dislocations," Tohoku Dagaiku, Sendai, Japan (Sci. Rep. Rsch. Inst. Tohoku Univ.) Ser. A, vol. 4, p. 455.

Taylor, J. L. (1963/64), "The Effect of Heat-Treatment on the Grain-Boundary Zones in High Purity Al-Zn-Mg," J. Inst. Metals, vol. 92, p. 301.

Thomas, G. and Nutting, J. (1959/60), "Electron-Microscopy Studies of Alloys Based on the Al-Zn-Mg System," J. Inst. Metals, vol. 88, p. 81.

Thomas, G. and Willens, H. (1964), "Defects in Al Quenched from the Liquid State," Acta Metall., vol. 12, p. 191.

TI-55 (1980), in "Calculator Decision-making Sourcebook," ISBN 0-89512-014-3, Lubbock, Texas: Texas Instruments Inc., p. A-3.

Turnbull, D. and Treaftis, H. N. (1957), "On the Rate of Formation of Guinier-Preston Zones in Al-Ag Alloys," Acta Metall., vol. 5, p. 534.

Turnbull, D., Rosenbaum, H. S. and Treaftis, H. M. (1960), "Kinetics of Clustering in some Al Alloys," Acta Metall., vol. 8, p. 277.

Unwin, P. N. T., Lorimer, G. W. and Nicholson, R. B. (1969), "The Origin of the Grain Boundary Precipitate-Free Zone," Acta Metall., vol. 17, p. 1363.

von Heimendahl, M. and Schneider, K. (1970), "Influence of Cold Work on Subsequent Precipitation in an Al-20 wt% Ag Alloy," J. Mater. Sci., vol. 5, p. 455.

von Koster, W. and Sperner, F. (1953), "Hardening of Al-Ag alloys. VII. Concentration Dependence of Hardening," Zeit. Metall., Vol. 44, p. 217.

Wakeman, D. W. and Raynor, G. V. (1948/49), "The Constitution of Al-Mn-Mg and Al-Mn-Ag Alloys with Special Reference to Ternary Compound Formation," J. Inst. Metals, vol. 75, p. 131.

Walker, C. B. and Guinier, A. (1953), "An X-ray Investigation of Age-hardening in AlAg," Acta Metall., vol. 1, p. 568.

Watanabe, Y., Hayashi, H. and Hayashi, K. (1963), "Direct Observation of the Al-Ag Alloy by Electron Microscope," Jap. Jour. Appl. Physics, vol. 2(8), p. 471.

Weaver, C. and Brown, L. C. (1968), "Diffusion in Evaporated Films of Ag-Al," Phil. Mag., vol. 17, p. 881.

Wert, J. A., Parker, E. R. and Zackay, V. F. (1979), "Elimination of Precipitate-Free Zones in an Fe-Nb Creep Resistant Alloy," Met. Trans. vol. 10A, p. 1313.

Williams, D. B. (1980), "Application of Electron Optical Techniques to Problems in Metallurgical and Materials Engineering," J. Metals, vol. 32, p. 16; "Considerations of the Current Potential and Limits of AEM," 38th Annual Proc. Electron Microscos. Soc. Amer., Bailey, G. W. (ed.) San Francisco, CA, p. 82.

Williams, R. O. and Easton, D. S. (1974), "The Solubility of Ag in Al," Scripta Metall., vol. 8(1), p. 27.

Wood, J. E. (1981), Lehigh University, private communication.

Wood, J. E., Williams, D. B. and Goldstein, J. I. (1981), "Determination of Cliff-Lorimer k-factors for a Philips EM400T," submitted to: Proc. of Jt. Confrn. by the Metals Society (London) and the Institute of Physics, 'Quantitative Microanalysis with High Spatial Resolution," UMIST, Manchester, March 1981.

Zaluzec, N. J. (1979), "Quantitative X-ray Microanalysis: Instrumental Considerations and Applications to Materials Science," in Introduction to Analytical Electron Microscopy, Hren, J. J., Goldstein, J. I. and Joy, D. C. (eds.), New York: Plenum Press, p. 121.

Zaluzec, N. J., Kenik, E. A. and Maziasz, P. J. (1980), "On the Limitations of X-ray Microanalysis of Heterogeneous Specimens Using Analytical Electron Microscopy," 38th Annual EMSA Meeting, San Francisco, CA, p. 132.

VITA

Sailesh Merchant was born to Meera and Mansinh Merchant on November 1, 1957 in Bombay, India. Having attended several schools, he completed his secondary education in 1973. He obtained his Bachelor of Engineering degree in Metallurgy at the College of Engineering, Poona, India in 1979. After a brief semester at the University of Oklahoma, he transferred to Lehigh in January 1980 and has since been a graduate student in the Department of Metallurgy and Materials Engineering.